Nano-composite material for respiratory filters against byssinosis

A thesis submitted to The University of Manchester for the degree of

Doctor of Philosophy

In the Faculty of Science and Engineering

2020

Muhammad Tauseef Khawar

School of Natural Sciences

Department of Materials

The University of Manchester

Table of Contents

Total word count: 45158

List of Tables

List of Figures

Abstract

Byssinosis is a type of chronic obstructive pulmonary disease (COPD), which is very common in textile cotton workers due to the inhalation of fine cotton dust, gram negative bacteria originated from cotton dust and their endotoxins for the long period of time repeatedly.

In this research, a three layer composite respiratory filter was developed for byssinosis prevention by using the combination of polypropylene (PP) based nonwoven layers and electrospun chitosan nanofibres (CSNF). Electrospinning process optimisation showed that smooth chitosan (CS) nanofibre production was achieved from 1% to 3.5% concentration of chitosan solution, while 4% and above concentration of chitosan could not produce nanofibres due to high viscosity and high surface tension of solutions. Performance of all the developed respiratory filter samples was evaluated by anti-bacterial resistance, protection efficiency against aerosol ranges from 100nm to 2.5µm, and quality factor. The developed filter samples with CSNF coating showed more than 99% filtration efficiency with a low pressure drop of 71.6 Pa and a high quality factor value of 0.082. The antibacterial performance of CSNF layers was 91% against the *Enterobacter agglomerans*. Conclusively, results showed that the developed nanocomposite material can potentially help to reduce byssinosis.

Furthermore, plasma surface modification has been selected to improve the surface activeness of the PP outer layer for the improvement of surface capturing mechanism. The outer surface of all the samples were activated by using low pressure plasma treatment. Results showed that all low pressure plasma treated samples showed higher filtration performance as compared to untreated samples due to more effective capturing mechanism. However, impact of surface modification was not significant in 50gsm meltblown filter samples and observed more significant in spunbonded 70gsm and 100gsm filter samples. Furthermore, decay of plasma treatment impact was also analysed by using drop shape analysis. It has been observed that the surface modification impact gradually decreases and the material surface changed from hydrophilic to hydrophobic over time.

Declaration

No portion of the work referred to in the thesis has been submitted in support of an application for another degree or qualification of this or any other university or other institute of learning.

Copyright Statement

I. The author of this thesis (including any appendices and/or schedules to this thesis) owns certain copyright or related rights in it (the "Copyright") and he has given The University of Manchester certain rights to use such Copyright, including for administrative purposes.

II. Copies of this thesis, either in full or in extracts and whether in hard or electronic copy, may be made only in accordance with the Copyright, Designs and Patents Act 1988 (as amended) and regulations issued under it or, where appropriate, in accordance with licensing agreements which the University has from time to time. This page must form part of any such copies made.

III. The ownership of certain Copyright, patents, designs, trademarks and other intellectual property (the "Intellectual Property") and any reproductions of copyright works in the thesis, for example graphs and tables ("Reproductions"), which may be described in this thesis, may not be owned by the author and may be owned by third parties. Such Intellectual Property and Reproductions cannot and must not be made available for use without the prior written permission of the owner(s) of the relevant Intellectual Property and/or Reproductions.

IV. Further information on the conditions under which disclosure, publication and commercialisation of this thesis, the Copyright and any Intellectual Property and/or Reproductions described in it may take place is available in the University IP Policy

(see http://documents.manchester.ac.uk/DocuInfo.aspx?DocID=487), in any relevant Thesis restriction declarations deposited in the University Library, The University Library's regulations (see http://www.manchester.ac.uk/library/aboutus/regulations) and in The University's policy on Presentation of Theses.

Dedication

This thesis is dedicated:

To my beloved parents and wife

Acknowledgements

I would sincerely like to acknowledge my supervisor Dr R Hugh Gong for his guidance, help and encouragement for my research work, especially his motivation towards my goals which I can never forget through my life.

Special thanks to my co-supervisor Dr Jiashen Ali to guide me towards my research work and providing me an excellent opportunity to perform my experimental work in Electrospinning process, which enabled me to successfully achieve my research goals.

I wish to thank School of Design, University of Leeds, especially Dr Muhammad Tausif to help me during the experimental work. I am also thankful to Xian Polytechnic University, China, for providing some of the characterisation facilities.

I would also like to thank my colleagues and friends, especially Dr Zeshan Yousaf, Dr Muhammad Umar, Qasim Zia, Dr Abida Younas and Dr Ayesha Abida for their help and support during my research work. I also acknowledge Punjab Education Endowment Fund (PEEF), Pakistan for the financial support to pursue my PhD studies.

Finally, I would like to express thanks to my family, especially my parents and wife who continuously encouraged me throughout my work.

Chapter 1: Introduction

Personal Protective Equipment (PPE) is critical for the prevention of respiratory diseases such as byssinosis and asthma. Byssinosis, being considered as an environmental lung disease, is defined as a narrowing of the airways caused by inhaling cotton, flax, or hemp particles. It may cause wheezing and tightness in the chest. It is a type of occupational chronic obstructive pulmonary disease (COPD). Controlling dust (e.g. using face masks and other measures) is the best way to reduce the risk of byssinosis. In a comprehensive review on long term respiratory health effects in textile workers, Lai and Christiani (2013), Harvard School of Public Health [1], point out that over 60 million people worldwide work in the textile or clothing industry are exposed to the risk of chronic lung diseases, in particular COPD in their workplaces, which could lead to considerable potential cost. It was also reported that the costs of occupational COPD from 2002 could be attributed to $5.0 billion for the USA annually. Therefore, a comprehensive study is required to reduce byssinosis and COPD by developing an effective respiratory filter for the textile workers.

1.1 Problem Definition

Cotton processing produces fine dust particulates and causes gram negative bacterial contamination in the work environment. Inhalation of these fine dust and bacterial endotoxins for a prolonged period of time creates symptoms of byssinosis. Due to the unavailability of effective personal protective equipment or respiratory filter, affected people of byssinosis are increasing day by day. Cotton dust is categorized in three ranges, micro dust, breathable dust, and fine particulates with size ranges of 15-50µm, 2.5-15µm, and 0.1-2.5µm respectively [2].

In addition, cotton dust contains gram negative bacteria and their endotoxins. There are three types of rod shape gram negative bacteria which are normally found in the cotton dust. These are *Enterobacter agglomerates, Pseudomonas Syringae* and *Agrobacterium (spp.). Enterobacter genus* is found in the abundance. Inhalation of these dust and bacteria is dangerous for the workers and has a strong possibility of causing the byssinotic symptoms.

The development of efficient personal protective equipment (PPE) for textile cotton workers can protect them from the exposure of cotton originated pathogenic dust and reduce byssinosis.

1.2 Research Aim

The aim of current research is to develop materials suitable for respiratory filters (PPE) which offer effective protection against fine cotton dust aerosols and their pathogenic species.

1.3 Research Objectives

- Optimisation of chitosan nanofibre production to spin with maximum concentration of chitosan and to produce nanofibres with a diameter range less than 500nm.
- Development of nanocomposite material by chitosan nanofibre coating with nano-level pore size distribution to capture fine cotton dust particulates and gram negative bacterial species.
- Filtration performance analysis of the nanocomposite filter materials against fine dust particles and gram negative bacterial species to achieve best combination with a filtration efficiency more than 95% and pressure drop value less than 250 Pa.

- Analyse the impact of plasma surface modification on the filtration performance of developed nanocomposite filter materials

1.4 Contribution of Research

Following is the contribution of research of all the participants and it implies to all the result and discussion chapters, which are written in journal format.

Muhammad Tauseef Khawar (Student):

Designed and conceptualised the reported work.

Selection of appropriate methodology and execution of all the involved experiments and characterisation.

Investigation of results and formal analysis to conclude the finding of the research.

Writing the original draft of the thesis on the basis of designed research.

Hugh Gong (Supervisor): Helped in designing and conceptualisation of the reported work. Supervised all the steps of experiments and characterisation. Contributed in formal analysis of the research findings. Reviewed and edited the thesis for the finalisation of research findings

Jiashen Li (Co-Supervisor): Helped in designing and conceptualisation of the reported work. Training and supervision of experimental work. Resource provision for the experimental work.

1.5 Thesis Layout

Chapter 2: Literature Review

In this chapter, relevant literature such as nonwoven web formation techniques, web bonding methods, finishing of nonwovens, applications of nonwovens, respiratory filters and past work on filtration performance against fine dust particles are reviewed and discussed.

Chapter 3: Material and Methods

This chapter gives the detailed information about materials used for the current research work, methodology adopted for the development of respiratory filters, surface modification method and characterisation techniques used for the performance analysis.

Chapter 4: Process optimisation for smooth nanofibres production of chitosan

This chapter describes the optimisation of the electrospinning process parameters to spin with the maximum concentration of chitosan for the production of nanofibres.

Chapter 5: Chitosan nanofibrous respiratory filter for prevention of byssinosis

This chapter gives the detailed information about the development of two-layer composite PP respiratory filter with chitosan nanofibre coating. The developed respiratory filter is analysed against fine dust particles ranging from 100nm to 2.5µm and against gram negative bacterial species.

Chapter 6: Effect of plasma surface modification on filtration performance of chitosan nanofibres based respiratory filter

Different samples of respiratory filters have been developed by using different nonwoven PP substrate and chitosan nanofibres coating. All the samples have been surface modified by using plasma surface modification. The filtration performances of plasma treated and untreated filter samples are compared.

Chapter 7: Conclusion and future work

In this chapter, conclusions of the work and possibility of the future work are provided.

Chapter 2: Literature View

2.1 Nonwovens

The term “Nonwovens” came during the late nineteenth and early twentieth centuries due to the three basic economic necessities worldwide. The first necessity was to reclaim acceptable quality fibres from waste or scrap clothing such as wool or cotton and reuse them for the production of economically competitive clothing; the second was to use coarse hair and vegetable origin coarse fibres for the production of viable products; and the third necessity was to reuse fibre waste from industry and utilize new developed fibres which are not suitable for conventional spinning such as wood pulp. Through this way, felts production from natural coarse fibres was started in the USA and UK in the late eighteenth century and commercialized for the manufacturing of viable products. [1]

The internationally acknowledged definition of nonwovens was described by the ISO standard 9092 and CEN EN 29092. The current definition of nonwovens by ISO were proposed by the two world famous associations EDANA and INDA.

“A nonwoven is a sheet of fibres, continuous filaments, or chopped yarns of any nature or origin, that have been formed into a web by any means, and bonded together by any means, with the exception of weaving or knitting. Felts obtained by wet milling are not nonwovens.”

"Wetlaid webs are nonwovens provided they contain a minimum of 50% of man-made fibres or other fibres of non-vegetable origin with a length to diameter ratio equals or superior to 300, or a minimum of 30% of man-made fibres with a length to diameter ratio equals or superior to 600, and a maximum apparent density of 0.40 gcm^{-3}."

"Composite structures are considered nonwovens provided their mass is constituted of at least 50% of nonwoven as per to the above definitions, or if the nonwoven component plays a prevalent role."

Nonwovens are unique and high-tech engineered fabrics made directly from fibres, and are employed worldwide in a wide range of products. The structural view of two bonded nonwovens is shown below in Figure 2.1.

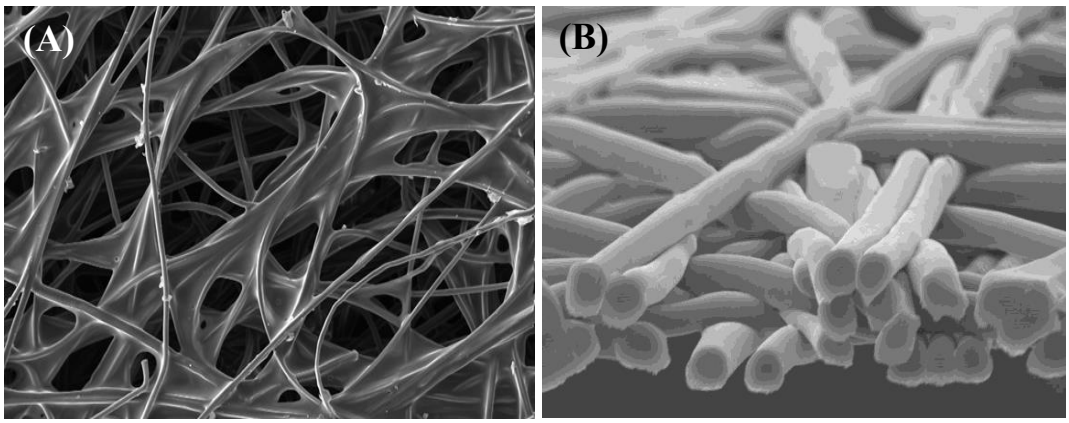

Figure 2.1: Structural view of (A) chemically (B) mechanically bonded nonwoven fabric [2][3]

The structure of nonwovens is quite different from knitted and woven fabric because nonwovens are manufactured by putting fibres together in the form of web or sheet in mainly

four different ways (dry-laid, wet-laid, air-laid and polymer-laid) on the basis of fibre laying technique for web making. The formed webs can be bonded by mechanical, thermal or chemical means. [4]

Under the umbrella of nonwovens, both durable and limited-life products can be produced with a variety of performance characteristics such as filtering, stretch, softness, absorbency, strength, cushioning, flame retardancy, washability, sterility, liquid repellence, resilience and bacterial barrier etc.

Nonwovens are employed for agriculture coverings, apparel linings, automotive headliners, automotive upholstery, civil engineering fabrics, envelops, house wrap, wipes, hygiene products, geotextiles, filtration products, substrates for roofing, shoe felts, blankets, tennis court surface, space shuttle exterior tiles, insulators, vinyl substrate, wall covering, synthetic leather, tennis ball covers, felts, shoulder padding, ceramic insulation, and in different other composites. Kevlar bullet proof vest, paper marker felts, interlining, carpet underlay pads, auto trunk liners, primary carpet backing, and blanket are also being produced by needle punching technology. [5]

2.1.1 Raw material for nonwovens

Both natural and man-made fibres are being used as a raw material for the production of nonwovens. However, man-made fibres including polypropylene and polyester are dominating according to the worldwide study by Tencon Limited. Furthermore, viscose rayon, acrylic,

polyamides and other speciality fibres are also being used as a raw material in nonwoven manufacturing. [6]

2.1.2 Web manufacturing techniques

Among all synthetic fibres, polypropylene is mostly being used due to its low density, low melting and glass transition temperature which leads to the energy-efficient thermal bonding, biological and mildew resistance, soil and stain resistance, good bulk cover with good tensile strength and abrasion resistance. Polyester fibre is mostly being used due to its low cost and durability. Due to the high moisture regain, use of regenerated cellulose base fibres like viscose rayon and Lyocell is increasing day by day in Europe. Viscose rayon is being used in the manufacturing of wipes, medical and hygiene sector. Lyocell consumption is also increasing due to its high wet strength with high moisture regain. [7]

There are four techniques for the web manufacturing which are drylaid, wetlaid, air-laid, and polymer-laid. They have their own different origins. Drylaid was based on textile spinning technique, wetlaid concept was acknowledged from paper-making industry, air-laid was based on assembling of fibres into the web by using air stream and polymer-laid technique was based on polymer extrusion and plastic making techniques. Brief descriptions of all these techniques are given below. [8]

2.1.2.1 Dry-laid web formation

Dry-laid method of web formation is based on carding mechanism of spinning and aerodynamically arrangement of fibres originated from the paper industry. In carding mechanism, all the fibres having the ability to bear carding can be used for the web formation.

Polymers, glass fibre, ceramic fibre, polyester, polypropylene and viscose rayon are mostly being used for the manufacturing of dry-laid nonwovens. The first step of this method is the opening of the fibres before feeding to the carding machine. “Well opened is half carded” is a famous statement in favour of the opening of the fibres because fibres mostly came in the form of bales as a raw material which needs to be opened for the removal of impurities, neps and inconsistency. Bale breakers, bale pickers, hooper feeder, fibre openers and disc openers are some of the machines which are mostly being used for the opening of fibre bales as shown in Figure 2.2.

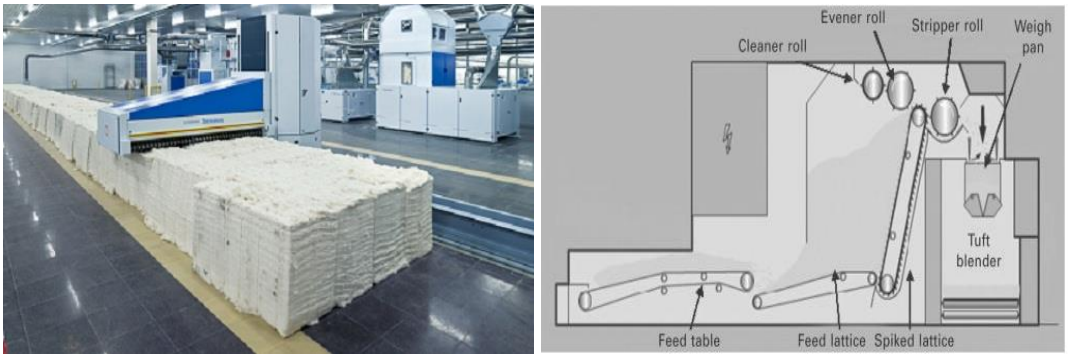

Figure 2.2: Pictorial view of bale opener and hooper feeder respectively [9] [10]

Mixing and blending of the fibres is the second step of this process to obtain homogeneous mixing of different fibres and their different blend ratios for achieving required mechanical or functional properties in a resultant web. For more precise blending or mixing, micro-processor controlled feed system is also being used. After this process, fibres are fed into the card machine for the homogeneous web formation. The whole mechanism of carding is based on working and stripping rollers situated around the main cylinder of the machine which makes sure the uniform distribution of the fibres and removal of tufts from the fibres. Consolidated fibres in

the form of the web are then condensed and removed with the help of doffer as shown in Figure 2.3.

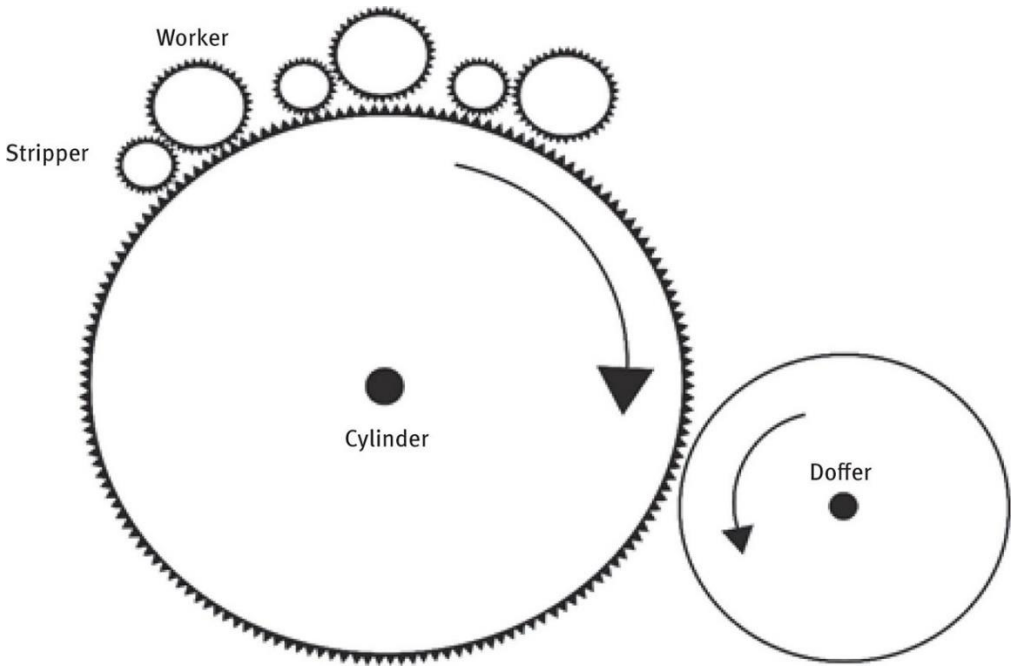

Figure 2.3: Carding mechanism for dry-laid web formation [11]

After that, consolidated web converted into required shape with the help of randomizing, cross-lapping and bonding respectively. Randomizing rollers are used to obtain required strength on machine direction and cross direction of the web respectively. Cross-lapper process involves the layering of the webs to achieve the required thickness and bonding technique governs the final strength of the web.

2.1.2.2 Air-Laid Web formation

Air laid technique involves the conversion of fibres in the form of the web with the help of aerodynamics or air stream and leading this air-fibre mixture towards a screen or conveyer;

where the air is separated and fibres are allowed to arrange in the form of web. Web formation mechanism through this technology is shown in Figure 2.4.

This method is used to make the isotropic web with respect to functional properties. A wide variety of fibres from conventional to high performance fibres range can be used through this process for web formation. Prior to web manufacturing, opening or fibre separation is essential to avoid web faults. After opening, fibres are fed to main cylinder with the help of feed rollers.

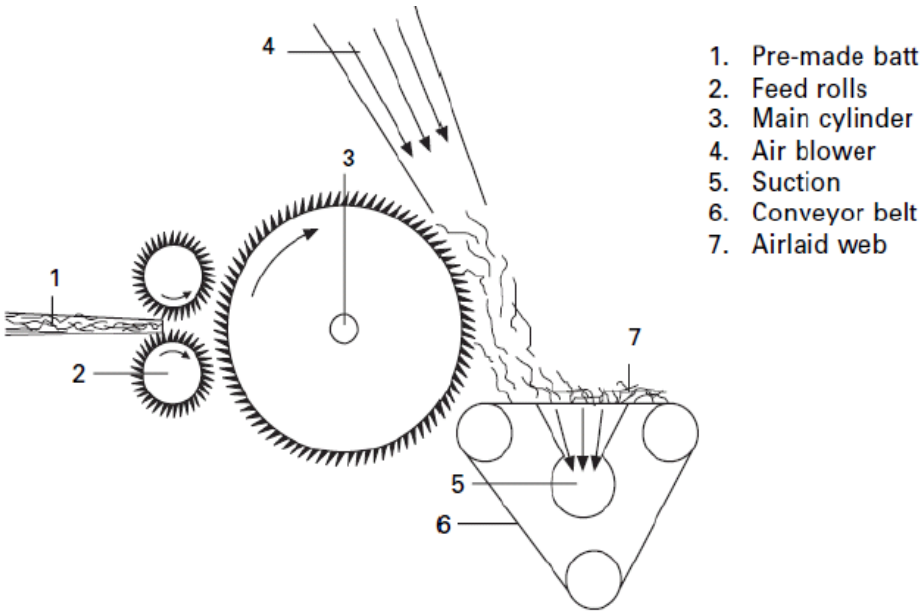

Figure 2.4: Principle of web formation through air-laid technique [12]

After that fibres transfer from the cylinder surface to conveyer surface, influenced by the air blower and suction under the conveyer. Then consolidated high loft web undergoes the required bonding process as shown in Figure 2.4. Web produced from air-laid method has properties like high strength, high resiliency, high loft, high porosity (if required), high absorbency and soft to handle. [13]

2.1.2.3 Wet-laid web formation

Wet-laid technique is based on the modified paper-making process in which the fibres are suspended in water. Natural, synthetic and high-performance fibres can be used to form the web as per the requirement. In this process, fibres are normally suspended in water by feeding the sheet of fibres or cut length fibres into a hydro pulper which is basically a shear mixer which breaks up the sheet and disperses the fibres and fibrils in water. After that, fibre water suspension is forced through two metal bars in a flow box to control the flow on a wire. Figure 2.5 shows the complete working process of wet-laid.

The way in which suspended fibres are deposited onto the wire is very important due to the influence of different forces around the flow. To increase the filtration process of fibres or separation of fibres from liquid, vacuum boxes can be used under the wire for the better quality of the web.

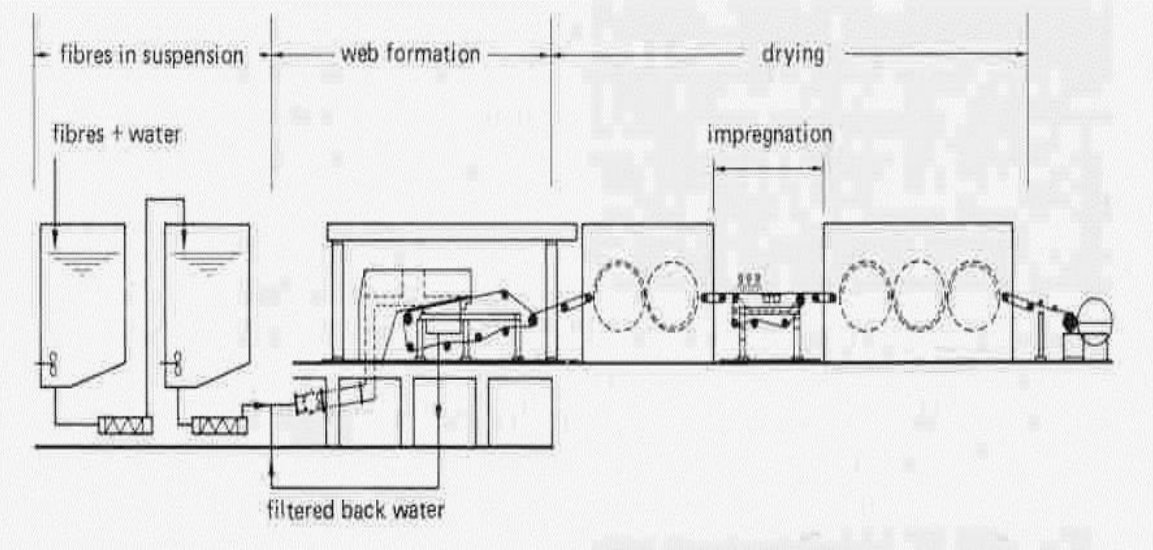

Figure 2.5: Working mechanism of wet-laid web formation [14]

After that, water removal through drying and bonding of the web complete this process as per the requirement. This process can be used for the brittle fibres due to its shearing mechanism. Production of nonwovens, by using this technique is 5-10% worldwide. [15]

2.1.2.4 Polymer-laid web formation

Polymer-laid, spunlaid or spunmelt nonwovens are produced by using extrusion spinning technique, in which web formation is based on filaments direct collection after extrusion during spinning. Intermediate process of yarn and tows formation is eliminated during this process which leads to cost effectiveness of this process. Generally, high molecular weight polymers processed by using spunbonding technique like, polyester, polypropylene, polyethylene and polyamides. Process of spunbonding involves control of filament extrusion, drawing, lay down and bonding respectively. For extrusion of polymers, dry, wet and melt spinning techniques are being used, while melt spinning is mostly being used for spunbonded nonwovens. Starting phase of this process is a polymer which ends with fabric form and required a continuous production line assembly. Process stages of spunbonding are given below in Figure 2.6. Low molecular weight or microfibres are preferred by using meltblown web production. Some micro fibres are found in nature like spider silk, pineapple leaf fibres.

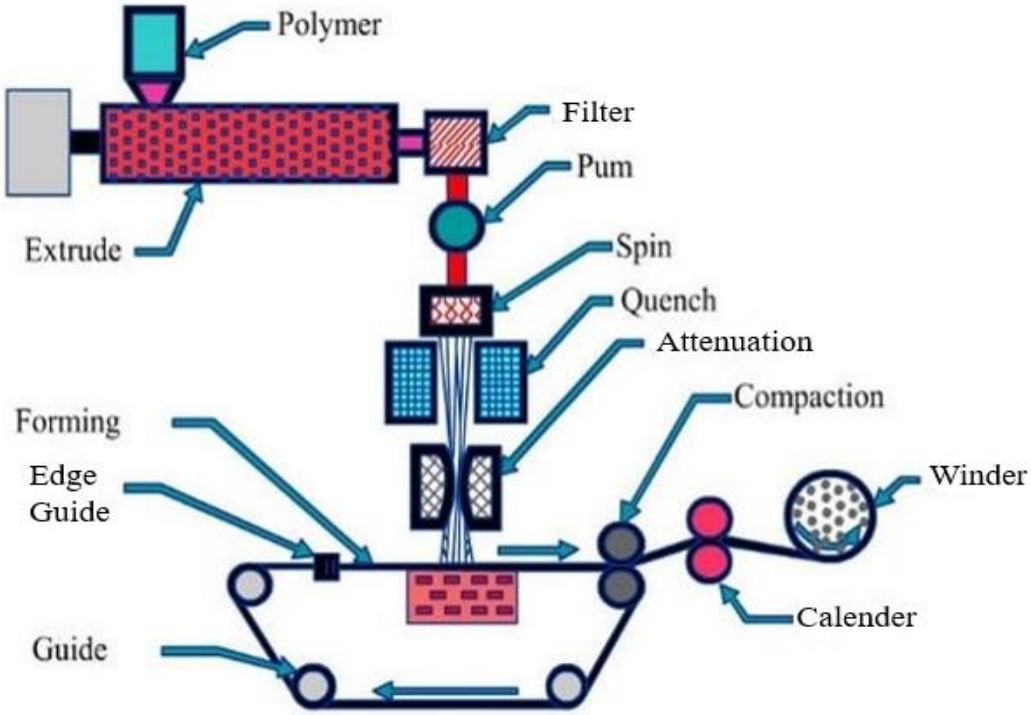

Figure 2.6: Process flow of spunbonding technique [16]

Manmade microfibres can be made by using different techniques like spray spinning, electro spinning and centrifugal spinning under the section of meltblown. This is very important and simple method involves molten state polymers which convert molten/ liquid polymers into microfibre with the help of high velocity streams of air or gas.

In this process, liquid polymer extruded from very fine orifices and passes through a convergent stream of hot air exiting from the top and bottom sides of the nosepiece which rapidly attenuates the polymer streams and converts it into very fine microfibres having diameter ranges from 1 to 5 µm. The process flow of meltblown web formation is given below in Figure 2.7. Meltblown fabrics due to the high surface area have high application in the field of filtration, insulation,

and liquid absorption. Greater surface area improves barrier properties and good barrier and wicking properties. [17]

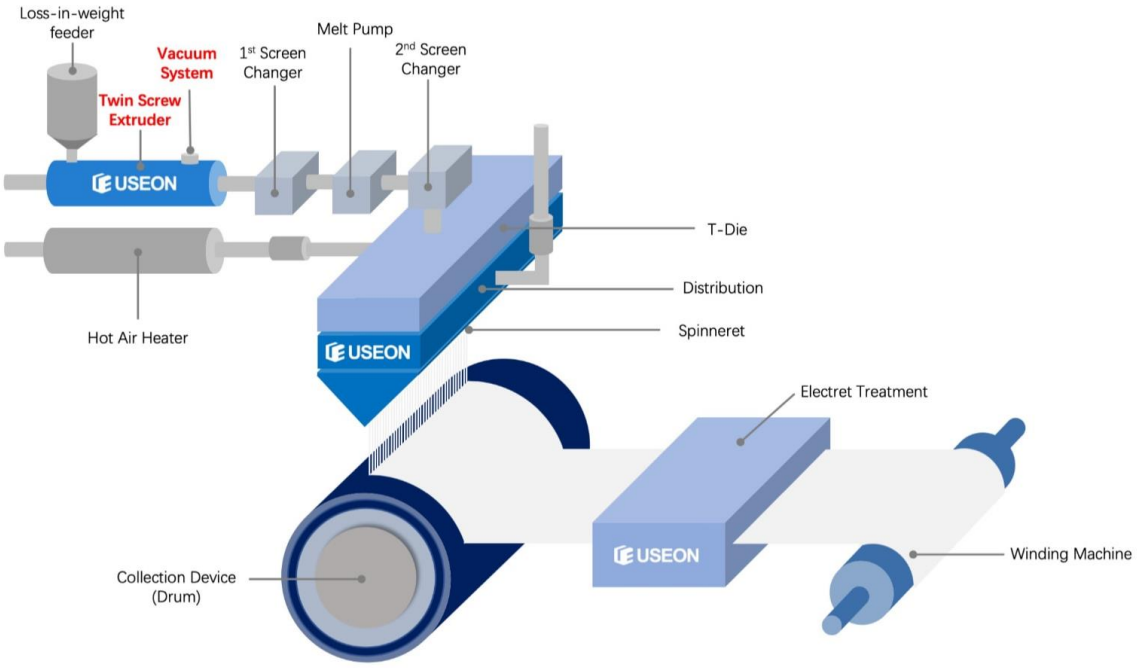

Figure 2.7: Process flow diagram of meltblown production line [18]

2.1.3 Nonwoven web bonding methods

Bonding is a vital step for web consolidation in the production of nonwovens fabric. There are three types of bonding techniques, thermal, chemical, and mechanical respectively. Strength, air permeability, porosity, flexibility, density, and softness of the nonwovens fabric can be predicted by the degree of bonding. The bonding process is stimulated after web formation in a production line. In some types of fabrics, multiple bonding options can be applied depending upon the required properties. A brief description of all types of bonding is given below. [19]

2.1.3.1 Thermal bonding

This method of bonding is applicable to all types of webs, manufactured from dry-laid, wet-laid and polymer-laid. Thermal bonding is applicable for thermoplastic synthetic fibres which can be soften or melt at low temperature and normally also called bi-component fibres. For this purpose, web manufacturing can be made with whole thermoplastic fibres or some proportion of low melt and bi-component fibres to achieve the required bonding after the application of heat source. Application of heat from different heat sources, soften or melt the bi-components which promotes bonding between the fibres and crossover points of the fibres in the web. An adhesive or mechanical bond is formed after subsequent cooling on bonded crossover points. The thermoplastic component can be in the form of powder, thin film, homofill fibre, web or sheath as a part of bonding source. Thermal bonding phenomenon through heated rollers is shown in Figure 2.8.

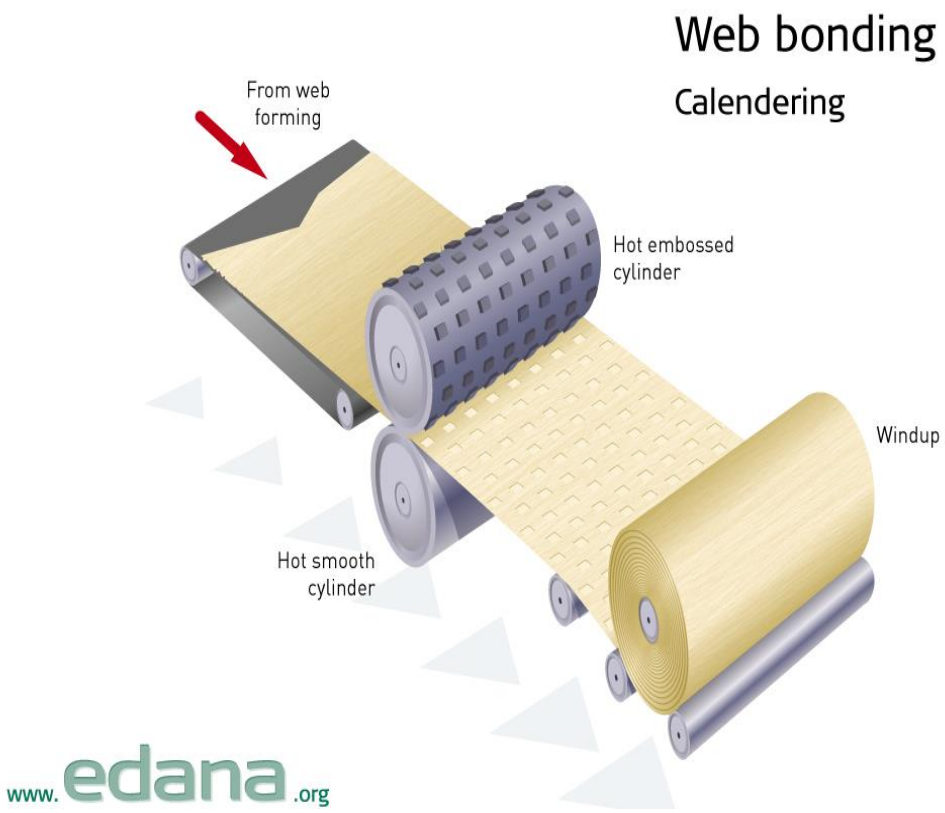

Figure 2.8: Web thermal bonding through heated calender rollers [20]

Calendering is one of the methods for heat supply. Through this way, fabric passes between the heated Calender rollers under heat and pressure to soften the thermoplastic portion of the web with good production speed. Through this process, we can apply the different pattern, area bonding and point bonding with the help of Calender rollers surface as shown in figure 2.8.

Bonding through hot air source is a good way to bond low melts fibres in the web. Through this way, we can produce high loft thermally bonded web for the required application. Drum and blanket system can also be used for the bonding of the web with the help of heat and pressure. Ultrasonic bonding and infrared bonding can also apply as an energy source to

provide heat for the softening or melting purpose of fibre to consolidate the web. A Grooved or patterned roller is used to apply high-frequency energy on the specified point of the web as per the applied roller pattern which promotes point bonding or area bonding. Thermal bonding is largely being used for the bonding of webs worldwide due to its low cost. Energy cost of this method is much lower than other bonding methods as shown in Figure 2.9. [21]

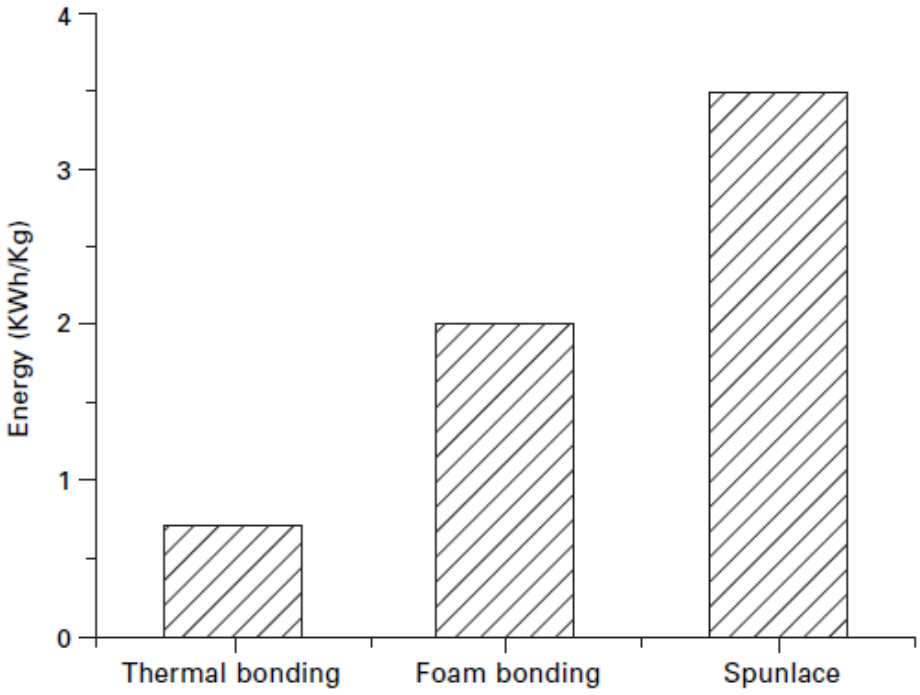

Figure 2.9. Energy cost comparison of thermal bonding with other methods [21]

2.1.3.2 Chemical bonding

Chemical bonding is a process in which liquid base bonding material is applied on the web for web consolidation. There are many polymer based binding materials available in the market like, acrylate polymer, styrene butadiene copolymers, and vinyl ethylene copolymers etc. Chemical bonding material can be water-based binders, powder adhesives, foam based and in

some cases organic solvent-based depending upon the functional properties requirement of the web.

Binders can be applied through a spray method, or uniformly impregnation of the whole web in binder solution, or the coating on the web and or through printing application of binding material. After the application of the material, drying is a subsequent process for the permanent consolidation through film formation on the web. Print bonding technique is gaining more attraction due to the application binders on specifies area of the web with a required design by leaving maximum un-bonded fibres for many other functional properties. Process flow of chemical bonding is given below in Figure 2.10.

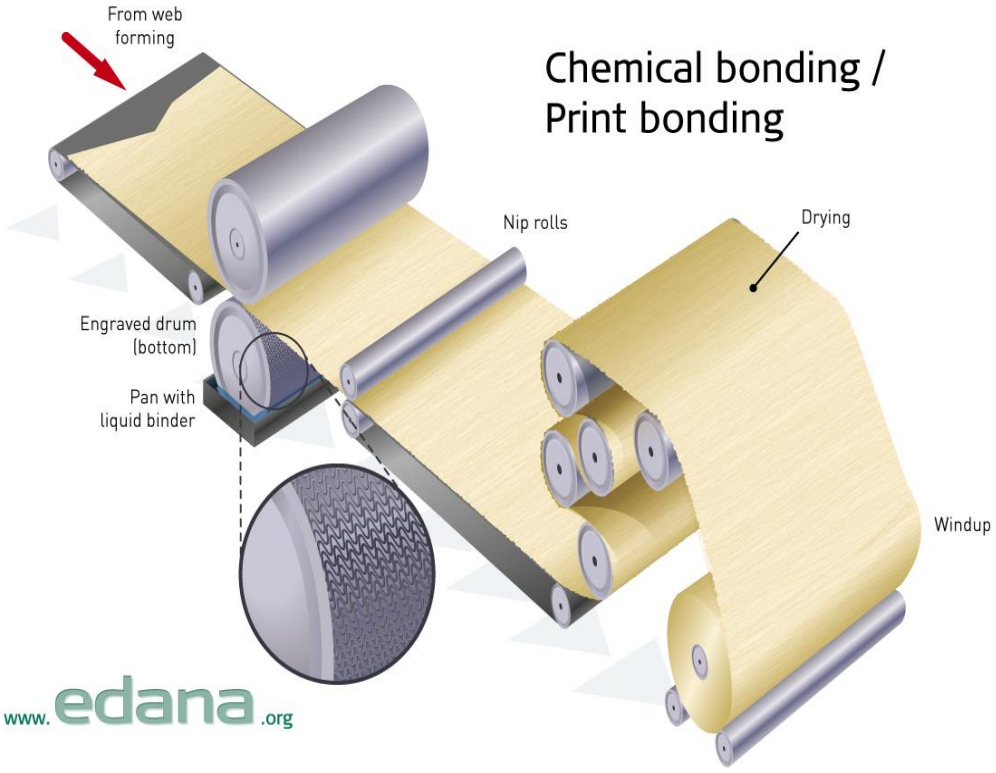

Figure 2.10: Process diagram of chemical bonding of nonwovens [20]

2.1.3.3 Mechanical bonding

Mechanical bonding is a process in which the web is strengthened by increasing the entanglement of the fibres and inter-fibre friction. There are two methods of mechanical bonding which is most commonly being used for web consolidation. One method is needlepunching and the second one is hydroentanglement. Brief description of these two methods is given below in the respective captions.

2.1.3.3.1 Needlepunching

Needlepunching methodology is also being used for the consolidation of the web as per the requirement. In this technique, fibres are entangled mechanically with the help of reciprocating barbed needles through a moving web on needle loom as shown in Figure 2.11. Barbed needles are attached on a loam board which oscillates between two fixed plates named as bed plate and stripper plate. The web passes between bed plate and stripper plate. These plates are porous and contain holes for the movement of the needles.

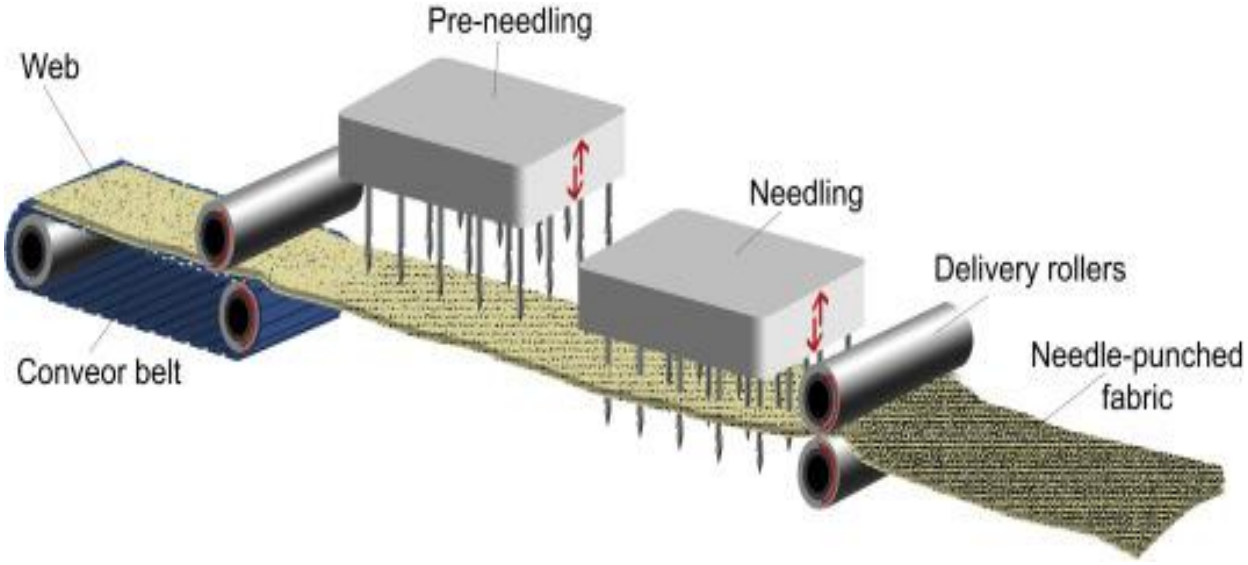

Figure 2.11: Needlepunching mechanism of web bonding [22]

During the oscillation of the needle board, fixed needles move upward and downward through these holes of the web holding plates for the entanglement of the fibres which leads to structural integrity in the fabric as shown in Figure 2.11. Web movement is totally dependent on the movement of nip rollers because the movement of these rollers governs the feeding and draw-off of the web during bonding. Barbed needle movement is shown below in Figure 2.12.

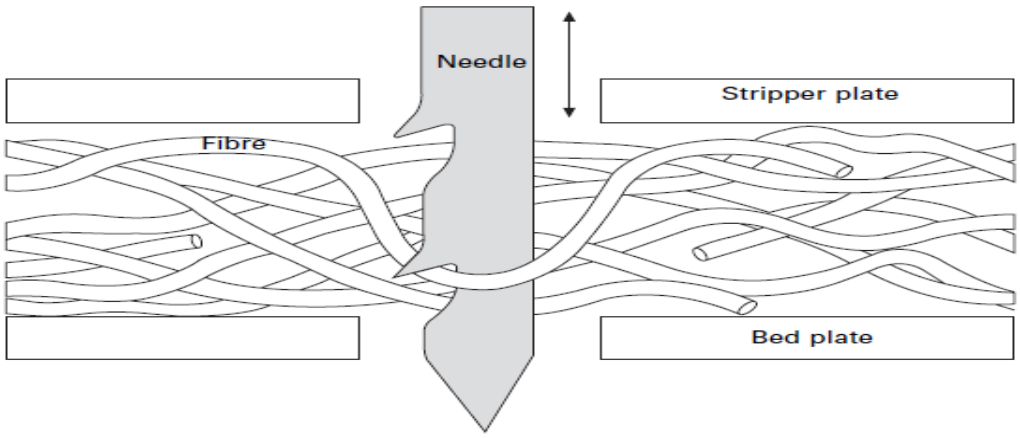

Figure 2.12. Barbed needle action during needlepunching [23]

Some draft normally occurs when we feed the web for bonding due to needling operation as the web or batt is pulled continuously through the needles. This draft can be minimized by the optimization of advance per stroke and by minimizing needle penetration through the web. But this mechanism leads to poor bonding or less entanglement of fibres. Needle loam can be classified into single board, multi-board and structuring or speciality as per the requirement. Normally coarse needles with larger barbs are used for coarse fibres and vice versa. [24]

2.1.3.3.2 Hydroentanglement

This technique is mostly applied to carded and wet-laid webs. During this methodology, high-pressure fine water jets directly strike with the web for the interlacement and entanglement of fibres. Interaction of high pressure water jets with web induces displacement and rearrangement of the fibres. This technology is also called spunlacing or hydraulic entanglement. Basically, hydroentanglement relies on the transfer of kinetic energy of water jets to the web which leads to mechanical bonding as shown in Figure 2.13. [24]

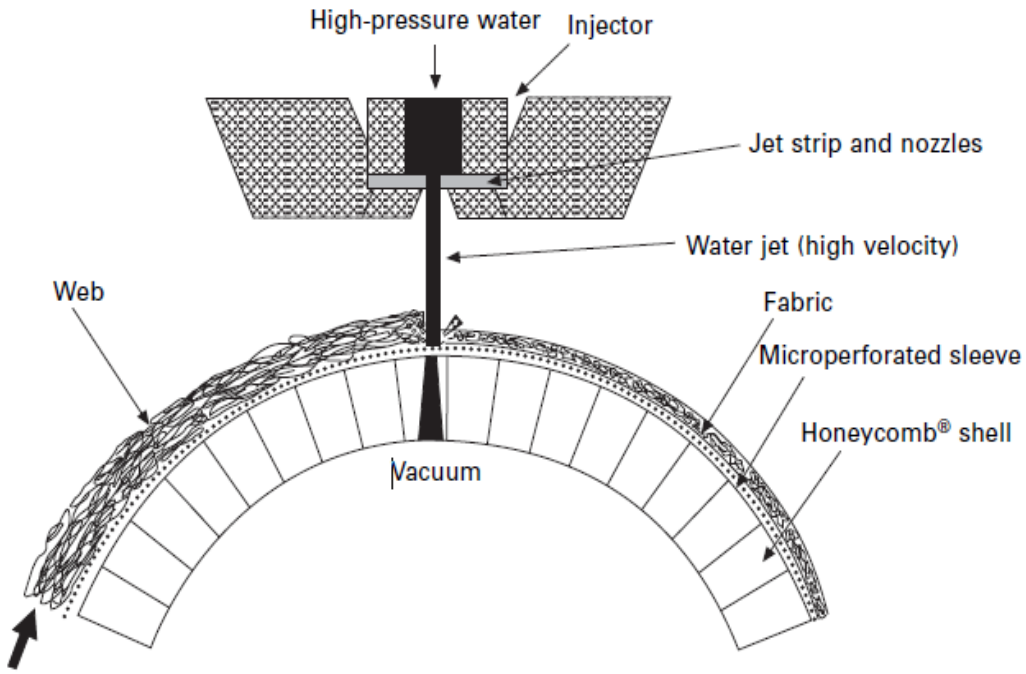

Figure 2.13: Hydroentanglement mechanism with captioned basic elements [25]

This process involves pre-wetting of the web for the removal of air bubbles, surface support for the web movement e.g. conveyer, injector working operation with respect to the quality of the jet, arrangement of the injectors as per the bonding requirements, de-watering of the web after injector operation, water circuit and filtration for the reuse of water and at the end drying and pattering the required effect as per requirement. Energy (kJ/kg) applied on the mass per unit area of the fabric describes the degree of bonding, economic efficiency and resultant bonding properties. Basically, energy transfer and resulting fibre entanglements totally depend upon the quality of jet and mechanical and physical properties of the fibres in the web. [24]

2.1.4 Finishing of nonwovens

Finishing is an integral part of nonwovens fabric manufacturing for the addition of technical performance and appearance fitness for the ultimate purpose. Finishing of nonwovens is totally

dependent on the required features in the end product and their application. Some finishing processes like dyeing, washing, calendering and printing have evolved from traditional processes of textile. Basically, there are many types of finishing processes named as mechanical finishing, chemical finishing and lamination. By the application of these finishes, nonwovens are gaining importance due to the improved and innovative features. [26]

2.1.4.1 Chemical finishing

Chemical finishing application has a vital role in the functionality enhancement of the nonwovens fabric. All these finishes have different application methods and dependent upon the end-use requirement of the product. Some finishes applied through wetting and some applied through other direct processes. Some masterbatch finishes are also available, which can be applied on yarn level before web manufacturing or other bonding methods. UV absorbers, UV stabilizer, UV filters, migratory, conductive and permanent anti-stats, antimicrobials and some fragrances are available in the form of masterbatch additives for the application on initial processes of web manufacturing.

The antistatic finish is applied on the synthetic base fabric to avoid from the clinging of dust, dirt, airborne soil through the removal of static electricity. By the application of antistatic finish, fibre conductivity and hydrophilicity are increased for the neutralization of the static charge. Antimicrobial finishes are also applied to avoid biological degradation which is the resultant of undesirable organism growth such as bacteria, fungus and fungi. Lubricants are also applied on some types of certain nonwoven fabrics for the reduction of fibre to fibre and fibre to metal or other substrate friction for the production feasibility.

Some fire retardant finishes are also applied in some cases where protection from the fire or flame propagation requires. These finishes are mostly nitrogen-phosphorous compounds based and normally applied with hygroscopic auxiliaries which ultimately reduce the flammability. Water repellent finishes are also being used to enhance the hydrophobicity of the fabric. These types of finishes based on silicon or fluorocarbon based and applied normally through aqueous dispersion or padding and spraying etc. Stiffeners are also applied to increase the abrasion resistance, weight and strength of the fabric. Softener finishes are also applied for the proper feel of the fabric which is required for the skin irritation. Softeners can be hydrophilic and hydrophobic which can be applied as per the ultimate requirement of the product. Sunlight degradation is a very common problem in which fabric is normally exposed to sunlight. So, to avoid this degradation, UV stabilizer and UV absorber finishes are mostly being used to avoid polymer from UV degradation by reflecting or absorption of the UV light. [27]

Wet finishing of nonwovens involves washing, colouration and printing processes as per the requirement of end-use. The washing process is the first process which is required for the subsequent process of colouration and printing. Normally detergent is mostly used for the washing in an aqueous bath for the surface clearance from dust particles and other hydrophobic impurities. The ultimate purpose of this process is to increase the wetting of the substrate for dyeing. During washing, temperature, process time, mechanical action and quantity of detergent govern the efficiency of the washing process. The washing process is followed by the rinsing of water for the dilution of detergent bath and removal of applied detergent from the surface of the substrate.

The washing process is continuous in nonwovens manufacturing with the help of guide rollers. Guide rollers help the fabric in passing from the scouring or washing and rinsing bath for the subsequent reaction and cleaning. This process can be performed in a machine having drum and other required chemicals and water feeding capacity normally called washing machine and the process is also called batch process. The ultimate goal of washing is the removal of spin finish oil on the substrate, dust, oil, waxes and other containments to enhance the wettability of the fabric.

2.1.4.2 Mechanical finishing

Mechanical finishing involves splitting, perforating, drying, compressive finishing and calendering. Every product has its own type of mechanical finish requirement from all these finishes. For achieving specific high density having a low thickness, splitting and winding methodology is applied to the fabric. In this process, fabric is split or levelled on required thickness by feeding on a table under the controlled tension and precisely feed to adjusted hoop knife. The main purpose of this finish is to produce thin fabrics by splitting.

In hygiene products of nonwovens, perforation of the fabric is required. In the perforation process, heated needles and modified calender rollers are mostly being used. Drying and heat setting is an important process with respect to producing dimensionally stable fabric with the help of stenter frames. Compression finishing is also applied to avoid from shrinkage factor on a very low extent in case of cellulosic fibres. During sanforising, shrinkage is stabilized by passing the pre-wetted or steamed fabric on a heated cylinder in contact with a rubber belt or

blanket. Fabric is compressed in-plane as it is held in contact with the blanket (usually elastomeric) and the drying cylinder. [28]

Softening, polishing, singeing, shearing and flocking are types of some surface finishes which are being used for the nonwoven fabrics. Softening is a process to improve surface feel and appearance by feeding through lightly touching belts on baffle plates at high speed. It can be achieved by applying functional chemicals, enzymes and softening agents later on with better-softening properties.

Low pressure hydroentanglement, thermal and chemical bonding also improve the softening of nonwoven fabric. Singeing process involves removal of protruding fibres by passing on a burner with high speed. This process is required to obtain a clean surface for the followed process of coating or printing. Shearing is also a process for the removal of protruding fibres for the surface clearance purpose. Flocking is a process of creating three dimensional piles on the surface of the fabric. This finish is required for the backing fabric having end-use in interior panels of shoes, apparel, filters and drapes for the pattern decoration purpose. [28]

2.1.4.3 Colouration of nonwovens

Colouration is a process to impart colour on the substrate by using dyes or pigments. There are many colouration methods being applied to impart colour, depending upon the substrate. During the process of dope dyeing, colour agents are applied in the spinning dope, prior to extrusion. This process results in excellent colour fastness properties.

2.1.4.3.1 Printing of nonwovens

Printing is another process to impart colour to the nonwoven substrate. In this process, the pigment is applied with the help of binder resin on the fabric, because it cannot be applied directly owing to no attraction for the substrate. Pigments are normally applied through printing process with the help of binder resin which normally works as a chemical bonding agent. Fixation of the pigments is dependent on the applied binder fixation through thermal drying or curing. To achieve the uniform shade on the fabric, even application of binder and pigment dispersion on the substrate. [28]

2.1.4.3.2 Dyeing of nonwovens

There are two methods for the dyeing of fabric; one is a continuous method and the second one is batch dyeing method. [28] But dope dyeing technique is also being used for the colouration of fabric on fibre level. This process requires the addition of colourant in the molten state of polymer before extrusion of filaments. By using this process, solid colour can be easily achieved but the different shade percentages of the same colour family are difficult to achieve. Exceptional colour fastness properties can achieve by dope dyeing method. [26]

Different studies have been carried on fibre level dyeing which further can be used for nonwovens manufacturing. Different colouration methods which can be applied are named as a continuous method, dope dyeing method and batch dyeing method. Mostly fibre dyeing is the main focus of industrialist for the nonwoven fabrication and pigments or dyes are added on the molten state of the polymer prior to extrusion.

Study of the many researchers' shows that pigment application is the most versatile method for colouration of nonwovens with the help of binder application. But the uniformity of the applied pigments is very important during drying and curing and still further working is required to control non-uniformity. This problem can be minimized by using a better selection of chemicals, antimigrants and proper control of drying conditions. [29]

Nonwoven fabric can also be dyed by using conventional methods either by continuous method or batch dyeing process. Selection of these processes depends upon the selection of the raw material which needs to dye. Dyeing of self-shade is easier in comparison to multiple colours. The continuous process of dyeing involves high tension during dyeing because fabric movement is totally dependent on the drives of guide roller for openly fabric movement from one bath to other.

To bear this high tension subsequent strength of the fabric required which is not normally possible in nonwovens. Nonwovens have less strength as compare to woven and knitted. So the application of colour through continuous method is very complex and has maximum chances of fabric degradation. Batch dyeing process involves less tension during the dyeing process and has multiple machine wise options having different methodologies of fabric and liquor movement. Availability of multiple options, this methodology can be applied for the dyeing nonwovens and can be explored with respect to bulk dyeing feasibility and machine settings. [29]

2.1.5 Multi-layer nonwovens

Joining of two or more than two pre-formed webs or the application of scrims or films on nonwovens fabric is an important process (as shown in figure 2.14) and impart some extra

mechanical and other functional properties as per the requirement. Multi-layer nonwovens consist of one nonwovens layer and the others can be nonwoven or woven and knitted. This process is normally applied to improve barrier properties, surface properties, dimensional stability and other mechanical properties.

Adhesion property or resin is required to permanently join the laminates. Ultimate bonding between laminates is achieved by applying heat and pressure. Lamination can be wet or dry. In wet lamination, the adhesives are applied from a solvent or water dispersion and the adhesive is commonly applied to one substrate. Application is by spraying, slop padding, knife coating or spreading and printing, depending on the solvent system used, application level and surface penetration required. [26]

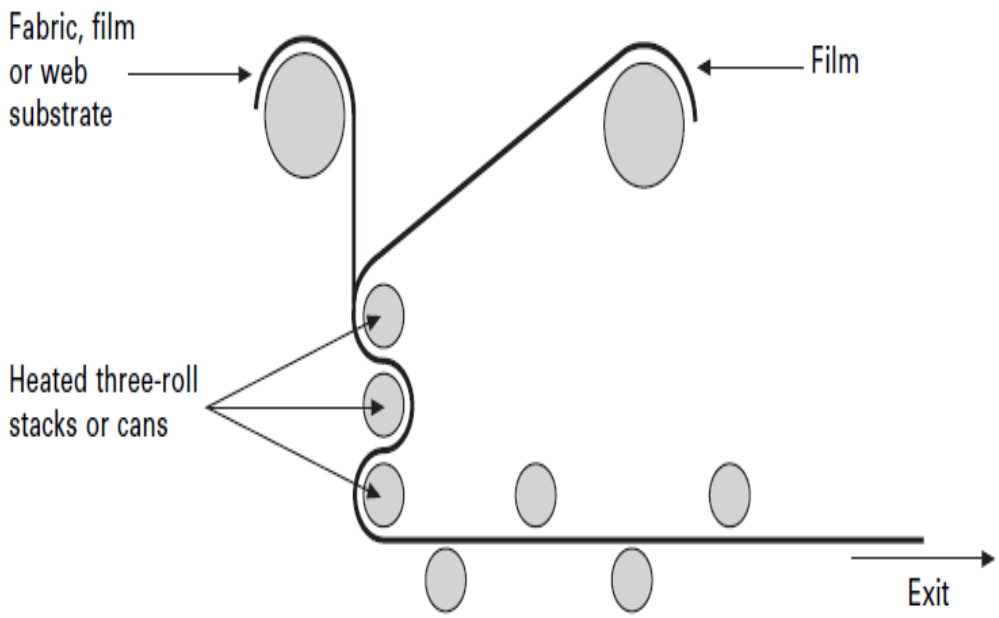

Figure 2.14. Calendering lamination process of nonwovens web substrate [30]

2.1.6 Application of nonwovens

Depending upon the fibre types, fibre orientation and bonding methodology, nonwovens have multiple applications with increasing demand all over the world. Nonwovens have wide range of applications. [31]

- Filtration products
- Roofing substrates
- Shoe lining felts
- Synthetic blankets
- Tennis court surface
- Space shuttle exterior tiles
- Insulators
- Auto trunk liners
- Primary carpet backing
- Wall covering
- Synthetic leather
- Tennis ball covers
- Shoulder padding
- Ceramic insulations
- Different colour composites
- Kevlar bullet proof vests
- Interlining of carpets under lay pads
- Geotextiles

2.2 Respiratory Filters

Human health is getting some serious effects due to the increasing trend of air pollution day by day. A major quantity of population is facing symptoms of asthma, nausea, skin irritation, high blood pressure, cancer and birth defects across the globe due to air pollution. Air filtration technology is very effective to control the pollution issue for the protection of different types of disease [32]. The respiratory filter is a type of protective clothing which is useful to protect the wearer from the inhalation of hazardous substances like airborne particles, dust, mist and pathogens etc. There are many types of filters available for the respiratory protection on the basis of specified functionality. Selection of right respirator for the required job is the most important for better protection efficiency. [33]

According to the different sizes of the air pollutants, particulate matter (PM) filter is divided into three categories, PM 10, PM 2.5 and PM 0.1 respectively. PM 10 provides protection against air particulates ranges from 2.5 µm to 10 µm while PM 2.5 is effective against 0.1 µm to 2.5 µm air particles. PM 0.1 is the finest type of respiratory filters having maximum protection efficiency against fine particulates raging below than 0.1 µm. [32] According to the title 30 CFR 11 (30 code of regulation, part 11), HEPA (High efficiency particulate air), dust-mist (DM) and dust-fume-mist (DFM) air respirators are certified and approved for the protection of air pollution before 1995. Due to replacement of code of regulation from 30CFR 11 to 42 CFR 84, it is decided that NIOSH approved authorities will not use these air filters (DM, DFM and HEPA) because the efficiency level of these filters is not up to the mark as NIOSH required. After those new filters under the NIOSH classification N, R and P series were developed and standardised on the basis of filtration performance. [34]

N, R and P series of NIOSH certified filters are further classified into nine categories according to the level of protection efficiency. Each series contains three protection levels: 95%, 99% and 99.97% respectively. Filters of N series are specialized to use for those environmental aerosols having no oil contents while R series filters can be used for the aerosols of oil mists but is limited to use for one work shift only. Filters of P series can be used for more than one work shift protection from oil mists. [33] The performance factor of the respiratory filter is very important and based on filtration efficiency, penetration, pressure drop and quality factor. Air filtration efficiency of the filter is dependent on the air resistance, minimum efficiency reporting value (MERV) and most penetrating particle size (MPPS). MPPS is a size range of particles which are not being blocked by the filter during characterization. It is very important to maintain the correct balance between the breathing efficiency and pressure drop of the filter during the development otherwise it will be difficult to use for the worker. Normally, high filtration efficiency can cause to raise pressure drop of the filter. So, it is mandatory to keep the pressure drop value below than 147 Pa during the development. Mathematical formulas of the technical characterization terms are given below in Equation 2.1, 2.2, 2.3 and 2.4. [32]

$$\eta = \frac{n2-n1}{n2} \qquad \text{(Equation 2.1)}$$

$$P = 1 - \eta \qquad \text{(Equation 2.2)}$$

$$\Delta P = P1 - P2 \qquad \text{(Equation 2.3)}$$

$$Q = \frac{-\ln(1-\eta)}{\Delta P} \qquad \text{(Equation 2.4)}$$

In the above picture η is filtration efficiency while n1 and n2 are the aerosol concentration on downstream and upstream of the filter respectively. P is showing the fractional aerosol penetration while **ΔP** is pressure drop. P1 and P2 are expressed as upstream and downstream air pressure respectively while Q denotes the overall quality factor of the filter. [32] The Capturing mechanism of the filter is also very important for protection efficiency. The Capturing mechanism is totally dependent on the nature of pollutants and the material of the filter. The whole filtration mechanism is categorized in diffusion, interception, intermolecular interaction, straining, inertial impaction, gravitation, and electrostatic interaction of the particle on the substrate. [35] The demonstration of the capturing mechanism is shown in Figure 2.15. From all these mechanisms, diffusion and interception is very important with respect to filtration protection efficiency. Particles having a diameter below than 500 nm can be captured or diffused by Brownian diffusion due to their random motion. [36]

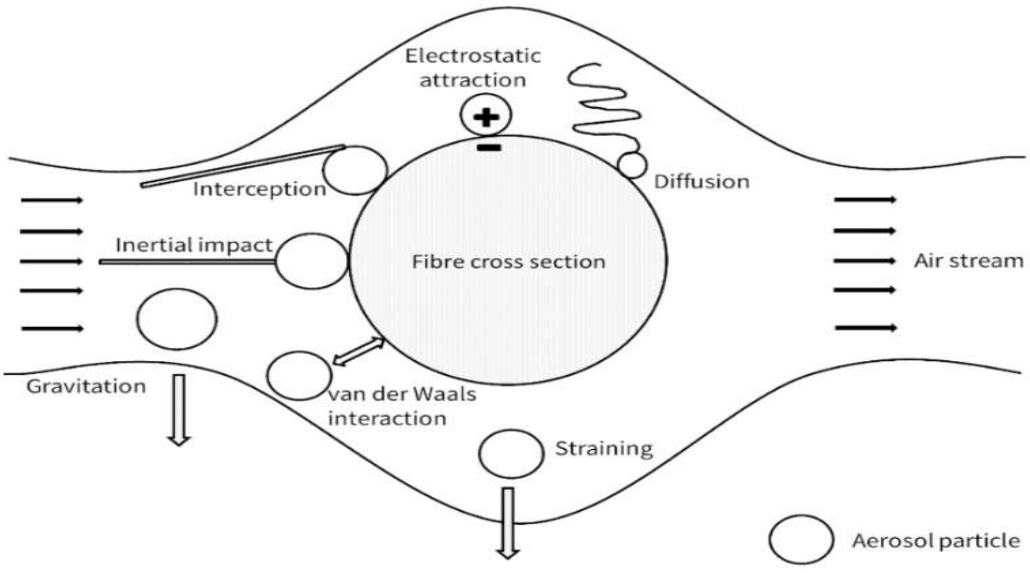

Figure 2.15. Filter capturing mechanism demonstration [32]

There are two basic capturing mechanism based on the trapping action of the filter names as physio-sorption and chemisorption. Capturing of fine particulates with the help of higher surface area and intermolecular attraction due to van der waal forces, termed as physio-sorption. In the chemisorption mechanism, pollutants are blocked or purified with the help of catalytic or non-catalytic reaction of the polymeric filter. This type of mechanism required some type of surface activation and fibre surface modification to improve the surface chemistry which can interact chemically with the pollutants. This type of filtration required targeted pollutants to block effectively. [37]

Wake et al (1997) investigated the bacterial filtration efficiency of performance filters. Half mask, fullface piece, nuisance dust mask, surgical mask, resuscitation mask, and filtering face piece were investigated made of glass fibre, resin wool and polyester materials. These filters were examined against pseudomonas alcaligenes (0.5µm diameter, 2-3µm length), mycobacterium tuberculosis (TB) (0.3-0.6µm diameter, 1-4µm length) and micrococcus luteus (0.9-1.8µm diameter) for the biological tests. NaCl particles (0.6µm diameter) and monodisperse urea (1.5, 3, 5, 7, 9µm diameter) were used for non-biological filtration efficiency test. Bacterial efficiency and non-biological particles efficiency were good in all types of masks except surgical mask and a nuisance dust mask. The pressure drop value was higher in all other types of masks except surgical facemask and a nuisance dust mask. [38]

Qian et al (1998) investigated the filtration performance of multi-layer polypropylene made N95 respirator by using poly-disperse NaCl, monodisperse polystyrene latex (PSL), and two gram negative bacterial species (bacillus subtilis & bacillus megatherium). The result showed that filtration performance against 100nm to 300nm particles was 95% and remained even better against 750nm particles. In addition, filter showed 99.5% filtration efficiency against bacterial aerosols. [39]

Balazy et al (2006) studied the protection efficiency level of polypropylene-based N95 filter and surgical facemask against MS2 virus (a non-harmful pathogen) by using air flow rate 85 l/min. Both filters were comprised of multi-layer assembly. The results showed that filtration efficiency of both N95 filters were 4.5 % and 5.6 % having the most penetrating particle size (MPPS) 40-50nm. Two surgical masks showed 20.5% and 84.5% protection efficiency with an 80nm MPPS which was very low in comparison to N95. [40]

Balazy et al (2006) evaluated the performance of two N95 multi-layer filtering facepiece respirator by using the nanoparticle-based aerosols (diameter 10nm to 600nm). The Manikin was used to fix the filter before the evaluation and surface of both filters were electrically charged. The results revealed that respirator showed better filtration efficiency ranges from 1.5% to 5 % particle penetration on two different airflows, 30 l/min and 85 l/min respectively. Respirator B showed 3% to 6% particle penetration on the same two flow rates as like respirator A. MPPS particle size ranged from 20nm to 100nm for both respirators. The difference between the filtration efficiency of these two filters was based on surface densities because the respirator had higher surface density as compared to respirator B. [41]

Eninger et al (2008) investigated the performance of PP based N95 and N95 facepiece respirators against ultrafine nanoparticles (NaCl) and viral species (Bacillus subtilis virus and Enterbacteriphage T4) on three different flow rates 30 l/min, 85 l/min, and 150 l/min respectively. The results explained that particle penetration increased in all types of filters by changing the flow rates on a higher level. Filtration efficiency was better at a 30 l/min flow rate and become worse on 150 l/min in all respirators. [42]

Eshbaugh et al (2008) analysed the filtration efficiency of PP based N95 and P100 under high and constant flow rate, by using NaCl and dioctyl phthalate (DOP) aerosols having a diameter range from 20nm to 2900nm. Mean inhalation flow rate and peak inhalation flow rate were 85

l/min to 270 l/min and 130 l/min to 430 l/min respectively. Results explained that penetration of the aerosols increased and filtration efficiency decreased by increasing the flow rate. MPPS also decreased to 50nm for N95 and 50nm to 200nm for P100 by increasing the inhalation flow rate. Conclusively, air flow rate has a strong inverse impact on filtration efficiency. [43]

Rengasamy et al (2009) examined the performance of NIOSH certified filtering facepiece respirators (N95, P100, FFP1 and FFP2) against MAT 1 silver nanoparticles (4nm-20nm) and NaCl based nanoparticles (20nm to 1000nm) by using an air flow rate 85 l/min. All the filters were made of polypropylene layers and had an electrically charged surface. Results explained that electrically charged surface filters showed most penetrating particle size (MPPS) between 30nm to 60nm and it remained between 200nm to 300nm for mechanical filters. Conclusively, the electrically charged surface showed better filtration efficiency and MPPS shifted below in terms of particle size. [44]

Shaffer and Rengasamy (2009) reviewed the performance of NIOSH certified filters against airborne nanoparticles. The review summarised that the protection performance of electrically charged surface is much better than the mechanical filter and most penetrating particle size (MPPS) shifted below to finer size. MPPS remained between 200nm to 300nm against mechanical filter while shifted below between 30nm to 100nm for an electrically charged filter. Improvement in filtration efficiency is attributed to the surface activeness of the charged filter which enhanced the capturing mechanism of the filter. [45]

Mostofi et al (2010) reviewed the performance of mechanical filters against nanoparticles to identify the limitation and further research improvements. The review summarised that MPPS reduction of electret filter is due to the Brownian motion of the fine particulates and notified between 30nm to 70nm by the researchers. Face velocity or air flow rate is inversely proportional to the filtration efficiency because the interception mechanism increases on higher

flow rates. The researcher emphasized improving and standardizes the filtration efficiency against MPPS to avoid the inhalation of fine particulate. Protection against aerosols on higher flow rates is also a limitation of research which needs the attention of the researchers for future work. [46]

Grinshpun et al (2009) investigated the filtration performance of N95 and surgical facemask during human breathing mechanisms. N95 filters were electrically charged and examined against 50nm to 1000nm particles like surgical facemask. Results showed that the filtration efficiency of the N95 filter was better than surgical facemask and face seal leakage of the N95 filter was more sensitive in comparison to the surgical facemask. Face seal leakage of the filter was higher during head movement from side to side and up and down. MPPS of the N95 filter was 59nm. In a conclusion, the researcher suggested focusing on the new development of the filter with better face fir properties to avoid leakage. [47]

Borkow et al (2010) investigated the viral protection efficiency of the four layers filter which contains 2.2% and 2 % copper oxide particles in the first two layers respectively. Protection efficiency was evaluated against 100nm to 500nm particles, virus H1N1 and H9N2 and staphylococcus aureus. Results explained that the filter showed a reduction in viral penetration, which can cause influenza while the bacterial filtration efficiency of the filter was 98.2% and 98.7 % respectively. Overall average filtration efficiency against latex polymer aerosol remained 93.54 %. The risk of skin irritation and inflammation of the filter due to copper oxide impregnation was also very low. [48]

Liu et al (2019) reported the filtration performance of five different baghouse filters against ultra-low emission. However, the objective of the research was to analyse the effect of pore size and fibre diameter on the filtration performance by using static and dynamic filtration tests. Filtration performance of all five filter samples was investigated by using 1.5µm average dust

particle diameter. Results illustrated that smaller pore size and diameter showed comparatively higher filtration efficiency. Furthermore, dynamic filtration performance results showed that smaller pore size filters were more effective against the irreversible blockage of dust particles inside membrane microspores. Therefore, higher filtration efficiency and a more stable dynamic filtration process were achieved by using small pore size filter media. [49]

According to a detailed literature review of respiratory filter, it is concluded that available respiratory filters and masks showed maximum filtration efficiency from 95% to 99% against 300nm and above diameter range particles. However, a surgical mask can only provide protection against 3µm and above particle diameters [50]. Therefore, there is an urgent need to investigate the performance of respiratory filters against below 300nm particle aerosols. Furthermore, a combination of higher filtration performance and higher antibacterial efficiency also needs attention for the future research and development of respiratory filters to achieve specified filtration performance goals.

2.2.1 Nanofibrous Filters

Due to air pollution of fine particulates and pathogens in the environment, nanofibrous based filters are being produced with the help of nanotechnology. The electrospinning technique is very common for the production of nanofibres by using different types of polymers on the basis of functionality. These types of filtration media contain either one or more layers of nanofibres on the conventional fibre web which enable them to increase the surface area more effectively up to nano size level. Due to the higher surface of the filter media, it becomes possible to capture the pollutant having size ranges 100nm to 500nm. [52]

A lot of nanofibres based membranes have been developed by the researcher by using different types of polymers which are possible to electrospun for the fine fibre production [51]. With the help of electrospinning, we can achieve higher surface area ranges from 1 m^2/g to 35 m^2/g which has better functionality enrichment up to fibre level and, even pore size distribution with good interconnectivity and high filtration efficiency of the membrane. But, researchers are still working to optimize the process energy cost with a high production level. [52]

Ahn et al (2006) worked on the development of single layer nylon 6 based nanofibrous filter by using the electrospinning technique. The thickness of the developed nanofibrous filters was 50µm and 100 µm, while pore size remained 0.24 µm in both samples. Filtration performance was analysed against particles size 85nm to 2µm while face velocity value remained between 3cm/s to 10cm/s during testing. Results showed that the filtration efficiency of sample 1 was 99.96% while the pressure drop remained 60 mmAq. Filtration efficiency of sample 2 remained 99.993% with a pressure drop value 154 mmAq. Conclusively, filtration efficiency of the nanofibrous filter remained excellent but the pressure drop value was very high. [53]

Qin and Wang (2006) investigated the filtration property of nanofibre based filters. PVA Nanofibres were coated on the supporting layers of spunbond and meltblown layers of PP by using the electrospinning technique. The addition of nanofibres was ranging from 0.5 g/m^2 to 2.5 g/m^2 respectively on both types of supporting layers. Results concluded that 2.54 g/m^2 nanofibres addition on meltblown supporting layer showed 100% filtration performance while the pressure drop remained high up to 1500 Pa. Addition of 2.9 g/m^2 nanofibres on spunbonded supporting layer showed 95% filtration efficiency but the value of pressure drop was remained low up to 900 Pa. Overall optimised view with low pressure drop value (200-400 Pa), filtration efficiency of meltblown nanofibre the coated layer remained 90-95% in comparison to spunbonded nanofibre coated the layer which remained less efficient around 20-60%. [54]

Gopal et al (2006) developed nanofibrous single layer membranes of polyvinylidene flouride (PVDF) by using an electrospinning technique for the liquid filtration. The thickness of the filter was 300µm and pore size distribution remained 4 to 10.6µm. Polystyrene micro particles of 1, 5 and 10µm size were used for the evaluation in 500ppm solution form. Results showed that developed membranes filtration can filter 5-10 micron particles effectively. [55]

Podgorski et al (2006) studied the application of nanofibrous filters against filtration of most penetrating aerosols. In preliminary work, researchers developed single layer meltblown nanofibres with variable thickness ranges from 2.1 to 4.3mm and evaluated against particles of 10nm to 500nm size. Results revealed that increasing the thickness of the filter by adding more nanofibres enhanced the filtration efficiency but pressure drop also increased which ultimately decreased the quality factor of the filter. After the preliminary work, researchers developed a multi-layer structure of the filter with single nanofibre layers. Evaluation of these multi-layer filters showed better performance in terms of filtration and pressure drop. The Overall quality factor of the filter was also improved from the previous preliminary work. [56]

Barhate et al (2006) studied the characterization of polyacrynitrile based nanofibrous filtration membranes developed by using the electrospinning technique. The thickness of the membranes remained 81-179 micron and porosity was 91.63% to 97.15%. Results showed that the produced nanofibre diameter remained 200nm. Researchers summarised that optimizing the collector distance and applied voltage, well porous and dried membranes of nanofibres can be achieved. 0.12m distance and 140000v/m were the best parameters for the development of PAN nanofibres. [57]

Gopal et al (2006) developed polysulfone-based nanofibrous membranes as a pre-filter application for the removal of particles from the liquid solution. The thickness and mean pore size diameter of the membranes were 135µm and 2.1µm respectively. Polystyrene-based

particulates of 0.1µm to 10µm were used in 100ppm solution for the evaluation of the filter membrane. Results showed that membranes filtration remained 99% against 7µm to 10µm particle size while the existence of permanent fouling was not prominent. During the evaluation, the membrane bubble point was observed at 4.6µm particulate size. [58]

Barhate and Ramakrishna (2007) reviewed the nanofibrous filter media to find out the current filtration problems and solutions for protection from tiny materials. The review summarised that the filtration efficiency of the nanofibrous filter can increase by using different types of surface modifications like ionic plasma coating of silver nano particles, physical coating, plasma treatment for free radical generation and chemical modification. Researchers also mentioned that different types of filters are being produced with enhanced properties like an antibacterial filter, ion exchange filter media, and multi-component filter media. [52]

Leung et al (2009) studied the effect of face velocity, thickness and packing density on the filtration performance of polyethylene oxide (PEO) based nanofibrous filtration media. PEO nanofibres were coated on the nonwoven sub-layer for the structural support. Results revealed that the filtration efficiency of the filter increased by increasing the weight and packing density of nanofibres and MPPS decreased slightly which showed better protection efficiency. But the pressure drop value of the filter increased which decreased the quality factor. In the case of thickness, filtration efficiency and MPPS size value improved slightly but the value of pressure drop remained high. Researchers concluded that the quality factor of the filter can improve by stacking the multiple nanofibre layers having fewer fibres with better porosity. [59]

Yun et al (2010) worked on the optimization of PAN and polymethylmethacrylate (PMMA) based nanofibre application in aerosol filtration. The characterization of the developed nanofibrous filter was done by using NaCl particles of 20nm to 300nm. Results illustrated that the pressure drop value increases by increasing the face velocity. Beaded nanofibres based

composite filter showed better filtration efficiency, especially against MPPS. The researcher concluded that enhancement for the quality factor was the improvement of volume fraction by the beads and PMMA particles in the nanofibre. [60]

Hung and Leung (2011) studied the behaviour of nanofibrous filters against the filtration of nano-aerosols. Filter media was consist of nylon 6 based nanofibrous coated nonwoven web with sufficient structural support. Filtration efficiency was examined by using NaCl aerosols having a diameter from 50nm to 500nm. Results illustrated that reduction of filtration efficiency observed by increasing the face velocity due to the increased diffusion phenomenon. The pressure drop of the filter was increased by reducing the nanofibres diameter in the resulting web. In the case of the base weight variable, filtration efficiency increased by increasing the weight of nanofibres but the quality factor was reduced due to higher pressure drop value. [61]

Sundarrajan et al (2013) studied the application of nanofibrous filter media for the protection against nano-aerosols. The researcher summarised that use of charcoal and glass fibres based filters can be replaced now with the application of nanofibre-based filters or functional nanofibre combination. By using electrospun nanofibrous membranes with conventional filters, we can improve the filtration efficiency for the removal of airborne, bacteria, and volatile organic compounds contaminations, which will ultimately contribute to reducing the pollution of breathing air as well as health issues related to asthma and lung disease. [62]

Wang et al (2014) studied the effectiveness of superamphiphobic nanofibrous membranes against airborne fine particulates. The nanofibrous membrane was made of fluorinated polyurethane modified PAN/PU composite nanofibres by the electrospinning process. The membrane was comprised of a multi-layer structure. Characterization was made by using NaCl aerosols having a size range 300nm to 500nm. Results revealed that the filtration efficiency

trend increased by increasing the base weight. The filtration efficiency was reduced against oil particulates while remained efficient against NaCl aerosols. The developed membrane showed superoleophobicity (151 degrees) and super hydrophobicity (154 degrees) with greater mechanical properties. [63]

According to the 3M technical data bulletin #171, face seal leakage is a very important factor for the development of nanotechnology-based respirator filter. Brownian diffusion is an important factor for capturing particles less than MPPS. Bulletin pointed out that electret media will reduce MPPS from mechanical media like the N95 filter, MPPS ranges between 40 to 100nm. According to the European standard (EN 149:2001+A1:2009), FFP2 has 94% efficiency while FFP3 has 99 % filtration efficiency. FFP3 (APF 20) generally used for precautionary measures and FFP3 (APF 40) preferably being used to protect airborne nanoparticles. The most updated measuring European standard for filtration performance is EN 529:2005. [64]

Kadam et al (2019) developed bilayer nanomembrane for the evaluation of low resistance respiratory filtration performance. Lightweight respiratory filter media was developed by using beaded electrospun nanofibres. The filtration performance of developed filter media was evaluated against particles from 0.3µm to 5µm diameter. Results illustrated that a mixture of beads and nanofibres altered the thickness, pore size distribution, and packing density of the developed filter. Furthermore, the filter sample having $0.5gm^{-2}$ stacking showed higher filtration performance as compared to commercial P2 type respirator. [36]

In conclusion, nanofibres are playing an important role in the field of air filtration by inducing higher surface area and barrier protection. However, nanofibres also has direct impact on the rise the pressure drop value which is also a very important in filtration characterisation. Therefore, mostly researchers developed nanofibres base membranes for water filtration and

air ventilation purpose where pressure drop value is not significant. However, researchers also developed respiratory filter base membrane, which significantly showed higher filtration performance up to 99% against nano-level aerosol particles but resulted in higher pressure drop value which creates difficulty in breathing for end users. Therefore, nanofibrous filter with higher filtration efficiency and optimised pressure drop value is still needs researchers' attention for commercial impact and localised application for end user.

2.3 Polypropylene (PP)

Polypropylene is a versatile polymer with respect to its worldwide application in the form of fibre and plastic. It has a linear chain of hydrocarbons, as like polyethylene. Both polypropylene and polyethylene called polyolefin. Polypropylene is categorized in thermoplastic polymer resins. Due to its chemical nature, PP has semi-rigid structure, good chemical resistance, good toughness, good fatigue resistance, integral hinge property, and good heat resistance. A table of PP physical and chemical properties is given below in Table 2.1. [65]

Table 2.1: Physical and chemical properties of PP [66] [67] [68]

Density	0.905 g/cm3
Tensile Strength	0.95-130 N/mm^2
Tensile Modulus	1-1.4 Gpa
Thermal Coefficient of expansion	100-150* 10^{-6}
Maximum Continuous Operating Temp	80 C
Weight	Low Weight
Moisture %	0.01-0.03
Resistance to Dilute Acids	Very Good
Resistance to Dilute Alkali	Very Good
Resistance to Oil and Greases	Moderate
Resistance to Alcohols	Very Good
Melt Temperature	210-290 C
Mould Temperature	20-60 C
Resistance to Cracking and Stress	Excellent

Methyl group presence in the chain is very important with respect to properties. Due to the location of substituents (methyl group), the chain configuration of polypropylene categorizes into the following three types shown in (Figure 2.16).

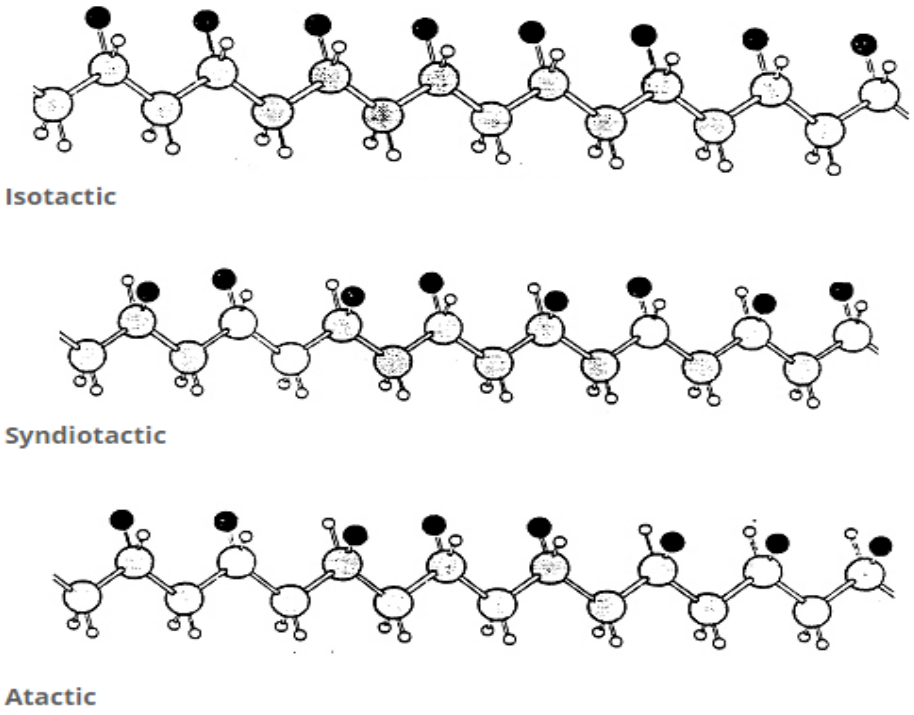

Figure 2.16: Isotactic, Syndriotactic and Atactic structure of PP [66]

Due to versatility and cost-effective properties, PP is being used worldwide in the manufacturing of plastic parts, carpeting (nonwoven) industry, in reusable product manufacturing, in paper binding, laboratory equipment and the most importantly in thermoplastic fibre reinforced composites. The high melting point of PP is also an advantage for the usage in food containers having the possibility of high temperature during microwave and dish washing process. PP can easily be dyed in different colours with the help of a dope dyeing technique. Due to its good mechanical properties and colouration possibility, PP is mostly being used for the manufacturing of carpets. Less specific weight, inexpensive availability, and non-toxic natures enable polypropylene for the usage in household products. PP is also being used in electrical products due to its low conductivity. [69]

Pure spunbonded polypropylene (PP) is being used for the production in barrier fabrics due to its lights weight and low price with a combination of good mechanical properties. It has very

low moisture regain and good resistance to mildew attack, which both are attractive properties for the filtration. Recycling of polypropylene is also an advantage for the usage in product manufacturing. [70] Annual production of PP is about 52.2 million tons worldwide while usage in Russia and Europe is 0.64 and 13.1 million tons respectively. Application area wise usage of polypropylene is given below in Figure 2.17.

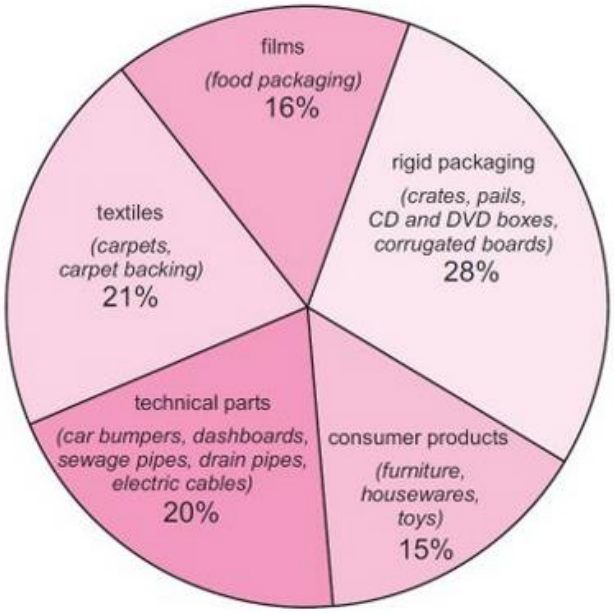

Figure 2.17: Division of percentage usage of Polypropylene [71]

2.3.1 Polypropylene base Filters

Polypropylene is being used in filtration applications worldwide. Spunbonded and melt-blown layers of PP (Figure 2.18) are considered as an important base for both gas and liquid filtration products. Due to the hydrophobicity and compatibility of PP with a variety of chemicals, it is beneficial for the filtration of non-aqueous chemicals and some solvents. Hydrophobicity of PP material is desirable for the usage in process air and liquids purification. Pleated depth of

the PP filter is very important during filtration because the pleated surface provides a high surface area with maximum range of pore size, that's why these deigns of filters are very important in the field of pharmaceutical, electrical, food and beverage filtration [72].

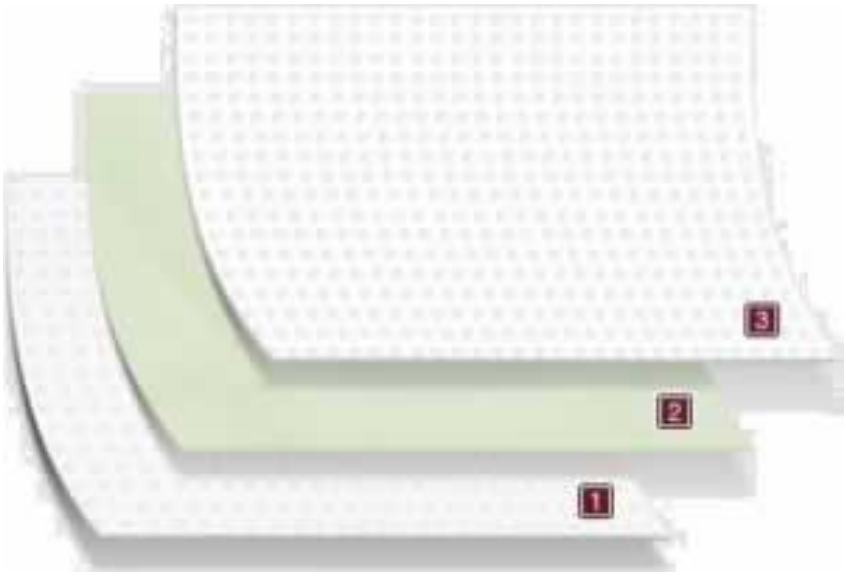

Figure 2.18: Polypropylene based filter layers [73]

Meltblown and Nano-spun technology-based PP filters provide protection to nano size particulate cost-effectively. Single-layer and multi-layers of PP are being produced by using both spunbonding and melt-blown techniques. Spunbonding technique produces coarse fibres as compare to meltblown that why the capturing mechanism of spunbonded PP filters is limited to large particle due to bigger pore size while melt-blown produces fine fibre due to the attenuation and drafting of the extruded filament by blown hot air. Multi-layer filters containing both spunbonded and meltblown layers are very effective for the filtration for large as well as fine particulates. The upper spunbonded layer blocks the bigger particles while the inner melt-blown layer provides protection against fine particulates due to finer pore size and higher surface area. [74]

Polypropylene has better chemical compatibility and pH tolerance which leads PP filter to provide better protection against non-aqueous chemical samples. It is very easy to sterilize and re-use PP based filters due to its good thermal stability. [75] Spunbonded PP prefilters are also being used to provide for the retention and blockage of coarse dust particles outside with minimum pressure drop. PP prefilters have high dirt-holding capacity and better for the use of organic solvent prefiltration. [76] Different types of PP filter media available in the market like polypropylene felt, PP mesh and PP microfibre felt depending upon the purpose of use. [77]

As a conclusion, PP is the most common polymer which is being used in filtration application in the form of nonwoven fabrics. However, microfibres based multilayer respiratory filters can only produce by use PP due to its limitation for nanofibre production. Currently, PP based multilayer surgical mask and N95 mask are most commonly being used all across the world as an effective respiratory filter. However, combination of nanofibres and conventional PP nonwoven can further enhanced the filtration performance from nano-level aerosols, bacterial and viral protection. Moreover, selection of material having natural anti-bacterial properties for nanofibre production can play an important towards bacterial protection.

2.4 Chitosan

Chitosan is an abundantly occurring amino polysaccharide of cationic nature. Chitosan is based upon chitin. The structures of chitin and chitosan are shown in Figure 2.19. Both chitin and chitosan are found abundant in nature from a number of natural renewable sources. The main sources of chitin are skeletal materials of sea creatures, including crabs, prawns, lobsters, shrimps, and cephalopods. [78] [79]

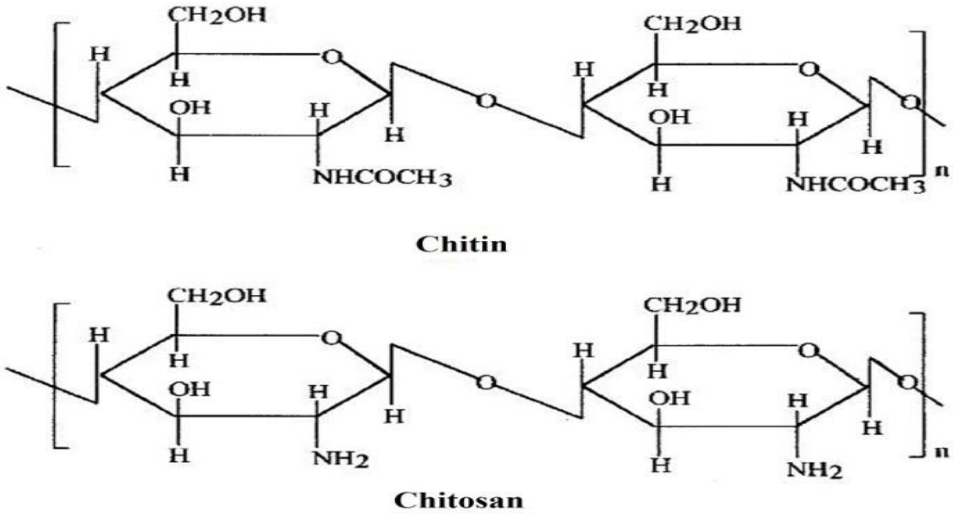

Figure 2.19: Structure of Chitin and Chitosan [80]

The chemical name of chitosan is 2-amino- 2-deoxy-b-D-glucopyranose and the molecular formula is (C6H11O4N)n. Chitosan is highly molecular and is composed mainly of monomers of β-(1,4) linked D-glucosamine and partly of β-(1, 4) linked N-acetyl-D-glucosamine. The ratio between D-glucosamine and N-acetyl-D-glucosamine is the degree of deacetylation. The acetylated units have typical degrees of deacetylation between 70 and 95% and molecular weights between 10 and 1,000 kDa [81] [82].

Chitosan is prepared by the deacetylation of chitin in a hot alkali solution (Figure 2.20). Chemically, chitin is poly-β-(1,4) linked-N-acetyl-D-glucosamine). When the C-2s of chitin's monomers substitute all or partial vinyl amine with amine groups then chitin becomes chitosan [82].

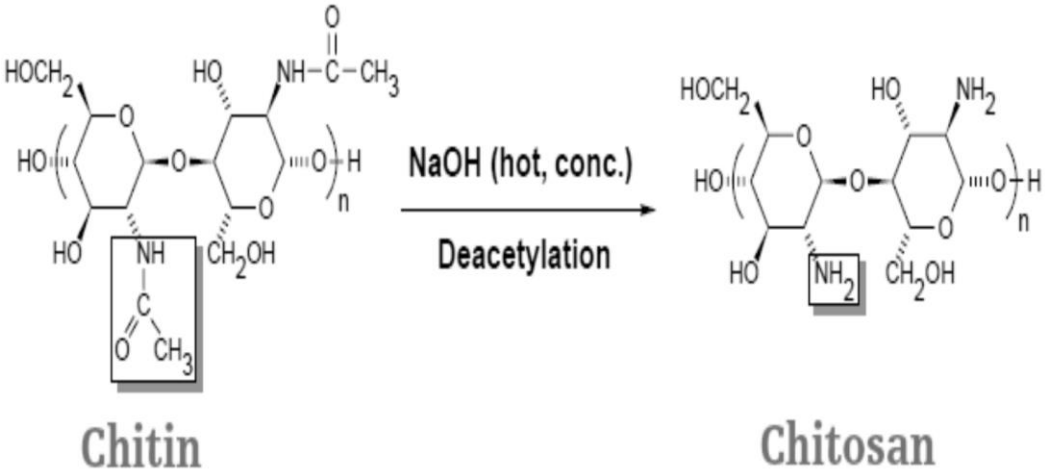

Figure 2.20: Conversion of Chitin into Chitosan [82]

Overall, chitosan consists of three kinds of reactive functional groups, an amino/acetamide group at C-2 position as well as both primary and secondary hydroxyl groups at C-6, and C-3 positions, respectively. These groups are mainly focused on when chemical modification of chitosan is done. [83][84] The cationic amino groups carried by the C2 position of the glucosamine units of chitosan are responsible for the formation of polyelectrolyte complexes with the anionic groups and different polyamines like carboxylic acids, alginate, xanthan gum, carrageenan, carboxymethyl cellulose, pectin, poly (L-lactide) etc. These complexes have various significant roles in biomedical applications. [85][86]

Chitosan is a semi-crystalline polymer with somehow organized polymer chains [87] which exhibit some rigidity and stiffness. It is also nontoxic, biodegradable, and biocompatible [88]–[90]. Various studies have shown that chitosan possesses anti-microbial effects against bacteria, fungi and viruses. [91], [92] Chitosan can be converted into fibre but it is costly. To cut the cost chitosan can be used by blending with other natural fibres and biomaterials. The blends of chitosan were reported with alginate, collagen, poly (ethylene oxide), starch, silk fibroin, poly (vinyl alcohol). [88]–[90]

To provide an antimicrobial agent for textiles, chitosan can be used as an additive when spinning antimicrobial fibres and also as a finishing agent for surface modification, mainly of cellulose, cellulose/poly- ester and wool fibres. Chitosan is positively charged and soluble in acidic to neutral solutions because the amino groups in chitosan have a pKa of ~6.5. Its antimicrobial function arises from its poly-cationic nature which is caused by protonation of the amino groups at the C-2 atoms of the glucosamine units; such antimicrobial function is a very similar to that determined for QAS (Quaternary Ammonium Salt). Positively charged amino groups can bind to the negatively charged bacterial surface, resulting in the disruption of the cell membrane and an increase in its permeability. [93]–[95]

Chitosan can also interact with the DNA of microorganisms to prevent protein synthesis. It is very effective to inhibit or kill gram-negative and gram-positive bacteria. [96] The antimicrobial efficiency of chitosan depends on its average molecular weight, degree of deacetylation and the ratio between protonated and un-protonated amino groups in the structure. It is believed that chitosan of low molecular weight is more active than chitosan oligomers for the antimicrobial property. The efficiency of chitosan also increases with increased deacetylation, which can exceed 90%. [93]

2.4.1 Chitosan based nanofibre and filters

Chitosan is being used all over the world due to the affordability, versatility, and anti-microbial activity. It has good defensive potential against the microbes, toxins, viruses and fungi etc. Chitosan is being used in food packaging to kill bacterial contaminations which enable the longer shelf life of the packed food. To get the high surface area with less weight, nanofibrous mats are being produced with the help of electrospinning which has applications not limited to tissue engineering, water filtration, wound dressings, control drug release, enzymatic

immobilization, and in the production of biosensors for the diagnostic studies. Nanofibres of chitosan are an effective material assembly for the specific biomedical application specifically due to its anti-microbial property. [97]

Due to the higher molecular weight and the viscosity of chitosan, it is very difficult to electrospun it into nanofibres. Low to medium molecular weight ranges between 50 kg/mole to 570 kg/mole is effective in the production of nanofibres. To improve its spin ability, the addition of co-spinning polymers gelatin or collagen, silk fibroin, polycaprolactone, poly (vinyl alcohol) PVA and mainly with poly (ethylene oxide) PEO is reported by many researchers. During the electrospinning, the concentration of chitosan is also very important because it is directly related to the viscosity of the polymer. The electrospun-able concentration of chitosan ranges between 2% to 5% because, beyond this, the viscosity of the polymers becomes too high, which is difficult to electrospun. [98]

Application of chitosan in filtration application is increasing day by day due to its biocompatibility, good electrospun possibility, better porosity and excellent anti-bacterial properties. A lot of study has been carried to produce the chitosan base membranes for water and air filtration having inherent anti-microbial property. Detailed literature review of chitosan-based nanofibre production and its application in filtration media is given below.

Geng et al (2005) studied the electrospinning possibility by using concentrated acetic acid for the development of nanofibres. The researcher performed the experiment by using various molecular weight ranges of chitosan on different concentrations of acetic acid. Results revealed that 7% chitosan (106000 g/mol) solution in 90% acetic acid produced best beads free fibres on a 4kv/cm electric field. The researcher summarised that increase in the electric field produced fine nanofibres with a possibility of beads formation. So, optimization of parameters is very important and these can differ depending upon the material characteristics. [99]

Jung et al (2006) developed a nanofibrous mat of PET/chitosan by using an electrospinning technique for the biomedical application. PET/chitosan nanofibres were produced on the surface of the PET nonwoven sub-layer and examined against bacterial species for the antibacterial property. Results revealed that fibre diameter was in the range of 500nm to 800nm and produced mat which showed better protection properties as compared to PET only nanofibres which can be beneficial towards better tissue compatibility. [100]

Zhang et al (2007) developed chitosan based nanofibres by using the ultra-high molecular weight polyethylene oxide (UHMWPEO) solution system. PEO is an excellent nanofibre forming agent which was added to form smooth fibre production of chitosan. Results revealed that excellent fibre formation was observed with beads free surface. Researchers concluded that chitosan-based large scale production of nanofibrous structure can easily fabricate by using PEO co-spinning agent for biomedical application. [101]

Homayoni et al (2009) worked for the optimization of pure chitosan nanofibres by using electrospinning technique. Due to high viscosity, electrospinning of pure chitosan seems impossible. To overcome this issue, chitosan hydrolysed for the reduction of molecular weight and its viscosity by alkali treatment for up to 48 hours. After alkali treatment, solution of chitosan was prepared by using different concentration of acetic acid (solvent). Results revealed that the concentration of acetic acid has inverse relation with fibre diameter. Developed nanofibres showed diameter remained around 140nm averagely. After the development of nanofibres, FTIR characterization explained that alkali treatment and the spinning process did not affect the chemical composition of chitosan while moisture regains property was improved 74% from the untreated sample. [102]

Cooper et al (2014) worked on the development of chitosan-based antibacterial membranes for the filtration application. In the field of water filtration, it is a big challenge to remove bacterial

contamination without using any types of chemicals which may create some hazardous by-products in water. Due to the biocompatibility of the chitosan, nanofibrous membranes were developed by using polycaprolactone (PCL) as a co-spinning agent. Results revealed that developed nanofibres showed better particle filtration as well as reduced the adhesion of staphylococcus aureus. A diameter of the developed nanofibres was in the range of 200nm-400nm and resultant membranes also showed better structural stability against high water flux. [103]

Arkoun et al (2017) worked on the development of chitosan-based nanofibre for the construction of bacterial protected membrane by using electrospinning. PEO was used with 10% to 30% during the development of nanofibrous membranes as a co-spinning agent with chitosan. Characterization of the membrane was made by using bacterial species, Escherichia coli, salmonella typhimurium, staphylococcus aureus and listeria innocua bacteria as a baseline. Results revealed that membrane showed good antibacterial property against the applied species. On the basis of antibacterial property, researchers suggested that these types of membranes can be used as a perforator in food packaging material, which can increase the shelf life of stored food by reducing the bacterial attack possibility. [104]

Maslakci et al (2017) worked for the inhibition of biofilm formation of Pseudomonas aeruginosa PA01, by using plasma surface modified chitosan-based nanofibre derivatives. Produced nanofibre combinations were chitosan-thiophene, chitosan-furan and chitosan-3,4-ethylenedioxythiophene. All these nanofibres were surface modified by using plasma treatment. FTIR characterization confirmed that chitosan surface was covered by applied derivatives thiophene, furan and 3,4-ethylenedioxythiophene respectively. After the development, these nanofibres were examined against Pseudomonas aeruginosa PA01 bacterial specie for the evaluation of biofilm formation. Results revealed that developed chitosan-based

nanofibres showed good bacterial protection efficiency and inhibited the film formation of Pseudomonas aeruginosa PA01. [105]

2.5 Electrospinning process

Electrospinning is an effective process for the production of nanofibres by using synthetic polymers and natural polymers as well as ceramics and metals. This technology is a combination of electrospray and solution dry spinning. [106] In the electrospinning process, high voltage is applied between the needle tip of the polymer containing a syringe and the collector, which induced the charge in the polymer solution. Induced charge in the polymer enables the deformation of the spherical droplet shape of the polymer to a conical shape. When the electrostatic repulsion force value increases from the value of polymer surface tension, a charged fine polymer jet ejects from the Taylor cone and collected on the opposite pole of the electric field. During the traveling distance from the tip to the collector, the solvent evaporates due to the bending and stretch of the polymer. [99]

According to the basic principle, electrospinning setup consists of three main parts, a high voltage source, a syringe based spinneret for the polymer feeding having a metallic needle tip, and a collector which should be a grounded conductor. In the first step of the operating the procedure, fill the polymer solution in the syringe it on the machine by providing basic machine settings like the volume of the solution, flow rate, and syringe diameter etc. After these initial settings, high voltage (10-50 KV) is applied between the tip of the syringe and collector.

The extrusion mechanism of the polymer is totally dependent between the electrostatic repulsion and surface tension of the polymer. After the high voltage application, the polymer starts getting charge and electrostatic repulsion generates on the polymer. When the

electrostatic repulsion forces overcome the surface tension of the polymer, then the polymer droplet spherical shape changes into the conical shape named Taylor cone and the charged polymer ejects from the Taylor cone to the grounded collector. Due to the stretch and bending between the eject mechanism of the polymer, it becomes narrower and solidify due to solvent evaporation and resulted in a nanometre range fibres on the collector surface. [107] A schematic diagram of the electrospinning process is given below in Figure 2.21.

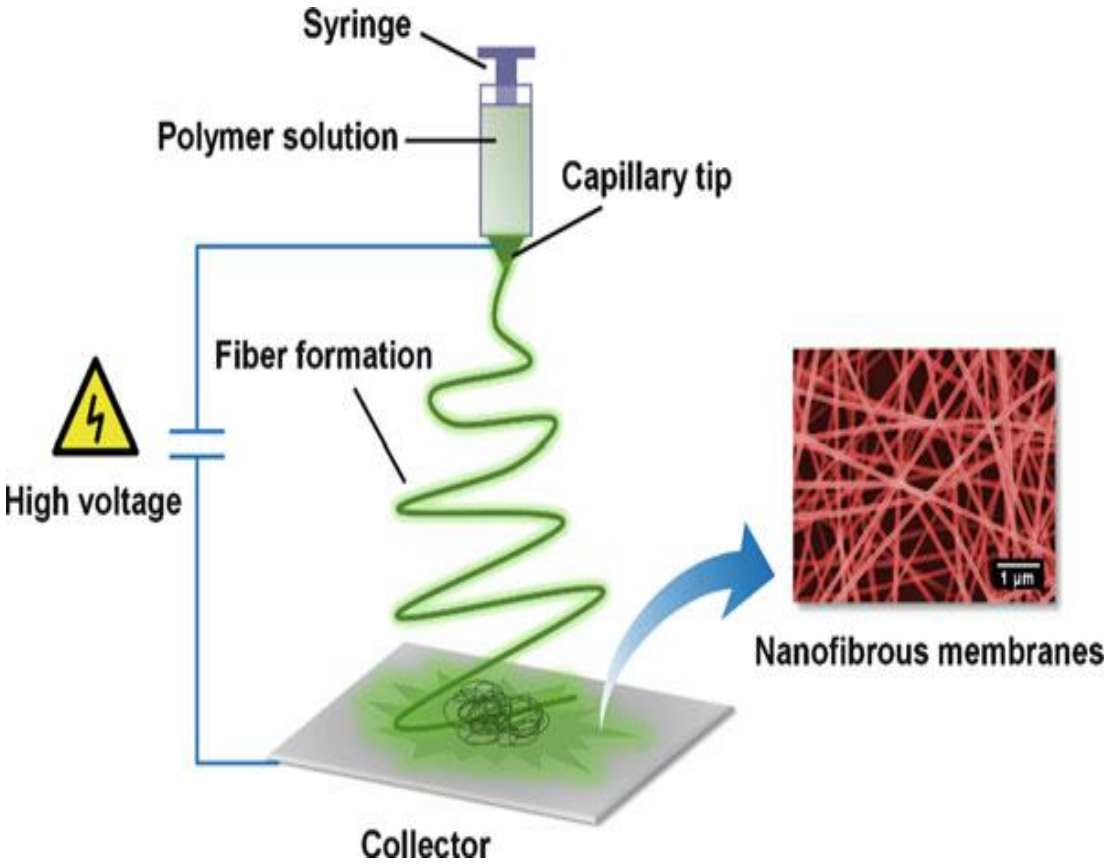

Figure 2.21: Schematic diagram of electrospinning process [108]

During the electrospinning, some parameters are very important to consider with respect to fibre formation like polymer chemistry, the viscosity of the polymer, molecular weight, surface tension, and conductivity. In addition to these polymer parameters, optimization of

electrospinning parameters is also very important for the collection of beads free nanofibres because voltage, flow rate, a needle gauge, and collector distance also vary from polymer to polymer. [51]

2.6 Plasma Surface Modification

Plasma treatment is an efficient way of surface modification for the polymers which helps the inert polymers to interact with different compounds for the secondary manufacturing application. During plasma generation, a specific electric field is applied to the known gas source for the generation of free energized positive and negative electrons, photons, and radicals for the collision with the targeted surface of the polymers. [109] Surface modification results of the polymer are totally dependent on the reaction of the exposed surface and processed gas generated plasma. This technique is very famous for surface cleaning, etching, coating, and activation properties. This process is cost-effective and environmently friendly way of surface modification. [110]

Atmospheric pressure plasma, low-pressure plasma and high-pressure plasma are three different types of plasma surface modification. Atmospheric pressure plasma treatment is the most common and cost effective way for the surface modification due to its simple application in normal atmospheric pressure but the uniformity of the application is a challenging role and difficult to achieve. High-pressure plasma is not suitable for the polymers due to its high intensity, expensive application, and damaging nature. While low pressure plasma is also being used widely for the industrial application due to its homogeneous application on the surface morphology. Low-pressure plasma required a separate vacuum chamber for the operation

which makes it a bit expensive from the atmospheric plasma treatment. [111] Schematic diagram of low pressure plasma treatment is shown in Figure 2.22.

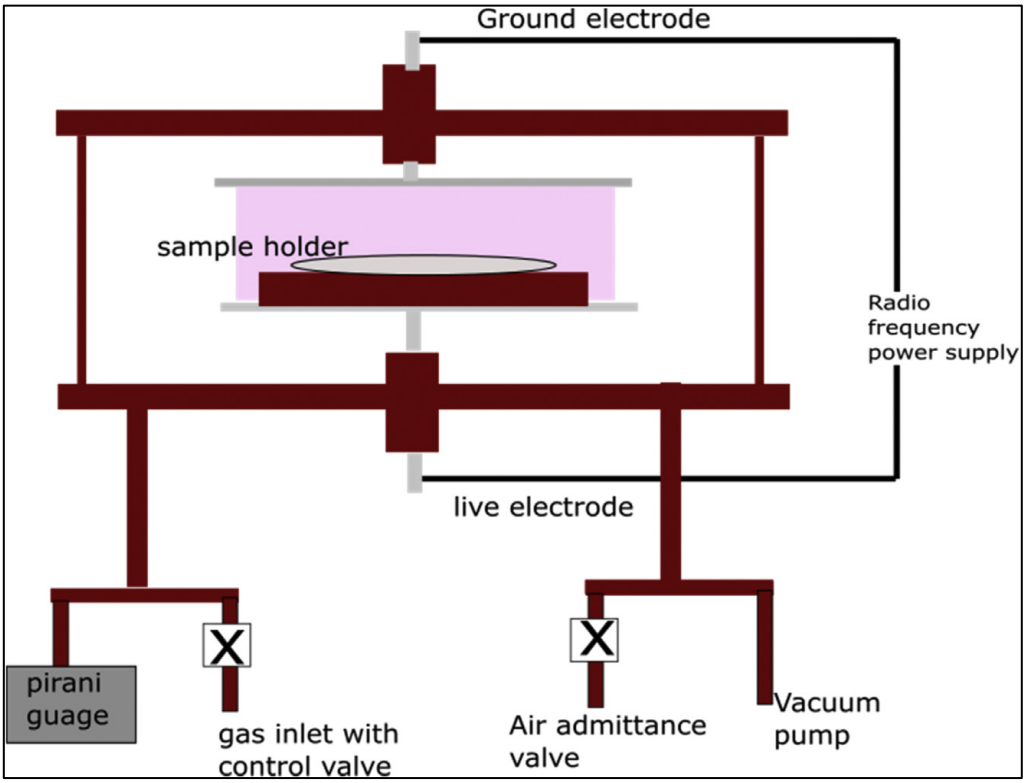

Figure 2.22: Low pressure plasma treatment setup [112]

Low pressure (LP) plasma techniques are non-thermodynamic-equilibrium processes which modify the surface chemistry of any solid polymer compound with the help of ionized gas items under low vacuum condition ranger from 10^{-3} - 1 Torr. With the help of low pressure plasma, a range of properties can achieve regarding chemical composition and surface morphology of the polymers such as wet stability, metal adhesion, dyeability, chemical inertness, lubricity, and biocompatibility. The biocompatibility of the polymer is very beneficial for the usage in medical applications. The source of the process gas is also very important for the plasma treatment process. A range of non-depositing (O2, N2, H2, NH3,

CO2, etc.) and inert (Ar, He) gases are being used in abundance as per the specification of the required functionality for the plasma generation. [113]

Conventional low-pressure plasma is operated under vacuum or low pressure ranges to a few Pa. Low pressure plasma treatment of polyolefin is implemented industrially for the required surface properties by reducing the inert nature of these polymers. The homogeneously treated surface is an advantage of low pressure plasma due to the vacuum chamber base operating procedure. [114]

2.7 Byssinosis

Byssinosis, being considered as environmental lung disease, is defined as a narrowing of the airways caused by inhaling cotton, flax, or hemp particles, which may cause wheezing and tightness in the chest. Basically, this disease is a type of occupational chronic obstructive pulmonary disease (COPD). Inhalation of cotton dust is a common problem in the working environment of the textile industry for employees while breathing. This type of condition is very dangerous for those people who are sensitive to cotton dust and can easily affect by asthma or byssinosis. [115]

Raw cotton contains some bacterial contamination from the crop level classified as gram-negative bacteria and their endotoxins. With the help of fine cotton dust, these bacteria and their endotoxins become the part of the working environment in the textile spinning mills, and transfer to the inhaler employee during work. After inhalation, these contaminations cause the tightening of airways and inflammation in the lungs with the help of bacterial endotoxins. [116]

Figure 2.23. Pictorial Explanation of Byssinosis [117]

At the start of this disease, worker feels symptoms of wheezing and tightness on the first working day after the rest, and symptoms start diminishes by time due to the repeated interactions of cotton dust. This process of irritation becomes disappears at the end of the workweek completely. By continuing this routine for several years, the worker will feel severity in wheezing and coughing up to two or three working days in a week and it can be prolonged to the whole week as well. The condition of this disease is totally dependent on the working environment of workers and workplace cotton dust exposure level. If the exposure to cotton dust is too high and persistent for many years then it can lead to the permanent disability of lung and ultimately can disable the person as well. [116] Preparatory processes of yarn manufacturing in textile spinning mills are very dusty and produce a lot of fine cotton dust that can be inhaled by employees. All men and women working in such departments (especially card room and blow room) are mostly interacted with cotton dust and more likely have chances to be affected by byssinosis. [118]

Identification of this disease can be done by three different medical tests named as chest x-ray, CT scan chest and Pulmonary function tests.. The pulmonary function test is the most common for the analysis and diagnosis of this disease. During the examination in the clinic, the doctor

may ask some questions about the symptoms and working conditions of the attendee and can also check the patient history for the analysis of severity [115]. With respect to the treatment point of view, doctors normally suggest some medicines to patients such as bronchodilators, which are effective to open lung airways for the short term solution. Physical exercise, breathing exercises, and patient awareness programs can also play an important role to reduce the risk. [1,2]

The Most effective way to cope with this disease is to control the dust level in the working environment by improving the functioning of the dust control mechanism of textile machines and by providing proper dust suction system on the work place with adequate ventilation. In addition to this, workplace personal protective equipment (PPE) or respiratory filter performance investigation and improvement can also play an important role to control the risk of Byssinosis.

Schilling et al (1955) carried out an epidemiological study on Byssinosis among Lancashire cotton workers. It was found that 60% of the cotton workers had symptoms of byssinosis characterized by the tightness of the chest and breathlessness on Mondays. 14% of cotton workers were seriously disabled (eight have since received disability pensions). The prevalence of byssinosis was inversely related to the distance of workers from the carding engines. Of all the employees in the 28 mills, 23% of the men and 33% of the women were exposed to the risk of developing disabling byssinosis. [118]

McKerrow et al (1958) studied the respiratory function during the day in cotton workers and studied the dust suppression effect on the fall of ventalitaory capacity of the workers, before and after installation and concluded that there is a pharmacologically pathogenic active component in the working environment of card-room which has strong relation with the fluctuation in ventilatory capacity. [119]

Bouhuys (1976) comprehensively review the possibilities of byssinosis in the textile industry. He reports that cotton dust contains some heat stable agents which are harmful to the lungs and water-soluble as well. According to the detailed study on US cotton workers and Spanish hemp workers, regular inhalation of cotton dust, due to work activities can disable the lungs permanently and it will be impossible to cure lungs at that stage. Review highlights the need to control the dust level in relevant dust causing industries e.g. cotton, hemp, and flax. It is concluded that still there is no adequate method to control this occupational chronic lung disease through a lot of studies have been conducted to obtain medical knowledge about this disease. In the end, the review emphasizes taking preventive measures for the control of Byssinosis effectively. [120]

Brown et al (1977) investigate the possibilities of byssinosis which is normally considered as the inhalation of cotton, flax, or soft hump dust in the textile workers. Research summarises that the contribution of external matter with the raw fibre has a strong influence while pure fibre is less likely can cause this disease. According to the research, it is very difficult to collect the waste having fine cotton dust ranging from 15µm to 20µm for the biological and chemical analysis in byssinosis research. The best way to take this respirable cotton dust is to collect it from air-cleaning system in the industrial mills. According to the results of two different mills card room analysis, the diameter of the respirable cotton dust ranged from 2.5µm to 20µm and chlorine contents are also found in the dust due to the residual of herbicides, pesticides or soil minerals. [121]

Fishwich et al (1994) investigated the effect of work environment symptoms and exposure of cotton dust on the workers of Lancashire mills for the byssinosis study. A Total 404 man-made fibre operative and 1408 cotton operative were selected and analysed for the outcome. Results showed that 3.7 % of people were founded affected by the byssinosis symptoms while

researchers correlated the severance of this disease with the interaction time period of the worker. [122]

Kobayashi et al (2004) investigated the inhalation effect of fine cotton dust on lung functioning. For this analysis, 66-year old man was selected having cotton dust exposure from the past 50 years. According to the chest CT scan, lung biopsy specimen analysis, and infrared spectrometry, it was summarized that patient has diffuse lung disease due to the excessive cotton inhalation but the clinical symptoms of the disease are totally different from byssinosis. [123]

In a comprehensive review on long term respiratory health effects in textile workers, Lai and Christiani (2013), Harvard School of Public Health, pointed out that over 60 million people worldwide work in the textile or clothing industry are exposed to the risk of chronic lung diseases, in particular, COPD in their workplaces, which could lead to the considerable potential cost. It was reported that the costs of occupational COPD from 2002 could be attributed to $5.0 billion for the USA annually. Animal models studies have suggested a shift in the lung macrophage: dendritic cell population as a potential mechanistic explanation for persistent inflammation in the lung due to repeated cotton dust related endotoxin exposure. Other types of textile dust, such as silk, may contribute to COPD in textile workers. They conclude that textile dust related obstructive lung disease has characteristics of both asthma and COPD. [124]

Fantahum et al investigated the type and frequency of the diseases in a textile mill of Bahir Dar, Northern Ethiopia in 1995/1996. The basic purpose of this research was to analyse the conditions of self-reported diseases by the workers for the health distribution estimation among the 394 workers by using a pretested questionnaires and professionally trained health staff. Results showed that 72 workers complained about more than one respiratory problem from the

spinning department only. On the basis of results, researchers suggested that the spinning department should take some steps like installation of hoods, dust filters, ventilators, and vacuum cleaners for the safety of the workers. [125]

Pnadey et al (2017) investigated the effect of cotton dust exposure and smoking habit on the lung function of textile workers of Varansi district, Uttar Pradesh, India. The textile sector is a larger employment provider in India due to the dependency of the large population with agriculture and its related industries. To analyse the previously mentioned study, 500 male weavers with 10-15 years of experience, were selected from different spinning outlets from Uttar Pradesh having an age range of 28-41 years having no lung related medical history. Some workers had a smoking history from 5-18 years. The investigation was made with the help of the peak expiratory flow rate (PEFR) test of workers. Results explained that workers from the spinning mills showed relatively low PEFR (lit/min) in comparison to the normal healthy workers while the effect of smoking was also significant. [126]

Mummadi et al (2017) studied the effect of cotton dust exposure on the respiratory related health of textile workers in Hydrabad, Telagana based factories. For the collection of data, a highly validated source (Medical Research Council (MRC) UK) base questionnaire was used. A Total population of 159 workers (men 9.4% and women 90.6), were selected for the analysis. Results elaborated that 3.8% of people were found affected by asthma, 2% pneumonia, 13.2% hypertension and 3.8% had diabetes. This report concluded that the duration of exposure to cotton dust is very significant and has a direct relation to the severity of the lung disease while suggested the textile factories to reduce the cotton dust level for a healthy environment. [127]

Anyfantis et al (2017) studied the effect of cotton dust exposure on the respiratory function of Greek textile cotton workers. For the experimental analysis, 256 workers from the cotton industry and 148 office workers were selected for the spirometry tests. Results showed that

textile workers had reported more affected by dyspnea and wheezing as compared to office workers. Cotton workers showed higher symptoms of respiratory problems in comparison to the control group while the most heavily impacted workers were related to the ginning industry. Researchers also concluded that the duration of exposure and work in the textile industry had a direct relation with the respiratory symptoms. [128]

2.7.1 Cotton Dust Endotoxin

In 1932, the home Office of Great Britain reported that cotton mills contain gram negative bacteria and their endotoxins which are very dangerous for the pulmonary function of the workers. Basically, these bacterial contaminations are originated from cotton leaves, cotton fibres and cotton dust from the crop level. During the process of yarn manufacturing, these contaminations become the part of mill and pollute the environment. During the breathing activity of the worker, there is a possibility of inhalation of these bacterial contaminations with the help of respirable dust. It was also reported that several workers from the mill found affected in pulmonary symptoms due to the short term and long term exposure of these contaminations which leads to the COPD and byssinosis. [129]

Gram negative bacteria species mostly found on agriculture dust, cotton leaves, bracts and fibres in large quantities. The Outer cell wall of these bacteria consists of endotoxins named as lipopolysaccrides (LPS). These endotoxins become the part of the human body with the inhalation of fine cotton dust from the mill environment. After inhalation, these bacterial endotoxins start pathogenic reactions in the lung airways and may cause inflammation in the lung tissues and airways. As a result of these reactions, the respiratory function of workers becomes less effective and may decrease the forced expiratory volume (FEV). These bacteria

found on different parts of the cotton plant particularly on the bract of the plant in a maximum quantity. [130] There are three types of rod shape gram negative bacteria which are normally found on the cotton. Names of these bacteria are *Enterobacter agglomerates, Pseudomonas syringae* and *Agrobacterium (spp.),* [129] while the *Enterobacter genus* is found in most abundance from all these. [130] Pictorial view of all prescribed species is given below in Figure 2.24.

(A) **(B)**

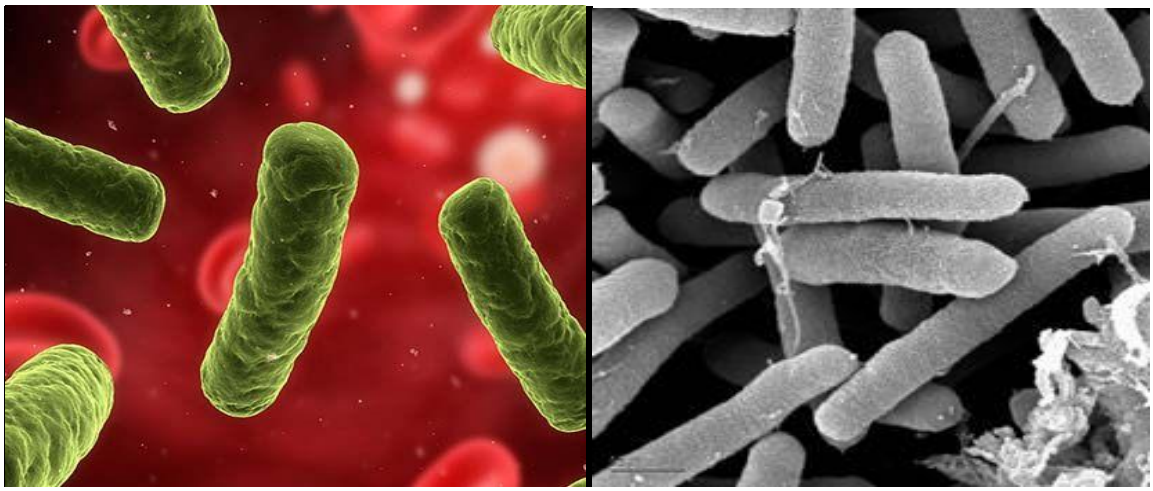

(C)

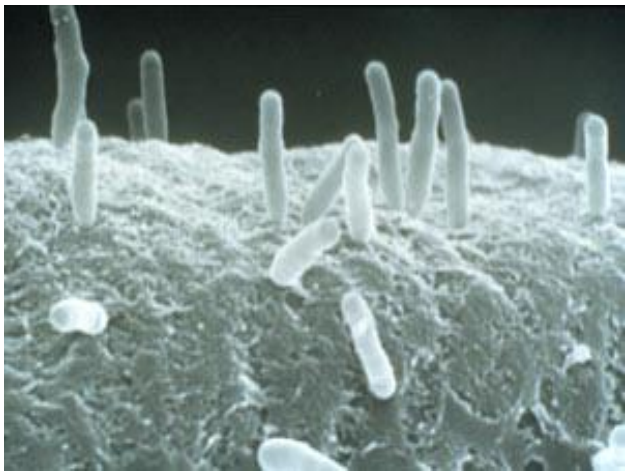

Figure 2.24: Pictorial view of rod shape gram negative bacteria. (A) *Enterobacter Genus* [131], (B) *Pseudomonas syringae*, [132] (C) *Agrobacterium spp.* [133]

Rylander and Lundholm (1978) studied different types of cotton originate bacterial contamination and fine dust for the analysis of bacterial species and their impact on the occurrence of byssinosis. The study concluded that three types of rod shape gram negative bacterial species were found in abundance known as typical cotton bacteria. The most prominent specie found in the cotton dust was the *Enterobacter genus*. For the experimental analysis, bacterial contaminations of cotton were inhaled by the guinea pigs which increased the number of leucocytes in the lung airways and caused acute pulmonary symptoms. In the end, it was also concluded that the occurrence of byssinosis can be correlated with the inhalation of cotton dust endotoxins and gram negative bacteria. [129]

Rylander et al (1985) studied the effect of cotton dust and their bacterial endotoxins on the health of spinning mill workers. Raw cotton was taken from different origins having a different amounts of bacterial contaminations. Environmental dust samples were taken with the help of a vertical elutriator and analysed for endotoxin levels. Analysis of output was made by examining field workers against forced expiratory volume test, and blood neutrophils test occurred before and after the work. Results concluded that there is a significant correlation between the number of endotoxins and the presence of byssinosis symptoms in the worker having the same working environment. Samples having increased value of endotoxins affected the worker more intensively as compared to fewer endotoxin samples. It was also concluded that symptoms of byssinosis are mostly dependent on the bacterial endotoxins level while the rest of the cotton dust factors are less important. [134]

Delucca and Shaffer (1989) conducted two-year study (1984, 1985) on the bacterial contamination analysis of cotton plant, bract, and fibres, by taking weekly samples throughout the season. The basic objective of this study was to check the effect of hot and humid conditions

on the existence of total and gram negative bacterial species in cotton plants. It was concluded that the amount of bacterial species remained sustain during the growth period of the plan while the amount of total and gram negative bacteria increased with the addition of frost in the environment to the end of plant growth which clearly expressed the bacterial growth shift influence by environmental conditions. Most abundance existence of *Enterobacter agglomerans* was reported among all gram negative bacteria. [135]

Milton et al (1989) studied the effect of cotton dust endotoxins and elastase on emphysema disease by using hamsters as a carrier. For the experimental analysis, cotton dust (0.75 mg/100g animal) and endotoxins (225µg/100g animals) injected every week into the hamsters for a period of six weeks regularly. After eight weeks of the last dose, they killed the hamsters and analyse the distensibility of the lungs by static pressure-volume deflation curve of air filled excised lungs. In the case of endotoxins dose animal, results showed increased distensibility and mild symptoms of emphysema with reduced surface-volume ratio while cotton dust sample had normal distensibility, reduced surface-volume ratio and mild centrilobular emphysema. According to the results, it can be summarised that cotton dust has a similar kind of elements that can cause centrilobular emphysema as like endotoxins. [136]

Mayan et al (2002) studied the respiratory effect among textile workers due to the interaction of cotton dust and their endotoxins. For the experimental analysis, total 231 workers of spinning mill and 186 workers of weavings mill were examined before and after the shift, after 36 hour rest from the work by using questionnaire administration and pulmonary function test. The Vertical elutriator having polyvinylchloride filter was used to collect the sample of the airborne cotton dust. Limulus amoebocyte lysate test was used for the airborne endotoxins level analysis of the cotton dust. The result showed that an average cotton dust level of spinning and weaving was 0.19-1.3 mg/m^3 and 0.11-0.58 mg/m^3 respectively while endotoxin level in the

card room area of spinning varied from 2.5-58 ng/m^3. The Weaving area showed zero value for the endotoxin level. In the case of the pulmonary function test, spinning workers showed higher rate of respiratory symptoms (28.3%) while ratio remained low up to (12.7%) in weaving area. It was also reported that endotoxins level has strong relation with the decreasing value of forced expiratory volume (FEV) among cotton workers. [130]

Jacobs and Chun (2004) worked on the reduction of variability between intra-laboratory and inter-laboratory analysis of endotoxin levels from cotton dust samples. Replicate samples of cotton dust were obtained from the standard card room with the help of vertical elutriator. Each laboratory analysed the samples by using two ways, one with their own normal extraction procedure and second with a common one between all laboratories while the assay kit type and a lot were the same in each case. Results showed the reduction in results variability between both inter and intra-laboratory by using a common type of assay kit and common extraction procedure in a standardized way. In the case of inter-laboratory results, variation was a bit higher and needs for the development of exposure assessment assay for the quantitative exposure standard. [137]

Astrakianakis et al (2006) studied the occurrence of lung cancer among textile cotton workers in Shanghai due to the long exposure to cotton dust and their endotoxins. This study was based on a quantitative data analysis of 3812 women workers having 7242 jobs in 503 different factories in the era of 1932 to 1998 for the historical development of cotton dust and endotoxin exposure level estimation. For the purpose of validation of this model, the quantitative estimation of two factories was compared with the individual collection of dust exposure measurements from the same two factories. Results showed that the relative bias factor of the estimation was minimal (<2%) and the accuracy factor was 61 % which was considered acceptable according to standard. It was concluded that on the basis of predicted cotton dust

exposure estimates, approximation measurement of endotoxin per unit of dust made in specific processes and retrospective exposures level was assigned. [138]

Tahir et al (2012) studied the presence of cotton dust base particulate matters (PM) and their effect on the health of small-scale waving industry workers situated in the Hafizabad district. Particulate matter was divided into four groups name as $PM_{1.0,}$ $PM_{2.5,}$ $PM_{4.0}$ and $PM_{10.0\ \mu m}$ for the quantitative analysis of these pollutants in the working environment. After the analysis of the particulate matter, it was concluded that $PM_{1.0}$ and $PM_{2.5}$ were found in abundance as compared to others. These are creating several disease issues during the working hours due to the inhalable and respirable size of these particulate matters. Normal diseases observed in the workers were flu, cough, eye and skin infection due to the interaction with cotton dust PM. It was concluded that poor medication and protection mask unavailability, due to the deficiency of financial resources, is also leading the workers towards these diseases. [139]

Dangi and Bhise (2017) studied the effect of cotton dust exposure on the respiratory symptoms of textile mill workers in the Ahmedabad city. For the experimental analysis, the researcher categorised the mill worker and normal residential people in two groups of hundred persons each, while residential people called as the control group. The medical analysis was done by using a spirometric test and by inquiring the populations about respiratory symptoms with the help questionnaire. Results showed that respiratory symptoms and decreased value of forced expiratory volume FEV in 1s were significantly found more common in mill workers compared to the control group. It was also explained that the duration of cotton dust exposure has a direct relation with the respiratory symptoms and spirometric abnormality of the workers. [140]

As a conclusion from above detailed literature, byssinosis (COPD) is a serious problem for textile workers due to the continuous exposure and inhalation of fine cotton dust and related gram negative bacterial endotoxins. Cotton aerosol ranges from 100nm to 2.5µm and nano-

level bacterial endotoxins are most problematic because workers are being protected from micro dust above 2.5µm by using conventional surgical mask. Therefore, thorough research for the development of effective respiratory filter material is necessary to protect textile workers from cotton related fine aerosols and bacterial contamination. Moreover, effective protection from cotton related aerosols will potentially reduced the symptoms of byssinosis in textile workers.

2.8 Summary of literature review:

According to a detailed literature review of respiratory filter, it is concluded that many researchers developed microfibres based multilayer respiratory filter against the aerosol particle ranges from 300nm and above diameter to achieve N95 (American standard NIOSH-42C FR84) and PPF2 (European Standard EN 149-2001) standard for commercial application. Moreover previously developed respiratory filters and masks showed maximum filtration efficiency from 95% to 99% against nano to micro level particles. However, a surgical mask can only provide protection against 3µm and above particle diameters. According to N95 and PPF2 standard requirement, developed filter should perform at least 95% filtration efficiency against 300nm particle aerosols and pressure drop value should not exceed beyond 343 Pa to fulfil the criteria of the mentioned standards. Therefore, filtration performance below 300m and protection from microbes are the limitation of currently developed N95 and FFP2 respiratory filters. Furthermore, in recent publication on NIOSH science blog, it was mentioned that N95 respirators use for more than one hour extended period of time can cause dizziness and elevated carbon dioxide amount in blood which is serious limitation for workers doing longer shift up to 8 to 12h. This limitation of N95 is directly associated with higher pressure

drop value and reduced breathing activity [141]. Therefore, there is an urgent need to investigate the performance of respiratory filters against below 300nm particle aerosols with lower pressure drop value for better breathing activity. Furthermore, a combination of higher filtration performance and higher antibacterial efficiency also needs attention for the future research and development of respiratory filters to achieve specified filtration performance goals.

Electrospun nanofibres are playing an important role in the field of air filtration by inducing higher surface area and barrier protection. However, nanofibres also has direct impact on the rise the pressure drop value which is also a very important in filtration characterisation. Therefore, mostly researchers developed nanofibres base membranes for water filtration and air ventilation purpose where pressure drop value is not significant. However, researchers also developed respiratory filter base membrane, which significantly showed higher filtration performance up to 99% against nano-level aerosol particles but resulted in higher pressure drop value which creates difficulty in breathing for end users. Therefore, nanofibrous filter with higher filtration efficiency and optimised pressure drop value is still needs researchers' attention for commercial impact and localised application for end user. However, combination of nanofibres and conventional PP nonwoven can further enhanced the filtration performance from nano-level aerosols, bacterial and viral protection. Moreover, selection of material having natural anti-bacterial properties (chitosan) for nanofibre production can play an important towards bacterial protection.

As a conclusion from detailed literature, byssinosis (COPD) is a serious problem for textile workers due to the continuous exposure and inhalation of fine cotton dust and related gram negative bacterial endotoxins. Cotton aerosol ranges from 100nm to 2.5µm and nano-level bacterial endotoxins are most problematic because workers can only protect themselves from

micro dust above 2.5µm by using conventional surgical mask. Therefore, thorough research for the development of effective respiratory filter material by using combination of nanofibres and conventional PP nonwoven can be investigated for higher filtration efficiency up to 99% and lower pressure drop value below 343 Pa. Successful development of composite structure respiratory filter material will be helpful to protect textile workers from cotton related fine aerosols and bacterial contamination. Moreover, effective protection from cotton related aerosols will potentially reduce the symptoms of byssinosis in textile workers.

2.9 Research Gap

According to the literature, COPD and byssinosis have attracted a lot of research attention in epidemiological studies, but protection against this disease has not been explored in any significant way. It was found that occupational agents causing COPD, include dust from cotton and other textile fibres. Workers reported to be at increased risk of developing occupational COPD (byssinosis) include farmers and cotton workers, as well as more general workers in textile mills. Furthermore, affected people of byssinosis are increasing day by day due to the lack of suitable respiratory filter for the protection against cotton dust and their pathogens in the textile industry.

A surgical mask is sometimes being used in the textile industry for the aerosol dust protection, but the filtration performance of surgical mask is only effective against large particles of 3µm and above. The N95 mask is also being used in few areas, but it is only effective against particle size of 300nm and above. However, N95 use for more than one hour extended period of time can cause dizziness and elevated carbon dioxide amount in blood, which is directly associated with breathing resistance due to its multilayer (4 to 7 layers) structure to gain higher surface

area. Furthermore, N95 is also not effective against cotton dust originated gram-negative bacterial pathogens. Therefore, it is concluded from the literature that there is no specified respiratory protection equipment as the standard protection requirement against byssinosis (COPD) in the textile industry. In addition to byssinosis, high filtration performance with a lower pressure drop is also a challenging issue for the development of suitable respiratory filters.

Conclusively, the development of efficient personal protective equipment (PPE) for textile cotton workers can protect them from the exposure of cotton originated pathogenic dust and reduces byssinosis. Therefore, thorough research for the development of effective respiratory filter material by using combination of nanofibres and conventional PP nonwoven can be investigated for higher filtration efficiency up to 99% and lower pressure drop value below 343 Pa. This research aims to develop the suitable respiratory protection equipment for textile workers against byssinosis by using nanocomposite material.

References

[1] P. D. Subhash K. Batra, and Behnam Pourdeyhimi, “Introduction to nonwovens technology,” 2012. [Online]. Available: http://www.textileworld.com/Issues/2012/May-June/Nonwovens-Technical_Textiles/Introduction_To_Nonwovens_Technology. [Accessed: 18-Aug-2020].

[2] “Entorno Saludable.” [Online]. Available: http://entornosaludable.com/31/03/2016/que-es-el-tejido-no-tejido/. [Accessed: 01-Sep-2020].

[3] “Ultra-Thin Wet-Laid Nonwovens.” [Online]. Available: http://www.hiroseamerica.com/products/ultra-thin-wet-laid-nonwovens/. [Accessed: 01-Sep-2020].

[4] EDANA, “What are nonwovens ?” [Online]. Available: http://www.edana.org/discover-nonwovens/what-are-nonwovens-. [Accessed: 18-Aug-2020].

[5] “What is a nonwovens fabric?,” *INDA Association of Nonwoven Fabric*. [Online]. Available: http://www.inda.org/about-nonwovens/. [Accessed: 18-Aug-2020].

[6] S. Jp, “Nonwoven: A Versatile Fabric,” *J. Text. Sci. Eng.*, vol. 04, no. 05, pp. 4–5, 2014.

[7] A. Wilson, “Handbook of nonwovens,” in *Development of the nonwovens industry,* S. J. Russell, Ed. woodhead publishing limited Cambridge England, pp. 9–10.

[8] A. Wilson, “Handbook of nonwovens,” in *Development of the nonwovens industry,* S.

J. Russell, Ed. woodhead publishing limited Cambridge England, pp. 4–5.

[9] "Spinning." [Online]. Available: http://textileinfo.blogspot.com/p/pinning.html. [Accessed: 01-Sep-2020].

[10] M. R. Mahmoudi, "Blending and composite yarn spinning," *Adv. Yarn Spinn. Technol.*, pp. 102–118, 2010.

[11] K. Shaker, M. Umair, W. Ashraf, and Y. Nawab, "Fabric manufacturing," *Phys. Sci. Rev.*, vol. 1, no. 7, pp. 1–25, 2019.

[12] Textnote, "Air Laid Web Formation Technique," 2013. [Online]. Available: https://texnoteblog.wordpress.com/2013/08/31/airlaid-web-formation-technique/. [Accessed: 01-Sep-2020].

[13] A. G. and A. P. Brydon, "Handbook of nonwovens," in *Dry-laid web formation*, S. J. Russell, Ed. woodhead publishing limited Cambridge England.

[14] "Wet-Laid Nonwovens." [Online]. Available: https://www.apparelsearch.com/education/research/nonwoven/2001_kermit_duckett/education_research_nonwoven_wet-laid_nonwovens.htm. [Accessed: 01-Sep-2020].

[15] R. Kotra, Haoming Rong, "Wet-Laid Nonwovens." [Online]. Available: https://www.apparelsearch.com/education/research/nonwoven/2001_kermit_duckett/education_research_nonwoven_wet-laid_nonwovens.htm. [Accessed: 18-Aug-2020].

[16] M. Madiwal, "Spun Bonding Technology with Types, Application and Market Future," *Textile Learner*. [Online]. Available: https://textilelearner.blogspot.com/2019/03/spun-bonding-technology-types.html. [Accessed: 01-Sep-2020].

[17] G. S. B. and S. R. Malkan, “Polymer-laid web formation,” in *Handbook of nonwovens*, S. J. Russell, Ed. woodhead publishing limited Cambridge England, pp. 143–173.

[18] “Process Flow of Meltblown Production Line.” [Online]. Available: https://www.useon.com/melt-blown-fabric-machine.html. [Accessed: 01-Sep-2020].

[19] A. Wilson, “Development of nonwoven industry,” S. J. Russell, Ed. woodhead publishing limited Cambridge England, p. 9.

[20] EDANA, “Bonding.” [Online]. Available: http://www.edana.org/discover-nonwovens/how-they’re-made/bonding. [Accessed: 18-Aug-2020].

[21] A. Pourmohammadi, “Thermal bonding,” in *Handbook of nonwovens*, S. J. Russell, Ed. woodhead publishing limited Cambridge England.

[22] E. Ramazan, *Advances in fabric structures for wound care*, Second Edi. Elsevier Ltd, 2019.

[23] V. Dhanabalan, “Needle punching technique.” [Online]. Available: https://www.slideshare.net/vigneshdhanabalan/needle-punching-technique-by-vignesh-dhanabalan. [Accessed: 01-Sep-2020].

[24] G. S. S C Anand, D B Runnschweiler, “Mechanical bonding,” in *Handbook of nonwovens*, S. J. Russell, Ed. woodhead publishing limited Cambridge England.

[25] A. Farag, “Nonwovens Web bonding processes.” [Online]. Available: https://www.linkedin.com/pulse/nonwovens-web-bonding-processes-1-dr-ahmad-farag/. [Accessed: 01-Sep-2020].

[26] A. I. Ahmad, “Nonwovens fabric finishing,” in *Handbook of nonwovens*, S. J. Russell, Ed. woodhead publishing limited Cambridge England.

[27] M. Patel, “Chemical finishes,” in *Nonwoven technology*, pp. 49–53.

[28] D. Aspland, “The Coloration and Finishing of Nonwoven Fabrics,” in *Nonwoven Enhancements*, 2005.

[29] J. R. Aspland, “The coloration and finishing of nonwoven fabrics,” *Sch. Mater. Sci. Eng. Univ.*, no. June, 2005.

[30] AI Ahmed, “Lamination,” in *Handbook of nonwovens*, S. J. Russell, Ed. woodhead publishing limited Cambridge England, 2007, pp. 385–386.

[31] R. A. Chapman, *Applications of Nonwovens in Technical Textiles*. woodhead publishing limited, 2010.

[32] V. V. Kadam, L. Wang, and R. Padhye, “Electrospun nanofibre materials to filter air pollutants - A review,” *J. Ind. Text.*, vol. 0, no. 00, pp. 1–28, 2016.

[33] OSHA, “General Respiratory Protection Guidance for Respiratory,” 2016.

[34] A. Rengasamy, Z. Zhuang, and R. Berryann, “Respiratory protection against bioaerosols: Literature review and research needs,” *Am. J. Infect. Control*, vol. 32, no. 6, pp. 345–354, 2004.

[35] A. Mukhopadhyay, “Pulse-jet filtration: An effective way to control industrial pollution Part I: Theory, selection and design of pulse-jet filter,” *Text. Prog.*, vol. 41, no. 4, pp. 195–315, 2009.

[36] V. Kadam, I. L. Kyratzis, Y. B. Truong, J. Schutz, and L. Wang, “2019 Electrospun bilayer nanomembrane with hierarchical placement of bead-on-string and fibres for low resistance respiratory air filtration.pdf,” *Sep. Purif. Technol.*, vol. 224, no. 1, pp. 247–254, 2019.

[37] A. Aluigi, C. Vineis, C. Tonin, C. Tonetti, A. Varesano, and G. Mazzuchetti, “Wool keratin-based nanofibres for active filtration of air and water,” *J. Biobased Mater. Bioenergy*, vol. 3, no. 3, pp. 311–319, 2009.

[38] D. Wake, A. C. Bowry, B. Crook, and R. C. Brown, “Performance of respirator filters and surgical masks against bacterial aerosols,” *J. Aerosol Sci.*, vol. 28, no. 7, pp. 1311–1329, 1997.

[39] Y. Qian, K. Willeke, S. a Grinshpun, J. Donnelly, and C. C. Coffey, “Performance of N95 respirators: filtration efficiency for airborne microbial and inert particles.,” *Am. Ind. Hyg. Assoc. J.*, vol. 59, no. 2, pp. 128–32, 1998.

[40] A. Bałazy, M. Toivola, A. Adhikari, S. K. Sivasubramani, T. Reponen, and S. A. Grinshpun, “Do N95 respirators provide 95% protection level against airborne viruses, and how adequate are surgical masks?,” *Am. J. Infect. Control*, vol. 34, no. 2, pp. 51–57, 2006.

[41] A. Bałazy, M. Toivola, T. Reponen, A. Podgórski, A. Zimmer, and S. A. Grinshpun, “Manikin-based performance evaluation of N95 filtering-facepiece respirators challenged with nanoparticles,” *Ann. Occup. Hyg.*, vol. 50, no. 3, pp. 259–269, 2006.

[42] R. M. Eninger, T. Honda, A. Adhikari, H. Heinonen-Tanski, T. Reponen, and S. A. Grinshpun, “Filter performance of N99 and N95 facepiece respirators against viruses and ultrafine particles,” *Ann. Occup. Hyg.*, vol. 52, no. 5, pp. 385–396, 2008.

[43] J. P. Eshbaugh, P. D. Gardner, A. W. Richardson, and K. C. Hofacre, “N95 and P100 Respirator Filter Efficiency Under High Constant and Cyclic Flow,” *J. Occup. Environ. Hyg.*, vol. 6, no. 1, pp. 52–61, 2008.

[44] S. Rengasamy, B. C. Eimer, and R. E. Shaffer, “Comparison of nanoparticle filtration

performance of NIOSH-approved and CE-marked particulate filtering facepiece respirators," *Ann. Occup. Hyg.*, vol. 53, no. 2, pp. 117–128, 2009.

[45] R. E. Shaffer and S. Rengasamy, "Respiratory protection against airborne nanoparticles: A review," *J. Nanoparticle Res.*, vol. 11, no. 7, pp. 1661–1672, 2009.

[46] R. Mostofi, B. Wang, F. Haghighat, A. Bahloul, and L. Jaime, "Performance of mechanical filters and respirators for capturing nanoparticles--limitations and future direction.," *Ind. Health*, vol. 48, pp. 296–304, 2010.

[47] S. a Grinshpun, H. Haruta, R. M. Eninger, T. Reponen, R. T. McKay, and S.-A. Lee, "Performance of an N95 filtering facepiece particulate respirator and a surgical mask during human breathing: two pathways for particle penetration.," *J. Occup. Environ. Hyg.*, vol. 6, no. 10, pp. 593–603, 2009.

[48] G. Borkow, S. S. Zhou, T. Page, and J. Gabbay, "A novel anti-influenza copper oxide containing respiratory face mask," *PLoS One*, vol. 5, no. 6, 2010.

[49] X. Liu, H. Shen, and X. Nie, "Study on the filtration performance of the baghouse filters for ultra-low emission as a function of filter pore size and fibre diameter," *Int. J. Environ. Res. Public Health*, vol. 16, no. 2, pp. 1–19, 2019.

[50] "Understanding Varying Levels of Face Mask Protection," *Face Mask UK*. [Online]. Available: https://facemasks-uk.com/2020/04/10/face-masks-standards-filtration-effectiveness-ratings/. [Accessed: 27-Sep-2020].

[51] Y. Si, X. Tang, J. Yu, and B. Ding, "Electrospun Nanofibres for Energy and Environmental Applications," *Nanostructure Sci. Technol.*, no. DOI 10.1007/978-3-642-54160-5__1, p. 525, 2014.

[52] R. S. Barhate and S. Ramakrishna, “Nanofibrous filtering media: Filtration problems and solutions from tiny materials,” *J. Memb. Sci.*, vol. 296, no. 1–2, pp. 1–8, 2007.

[53] Y. C. Ahn *et al.*, “Development of high efficiency nanofilters made of nanofibres,” *Curr. Appl. Phys.*, vol. 6, no. 6 SPEC. ISS., pp. 1030–1035, 2006.

[54] X. H. Qin and S. Y. Wang, “Filtration properties of electrospinning nanofibres,” *J. Appl. Polym. Sci.*, vol. 102, no. 2, pp. 1285–1290, 2006.

[55] R. Gopal, S. Kaur, Z. Ma, C. Chan, S. Ramakrishna, and T. Matsuura, “Electrospun nanofibrous filtration membrane,” *J. Memb. Sci.*, vol. 281, no. 1–2, pp. 581–586, 2006.

[56] A. Podgórski, A. Bałazy, and L. Gradoń, “Application of nanofibres to improve the filtration efficiency of the most penetrating aerosol particles in fibrous filters,” *Chem. Eng. Sci.*, vol. 61, no. 20, pp. 6804–6815, 2006.

[57] R. S. Barhate, C. K. Loong, and S. Ramakrishna, “Preparation and characterization of nanofibrous filtering media,” *J. Memb. Sci.*, vol. 283, no. 1–2, pp. 209–218, 2006.

[58] R. Gopal *et al.*, “Electrospun nanofibrous polysulfone membranes as pre-filters: Particulate removal,” *J. Memb. Sci.*, vol. 289, no. 1–2, pp. 210–219, 2007.

[59] W. W. F. Leung, C. H. Hung, and P. T. Yuen, “Effect of face velocity, nanofibre packing density and thickness on filtration performance of filters with nanofibres coated on a substrate,” *Sep. Purif. Technol.*, vol. 71, no. 1, pp. 30–37, 2010.

[60] K. M. Yun, A. B. Suryamas, F. Iskandar, L. Bao, H. Niinuma, and K. Okuyama, “Morphology optimization of polymer nanofibre for applications in aerosol particle filtration,” *Sep. Purif. Technol.*, vol. 75, no. 3, pp. 340–345, 2010.

[61] C. H. Hung and W. W. F. Leung, “Filtration of nano-aerosol using nanofibre filter

under low Peclet number and transitional flow regime," *Sep. Purif. Technol.*, vol. 79, no. 1, pp. 34–42, 2011.

[62] S. Sundarrajan, K. L. Tan, S. H. Lim, and S. Ramakrishna, "Electrospun nanofibres for air filtration applications," *Procedia Eng.*, vol. 75, pp. 159–163, 2014.

[63] N. Wang, Z. Zhu, J. Sheng, S. S. Al-Deyab, J. Yu, and B. Ding, "Superamphiphobic nanofibrous membranes for effective filtration of fine particles," *J. Colloid Interface Sci.*, vol. 428, pp. 41–48, 2014.

[64] "Nanotechnology and Respirator Use."

[65] C. Hindle, "Polypropylene (PP)," *British Plastic Federation*. [Online]. Available: http://www.bpf.co.uk/plastipedia/polymers/PP.aspx. [Accessed: 21-Jul-2017].

[66] C. Hindle, "Polypropylene (PP)," *British Plastic Federation*. .

[67] "Polypropylene (PP)," *NYLACAST*. [Online]. Available: https://www.nylacast.com/polypropylene-pp. [Accessed: 21-Jul-2017].

[68] "Water Absorption 24 hours," *Omnexus*. [Online]. Available: https://omnexus.specialchem.com/polymer-properties/properties/water-absorption-24-hours. [Accessed: 21-Jul-2017].

[69] "Learn the Basics of the Plastic Resin Polypropylene," *ThoughtCo.* [Online]. Available: https://www.thoughtco.com/what-is-polypropylene-820365. [Accessed: 23-Jul-2017].

[70] "Spunbonded Polypropylene," *techtex*. [Online]. Available: http://www.techtex.co.uk/industrial/products/non-woven/spunbonded-polypropylene. [Accessed: 23-Jul-2017].

[71] “Poly(propene) (Polypropylene),” *The Essential Chemical Industry-online*. [Online]. Available: http://www.essentialchemicalindustry.org/polymers/polypropene.html. [Accessed: 23-Jul-2017].

[72] “Polypropylene Membrane and Media Filters,” *Critical Process*. [Online]. Available: http://www.criticalprocess.com/filters/poly.php. [Accessed: 01-Sep-2019].

[73] “Polypropylene Filter Cloth.” [Online]. Available: https://www.google.co.uk/imgres?imgurl=https%3A%2F%2F4.imimg.com%2Fdata4%2FGM%2FBH%2FMY-2545248%2Fpolypropylene-filter-cloth-250x250.jpg&imgrefurl=https%3A%2F%2Fdir.indiamart.com%2Fimpcat%2Fpolypropylene-filter-cloth.html&docid=6IYFeNC65FzYGM&tbnid=u7YFag. [Accessed: 23-Jul-2017].

[74] “Introduction to Filtration.” [Online]. Available: http://www.filters-cartridges.com/filtrationFAQs.html. [Accessed: 23-Jul-2017].

[75] “Polypropylene Membranes,” *SterliTech*, 2019. [Online]. Available: https://www.sterlitech.com/polypropylene-membrane-filters.html. [Accessed: 01-Sep-2019].

[76] “Polypropylene Prefilters and Membranes,” *Merckmilipore*. [Online]. Available: https://www.merckmillipore.com/GB/en/product/Polypropylene-Prefilters-and-Membranes,MM_NF-C758?ReferrerURL=https%3A%2F%2Fwww.google.co.uk%2F&bd=1. [Accessed: 23-Jul-2017].

[77] “Filter Media.” [Online]. Available: http://www.filterbag.com/Filter-Media-20.html. [Accessed: 23-Jul-2017].

[78] K. Kurita, “Chitin and chitosan: Functional biopolymers from marine crustaceans,” *Mar. Biotechnol.*, vol. 8, no. 3, pp. 203–226, 2006.

[79] P. B. Malafaya, G. A. Silva, and R. L. Reis, “Natural-origin polymers as carriers and scaffolds for biomolecules and cell delivery in tissue engineering applications,” *Adv. Drug Deliv. Rev.*, vol. 59, no. 4–5, pp. 207–233, 2007.

[80] N. V. Majeti and R. Kumar, “A review of chitin and chitosan applications,” *React. Funct. Polym.*, vol. 46, no. 1, pp. 1–27, 2000.

[81] F. Esmaeili, S. Heuking, H. E. Junginger, and G. Borchard, “Progress in chitosan-based vaccine delivery systems,” *J. Drug Deliv. Sci. Technol.*, vol. 20, no. 1, pp. 53–61, 2010.

[82] L. Martinová and D. Lubasová, “Electrospun Chitosan Based Nanofibres,” *Rjta*, vol. 12, no. 2, pp. 72–79, 2008.

[83] M. S. Viarsagh, M. Janmaleki, H. R. Falahatpisheh, and J. Masoumi, “Chitosan Preparation from Persian Gulf Shrimp Shells and Investigating the Effect of Time on the Degree of Deacetylation,” *J. Paramed. Sci.*, vol. 1, no. 2, pp. 2–7, 2010.

[84] J. Berger, M. Reist, J. M. Mayer, O. Felt, and R. Gurny, “Structure and interactions in chitosan hydrogels formed by complexation or aggregation for biomedical applications,” *Eur. J. Pharm. Biopharm.*, vol. 57, no. 1, pp. 35–52, 2004.

[85] J. H. Hamman, “Chitosan based polyelectrolyte complexes as potential carrier materials in drug delivery systems,” *Mar. Drugs*, vol. 8, no. 4, pp. 1305–1322, 2010.

[86] M. Rinaudo, “Chitin and chitosan: Properties and applications,” *Prog. Polym. Sci.*, vol. 31, no. 7, pp. 603–632, 2006.

[87] S. Bagheri-Khoulenjani, S. M. Taghizadeh, and H. Mirzadeh, “An investigation on the short-term biodegradability of chitosan with various molecular weights and degrees of deacetylation,” *Carbohydr. Polym.*, vol. 78, no. 4, pp. 773–778, 2009.

[88] C. V Stevens, “Chitosan as Antimicrobial Agent : Applications and Mode of Action Chitosan as Antimicrobial Agent : Applications and Mode of,” vol. 4, no. SEPTEMBER, 2003.

[89] H. Sashiwa and S. I. Aiba, “Chemically modified chitin and chitosan as biomaterials,” *Prog. Polym. Sci.*, vol. 29, no. 9, pp. 887–908, 2004.

[90] E. a El-hefian, M. M. Nasef, and A. H. Yahaya, “Chitosan Physical Forms : A Short Review,” *Aust. J. Basic Appl. Sci.*, vol. 5, no. 5, pp. 670–677, 2011.

[91] K. M. Vårum, M. M. Myhr, R. J. N. Hjerde, and O. Smidsrød, “In vitro degradation rates of partially N-acetylated chitosans in human serum,” *Carbohydr. Res.*, vol. 299, no. 1–2, pp. 99–101, 1997.

[92] P. J. VandeVord, H. W. T. Matthew, S. P. DeSilva, L. Mayton, B. Wu, and P. H. Wooley, “Evaluation of the biocompatibility of a chitosan scaffold in mice,” *J. Biomed. Mater. Res.*, vol. 59, no. 3, pp. 585–590, 2002.

[93] B. Simoncic and B. Tomsic, “Structures of Novel Antimicrobial Agents for Textiles - A Review,” *Text. Res. J.*, vol. 80, no. 16, pp. 1721–1737, 2010.

[94] T. Tsai, H. F. Chien, T. H. Wang, C. T. Huang, Y. B. Ker, and C. T. Chen, “Chitosan augments photodynamic inactivation of gram-positive and gram-negative bacteria,” *Antimicrob. Agents Chemother.*, vol. 55, no. 5, pp. 1883–1890, 2011.

[95] D. Raafat, K. Von Bargen, A. Haas, and H. G. Sahl, “Insights into the mode of action

of chitosan as an antibacterial compound," *Appl. Environ. Microbiol.*, vol. 74, no. 12, pp. 3764–3773, 2008.

[96] M. Kong, X. G. Chen, K. Xing, and H. J. Park, "Antimicrobial properties of chitosan and mode of action: A state of the art review," *Int. J. Food Microbiol.*, vol. 144, no. 1, pp. 51–63, 2010.

[97] M. Arkoun, F. Daigle, M. C. Heuzey, and A. Ajji, "Mechanism of action of electrospun chitosan-based nanofibres against meat spoilage and pathogenic bacteria," *Molecules*, vol. 22, no. 4, 2017.

[98] S. M. Lemma, F. Bossard, and M. Rinaudo, "Preparation of pure and stable chitosan nanofibres by electrospinning in the presence of poly(ethylene oxide)," *Int. J. Mol. Sci.*, vol. 17, no. 11, 2016.

[99] X. Geng, O. H. Kwon, and J. Jang, "Electrospinning of chitosan dissolved in concentrated acetic acid solution," *Biomaterials*, vol. 26, no. 27, pp. 5427–5432, 2005.

[100] I.-K. K. Kyung-Hye Jung, Man-Woo Huh, Wan Meng, Jiang Yuan, Seok Hee Hyun, Jung-Sook Bae4, Samuel M. Hudson, "Preparation and Antibacterial Activity of PET/Chitosan Nanofibrous Mats Using an Electrospinning Technique," *J. Appl. Polym. Sci.*, vol. 105, pp. 2816–2823, 2007.

[101] Y. Z. Zhang, B. Su, S. Ramakrishna, and C. T. Lim, "Chitosan nanofibres from an easily electrospinnable UHMWPEO-doped chitosan solution system," *Biomacromolecules*, vol. 9, no. 1, pp. 136–141, 2008.

[102] H. Homayoni, S. A. H. Ravandi, and M. Valizadeh, "Electrospinning of chitosan nanofibres: Processing optimization," *Carbohydr. Polym.*, vol. 77, no. 3, pp. 656–661, 2009.

[103] H. Daniell, “Chitosan-based nanofibrous membranes for antibacterial filter applications,” *Carbohydr Polym.*, vol. 76, no. October 2009, pp. 211–220, 2012.

[104] M. Arkoun, F. Daigle, M. C. Heuzey, and A. Ajji, “Antibacterial electrospun chitosan-based nanofibres: A bacterial membrane perforator,” *Food Sci. Nutr.*, no. January, pp. 1–10, 2017.

[105] N. N. Maslakci, S. Ulusoy, and A. U. Oksuz, “Investigation of the effects of plasma-treated chitosan electrospun fibres onto biofilm formation,” *Sensors Actuators, B Chem.*, vol. 246, pp. 887–895, 2017.

[106] D. J. Lockwood, “Overview of the Electrospinning,” in *Electrospun Nanofibres for Energy and Environmental Applications*, B. Ding and J. Yu, Eds. Springer-Verlag Berlin, 2014, p. 6.

[107] D. J. Lockwood, “Basic Principles,” in *Electrospun Nanofibres for Energy and Environmental Applications*, B. Ding and J. Yu, Eds. Springer-Verlag Berlin, 2014, pp. 8–9.

[108] D. J. Lockwood, “History of Electrospinning,” in *Electrospun Nanofibres for Energy and Environmental Applications*, B. Ding and J. Yu, Eds. Springer-Verlag Berlin, 2014, pp. 6–8.

[109] “Plasma Treatment of Surfaces,” *TriStar*. [Online]. Available: http://www.tstar.com/plasma-treatments-surfaces. [Accessed: 24-Jul-2017].

[110] “Plasma Knowledge.” [Online]. Available: http://www.thierry-corp.com/plasma/knowledge/types-of-plasma-treatments. [Accessed: 24-Jul-2017].

[111] “Plasma treatment at atmospheric pressure conditions.” [Online]. Available:

http://www.ferben.com/Technology/Atmospheric_Plasma_Treatment.kl. [Accessed: 24-Jul-2017].

[112] C. Sarangapani, R. Yamuna Devi, R. Thirumdas, A. M. Trimukhe, R. R. Deshmukh, and U. S. Annapure, "Physico-chemical properties of low-pressure plasma treated black gram," *LWT - Food Sci. Technol.*, vol. 79, pp. 102–110, 2017.

[113] P. Favia and R. d'Agostino, "Plasma treatments and plasma deposition of polymers for biomedical applications," *Surf. Coatings Technol.*, vol. 98, no. 1–3, pp. 1102–1106, 1998.

[114] Michael Thomas and K.L. Mittal, "Selective Surface Modification of Polymer Materials by Atmospheric Pressure Plasmas," in *Atmospheric Pressure Plasma Treatment of Polymers: Relevance to Adhesion*, WILEY Publishers, 2013.

[115] MedlinePlus, "Byssinosis." [Online]. Available: https://medlineplus.gov/ency/article/001089.htm. [Accessed: 08-Jul-2017].

[116] L. S. Newman, "Byssinosis," *MSD MANUAL*. [Online]. Available: http://www.msdmanuals.com/en-gb/home/lung-and-airway-disorders/environmental-lung-diseases/byssinosis. [Accessed: 08-Jul-2017].

[117] "Lung Information Center: Swine Flu, BOOP Disease, Byssinosis, Caplan's Syndrome, SARS." [Online]. Available: https://www.epainassist.com/chest-pain/lungs. [Accessed: 08-Jul-2017].

[118] R. S. F. Schilling, J. P. W. Hughes, I. Dingwall-Fordyce, and J. C. Gilson, "an Epidemiological Study of Byssinosis Among Lancashre Cotton Workers," *Brit. J. Ind. Med*, vol. 12, 1955.

[119] K. C. Mc, D. M. Mc, J. C. Gilson, and R. S. Schilling, “Respiratory function during the day in cotton workers: a study in byssinosis,” *Br J Ind Med*, vol. 15, no. 2, pp. 75–83, 1958.

[120] A. Bouhuys, “Byssinosis Scheduled Asthma in Textile Industry,” vol. 16, pp. 3–16, 1976.

[121] D. F. Brown and R. J. Berni, “Collection of Large Quantities of Respirable Cotton Dust for Byssinosis Research.,” *Text. Res. J.*, vol. 47, no. 2, pp. 152–154, 1977.

[122] D. Fishwick, A. M. Fletcher, C. A. Pickering, R. M. Niven, and E. B. Faragher, “Respiratory symptoms and dust exposure in Lancashire cotton and man-made fibre mill operatives,” *Am. J. Respir. Crit. Care Med.*, vol. 150, no. 2, pp. 441–447, 1994.

[123] H. Kobayashi, S. Kanoh, K. Motoyoshi, and S. Aida, “Diffuse lung disease caused by cotton fibre inhalation but distinct from byssinosis.,” *Thorax*, vol. 59, no. 12, pp. 1095–7, 2004.

[124] P. S. Lai and D. C. Christiani, “Long Term Respiratory Health Effects in Textile Workers,” *Curr Opin Pulm Med. J.*, vol. 19, no. 2, pp. 152–157, 2014.

[125] M. Fantahun and Y. Abebe, “Self-reported disease conditions among workers of the textile mill in Bahir Dar , Northwest Ethiopia,” no. 3.

[126] S. Pandey, A. Singh, and T. B. Singh, “A Statistical study to estimate the effects of smoking and cotton dust exposure on lung function of cotton workers of Varanasi district , Uttar,” vol. 4, no. 3, pp. 743–746, 2017.

[127] M. K. Mummadi and G. N. Kusneniwar, “A cross sectional study on respiratory related morbidities at cotton factories in Hyderabad , Telangana,” vol. 4, no. 4, pp.

959–961, 2017.

[128] G. R. Ioannis D Anyfantis, C. Hadjichristodoulou, and K. I. Gourgoulianis, "Respiratory Symptoms and Lung Function among Greek Cotton Industry Workers: A Cross-Sectional Study," *Int. J. Occup. Environ. Med.*, vol. 8, no. 1 January, pp. 888-32–8, 2017.

[129] R. Rylander and M. Lundholm, "Bacterial contamination of cotton and cotton dust and effects on the lung.," *Br. J. Ind. Med.*, vol. 35, no. 3, pp. 204–207, 1978.

[130] O. Mayan, J. T. Da Costa, P. Neves, F. Capela, and A. S. Pinto, "Respiratory effects among cotton workers in relation to dust and endotoxin exposure," *Ann. Occup. Hyg.*, vol. 46, no. 1999, pp. 277–280, 2002.

[131] Bioquell, "Enterobacter aerogenes." [Online]. Available: http://www.bioquell.com/en-us/resources-and-support/microbiology/enterobacter-aerogenes. [Accessed: 15-Jul-2017].

[132] "Pseudomonas syringae." [Online]. Available: http://wishart.biology.ualberta.ca/BacMap/cgi/getSpeciesCard.cgi?accession=NC_004578. [Accessed: 15-Jul-2017].

[133] "Department of Microbiology, Cornell University." [Online]. Available: https://micro.cornell.edu/research/epulopiscium/bacterial-genomes. [Accessed: 15-Jul-2017].

[134] R. Rylander, P. Haglind, and M. Lundholm, "Endotoxin in cotton dust and respiratory function decrement among cotton workers in an experimental cardroom.," *Am. Rev. Respir. Dis.*, vol. 131, no. 2, pp. 209–213, 1985.

[135] A. J. DeLucca and G. P. Shaffer, “Factors influencing endotoxin concentrations on cotton grown in hot, humid environments: a two year study.,” *Br. J. Ind. Med.*, vol. 46, no. 12, pp. 887–891, 1989.

[136] D. K. Milton, J. J. Godleski, H. A. Feldman, and I. A. Greaves, “Toxicity of intratracheally instilled cotton dust, cellulose, and endotoxin.,” *Am. Rev. Respir. Dis.*, vol. 142, no. 1, pp. 184–192, 1990.

[137] R. R. Jacobs and D. Chun, “Inter-laboratory analysis of endotoxin in cotton dust samples,” *Am. J. Ind. Med.*, vol. 46, no. 4, pp. 333–337, 2004.

[138] G. Astrakianakis *et al.*, “Modeling, estimation and validation of cotton dust and endotoxin exposures in Chinese textile operations,” *Ann. Occup. Hyg.*, vol. 50, no. 6, pp. 573–582, 2006.

[139] M. W. Tahir *et al.*, “Monitoring of cotton dust and health risk assessment in small-scale weaving industry,” *Environ. Monit. Assess.*, vol. 184, no. 8, pp. 4879–4888, 2012.

[140] B. Dangi and A. Bhise, “Cotton dust exposure: Analysis of pulmonary function and respiratory symptoms,” *Lung India*, vol. 34, no. 2, p. 144, 2017.

[141] J. Williams, J. K. Cichowicz, A. Hornbeck, J. Pollard, and J. Snyder, “The Physiological Burden of Prolonged PPE Use on Healthcare Workers during Long Shifts,” *NIOSH Science Blog*, 2020. [Online]. Available: https://blogs.cdc.gov/niosh-science-blog/2020/06/10/ppe-burden/. [Accessed: 16-Feb-2020].

Chapter 3: Material and Methods

The aim of current research is to develop materials suitable for respiratory filters (PPE) which offer effective protection against fine cotton dust aerosols and their pathogenic species. In this study, a sandwich structured composite of two PP nonwoven layers and a chitosan nanofibres layer was designed for the development of respiratory filter. The upper layer is composed of PP and serves as a barrier for large dust particles and the bottom layer serves as supporting material for the chitosan nanofibres. Chitosan nanofibres were produced with the help of electrospinning. Polyethylene oxide (PEO) was used as a co-spinning agent of chitosan for smooth nanofibre production. The barrier performance of prepared respiratory filters against possible causes of byssinosis was examined. The barrier performance parameters, including filtration efficiency (η), pressure drop (ΔP), and quality factor (Q), against fine dust particles with a size range from 100 nm to 2.5 µm were discussed and the antibacterial performance of the CSNF layer was also evaluated to conclude the effectiveness of filter against byssinosis. Structural design explanation and details of materials and methods are given in the following sections.

3.1 Structural Design and Methodological Contribution

Three layers composite structure was developed by using one sandwiched nanofibrous layer and two (inner and outer) layer of different PP nonwovens as shown in Figure 3.1. Inner or bottom PP microfibres based nonwoven layer was used to support the structural stability of chitosan nanofibrous layer as nanofibrous layer lose its structural integration individually due to very fine thickness.

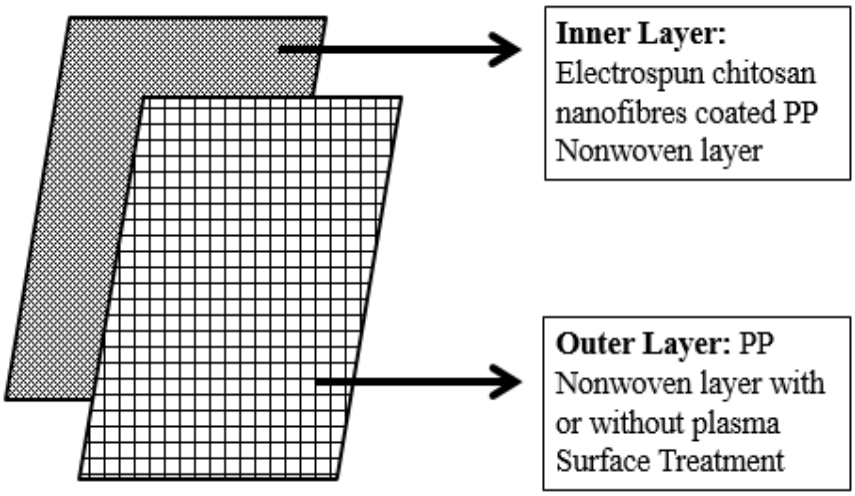

Figure 3.1: Structural design for composite respiratory filter development

However, chitosan nanofibrous layer acted as a sandwiched layer, which was developed by directly coating nanofibres on inner layer with the help of electrospinning. Addition of nanofibrous layer increased the surface area by reducing the pore size up to nano-level which is desirable to capture nano scale aerosol for targeted research problem. After that, outer PP nonwoven layer of same composition of PP inner layer was attached to make three layer composite structure of filter material. Purpose of additional outer microfibrous PP layer was to provide protection from larger micro scale particles and share the overall filtration load of inner nanofibrous layer.

Furthermore, outer surface PP nonwoven layer was plasm surface modified to induced polarity in the resultant composite filter structure. The basic objective of plasma surface modification was to capture fine particles on outer surface of resultant filter material by inducing polarity and further reducing the filtration load of inner nanofibrous layer for better filtration efficiency and lower pressure drop value.

On the basis of above structural design, three chapters of results and discussion were reported based on step by step process. As a first step, chitosan base nanofibres were produced by

varying different concentrations of chitosan. Use of chitosan was due to its natural antibacterial property and ability to electrospun for nanofibre production which were both required to tackle byssinosis related cotton dust bacterial endotoxins. The basic object of this chapter was to produce chitosan nanofibres with highest possible polymer concentration for better antibacterial efficiency with fine distribution of nanofibres diameter. Best combination of electrospun parameter with highest chitosan concentration were reported and further used for the development of all respiratory filter samples.

After the development of all nanocomposite respiratory filter samples with and without plasma surface modification, characterisation was done to find out the best nanocomposite combination effective against the fine cotton dust related aerosols and bacterial endotoxin base contamination. Results of best samples against targeted aerosols were reported in chapter 5 and concluded its effectiveness towards the potential reduction of byssinosis in textile cotton workers.

In chapter 6, impact of plasma surface modification on filtration efficiency of filter samples was explained. On the basis of results, conclusion was made on the effectiveness of surface treatment towards the filtration performance.

3.2 Materials

Chitosan was used for the production of nanofibres with the help of electrospinning. Chitosan is an abundantly occurring amino polysaccharide of cationic nature. Chitosan is based upon chitin [1] and being used all over the world due to the affordability, versatility and anti-microbial activity. It has good defensive potential against the microbes, toxins, viruses, and fungi, etc. [2][3] Therefore, chitosan nanofibres were used to examine specified antibacterial

functionality as well as to increase the surface area of the proposed respiratory filter for the analysis of filtration performance against byssinosis. Low molecular weight powdered chitosan having a 75-85% degree of deacetylation was purchased from Sigma Aldrich. The molecular weight of the purchased chitosan ranges from 50000-190000 Da which is totally based on the viscosity of the polymer. Polyethylene oxide (PEO) was purchased in powder form, from Sigma Aldrich with a molecular weight value, of 600 KDa. Glacial acetic acid (AcOH 99-100%) was also purchased from Sigma Aldrich and used as a solvent for chitosan and PEO. Deionized water was used for the dilution of glacial acetic acid concentration up to 50%.

Polypropylene (PP) nonwoven substrates layers were used as a support fabric to make sandwiched respiratory filter structure. Pure spunbonded and nonwoven polypropylene (PP) is being used for the production in barrier fabrics due to its lights weight and low price with a combination of good mechanical properties. It has very low moisture regain and good resistance to mildew attack, which both are attractive properties for the filtration. Furthermore, recycling polypropylene is also an advantage for the usage in product manufacturing. [4] Different PP nonwoven substrate was purchased with a range of areal density (g/m^2) and fibre diameters (µm) as shown in Table 3.1. Spunbonded and meltblown polypropylene sheets were used as an outer layer as well as a supporting web layer for the coating of chitosan nanofibres to produce an effective filter.

Table 3.1: PP nonwoven substrate details

Sr. #	GSM	Supplier	Average Fibre Diameter (µm)	Average Pore Size (µm)
1	25 (Meltblown)	Jiangxi Haorui Industry China	2.56	2.08 ± 0.62
2	50 (Meltblown)	Jiangxi Haorui Industry China	2.56	2.08 ± 0.62
3	70 (Spunbonded)	KBT Ltd Birmingham	23	10.08 ± 4.64
4	100 (Spunbonded)	Veijun Nonwoven China	34	16.81± 4.54

3.3 Methodology

The PP inner layer will be coated by nanofibres of chitosan for the improvement in filtration properties against fine cotton dust particulates and bacterial contaminations. The electrospinning methodology of chitosan is described below.

3.3.1 Solution Preparation for Electrospinning

Low molecular weight chitosan (CS) from 1g to 7g was dissolved in a solvent containing 50% (v/v) glacial acetic acid (as shown in Table 4.1) by continuous magnetic stirring for 24 hours to obtain 1% to 7% (w/v) chitosan solution. PEO (3g) was also dissolved in a solvent containing 50% (v/v) glacial acetic acid separately by overnight magnetic stirring. After that, a blend of each chitosan solution and PEO solution was prepared with 8:2 ratio respectively by four hours of continuous mixing. Every sample of chitosan solution were prepared with the addition of co-spinning agent PEO. As an example, 8 parts of the 1% chitosan solution is mixed with 2 parts of 3% (w/v) PEO solution to obtain the solution for electrospinning of sample N1 TO N4 in Table 4.1. This means that the final electrospinning solution contains 0.8% of chitosan and 0.6% PEO.

Table 3.2: Electrospinning process optimisation plan with different % of chitosan

Chitosan Electrospinning Process Optimisation				
Sample ID	**Chitosan Solution (%*)**	**Spinning Solution of Chitosan (%*)**	**Voltage (kV)**	**Working Distance (cm)**
N1	1	0.8	15	15
N2	1	0.8	15	10
N3	1	0.8	20	15
N4	1	0.8	20	10
N5	2	1.6	15	15
N6	2	1.6	15	10
N7	2	1.6	20	15
N8	2	1.6	20	10
N9	3	2.4	15	15
N10	3	2.4	15	10
N11	3	2.4	20	15
N12	3	2.4	20	10
N13	4	3.2	15	15
N14	4	3.2	15	10
N15	4	3.2	20	15
N16	4	3.2	20	10
N17	5	4	15	15
N18	5	4	15	10
N19	5	4	20	15
N20	5	4	20	10
N21	6	4.8	15	15
N22	6	4.8	15	10
N23	6	4.8	20	15
N24	6	4.8	20	10
N25	7	5.6	15	15
N26	7	5.6	15	10
N27	7	5.6	20	15
N28	7	5.6	20	10

*Note: The % in the table refers to % of chitosan in the solution

However, in all the prepared samples percentage contribution of PEO remained 0.6% due to its fixed solution ratio, while chitosan percentages were increased with increase of solution percentage. The solubility of chitosan in glacial acetic acid enables the process to be non-toxic and eco-friendly with respect to solvent usage. Detailed sample identification of all chitosan concentrations and process variables are shown in Table 3.2.

3.3.2 Electrospinning Parameters

Chitosan (CS) nanofibres were produced by using electrospinning and collected on a rotating drum collector. The electrospinning setup for all the experiments is shown in Figure 3.2. Each blended CS:PEO solution was poured in a 20 ml syringe and mounted on the pump with a tight grip holder. The syringe was connected with a 19-gauge blunt tip needle. Combination of optimal parameters including, 1 mL/hour flow rate and 15kV to 20 kV voltages were applied for the production of nanofibres. The distance between the needle tip and the PP substrate mounted collector was maintained to 10 cm. Samples identification of different % solution of chitosan and process parameters for electrospinning are shown in Table 3.2. All the experiments were performed in (22±1 °C) and relative humidity was 42% under the atmospheric condition. The electrospinning process for each combination of CS/PEO solution was repeated thrice.

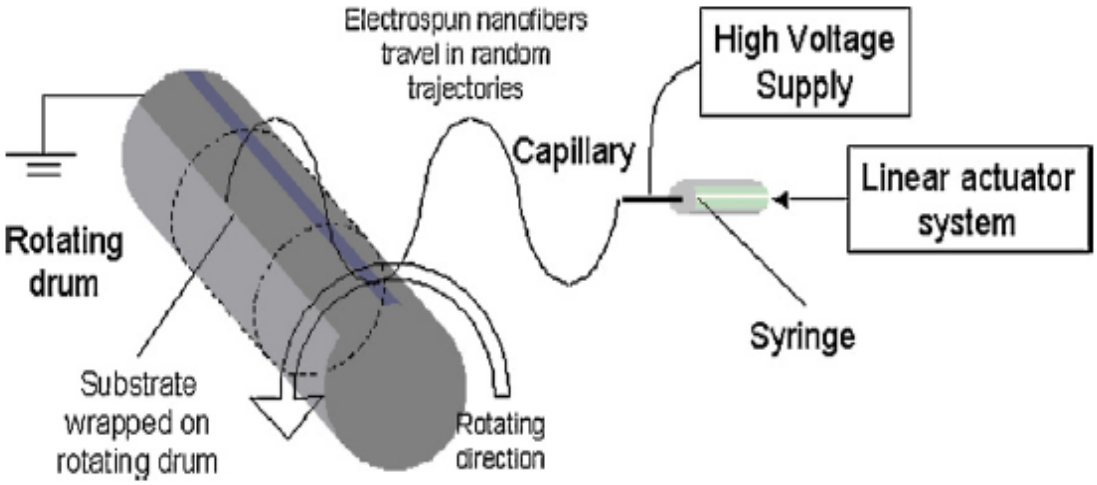

Figure 3.2: Schematic diagram of electrospinning unit for nanofibre production [5]

3.3.3 Preparation of respiratory filters with nanofibre coating

Chitosan (CS) nanofibres were produced by using the electrospinning method and directly coated on the each PP nonwoven substrate (Table 3.3) by wrapping it on the rotating drum collector. Three layer respiratory filter design is shown in Figure 3.1.

The surface area and pore size distribution of the filter are dependent on the amount of nanofibre and its uniform dispersion on the collecting PP substrate. However, excessive nanofibre coating can lead to a higher pressure drop and poor quality factor of the resultant respiratory filter [6]**.** Therefore, optimisation of nanofibre coating was carried out by varying different coating times (2h, 4h, 6h, and 8h). Thus, four different nanofibres coated PP substrate samples were produced in each category as mentioned in Table 3.3.

Table 3.3: Sample description of each PP nonwoven category after Nanofibre Coating

Sr. #	Description	Nanofibre Coating Time (h)
Sample 1	25 (Meltblown)	2
Sample 2		4
Sample 3		6
Sample 4		8
Sample 5	50 (Meltblown)	2
Sample 6		4
Sample 7		6
Sample 8		8
Sample 9	70 (Spunbonded)	2
Sample 10		4
Sample 11		6
Sample 12		8
Sample 13	100 (Spunbonded)	2
Sample 14		4
Sample 15		6
Sample 16		8

After the coating, each PP substrate was removed from the collector and placed in a fume cupboard for 12 hours to ensure the complete removal of volatile solvent from the coated nanofibres. Subsequently, all sixteen samples were dried in hot air oven later on. After that new uncoated PP substrate layer was placed on the top of the nanofibre holding PP substrate and joined them to make a multi-layer structure for the development of the composite respiratory filter. The whole process was repeated thrice in each category of each sample as shown in Table 3.3.

3.3.4 Plasma Surface Modification

All the developed respiratory filter samples were surface modified by using Low pressure plasma machine made of diener Electronic as shown in Figure 3.3. Oxygen (O_2) was used as a source of plasma generation, while plasma treatment time was five minutes for each sample. After the plasma treatment, each sample was placed in an airtight polybag to avoid further surface reactions caused by an open environment.

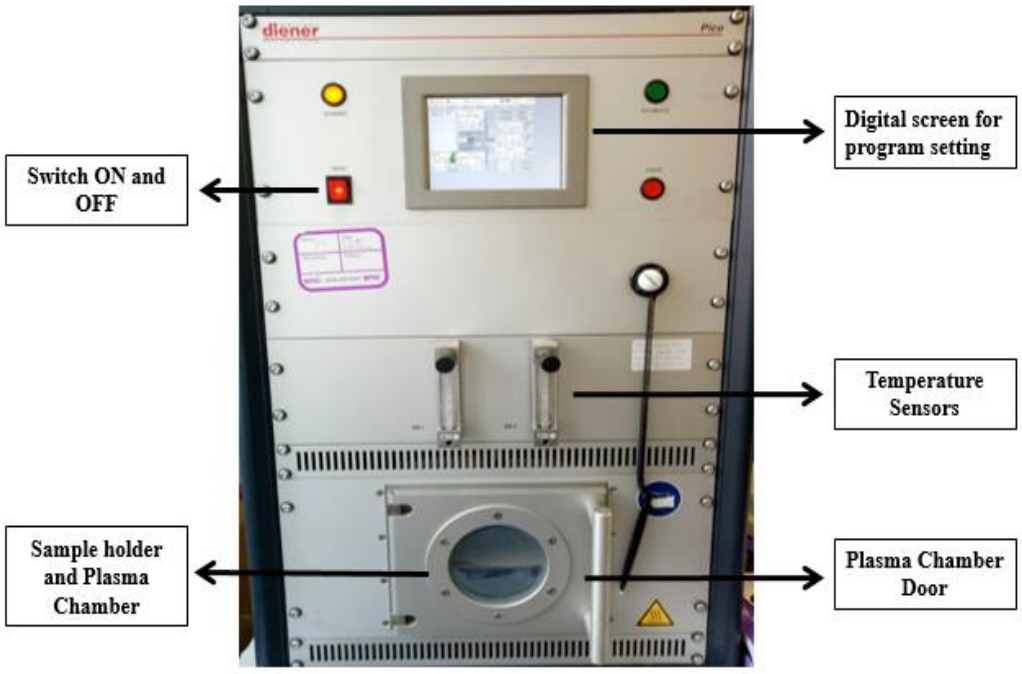

Figure 3.3: Low pressure plasma surface modification machine

The purpose of low-pressure plasma treatment is to increase the surface energy of the outer layer of the respiratory for the effective capturing mechanism which will help to reduce the pressure drop by keeping the same surface area. After that, all sixteen filter samples were evaluated against filtration performance and compared with the same twelve untreated samples

for the analysis of the results. Figure 3.4 shows the whole procedure of filter samples development and plasma surface modification.

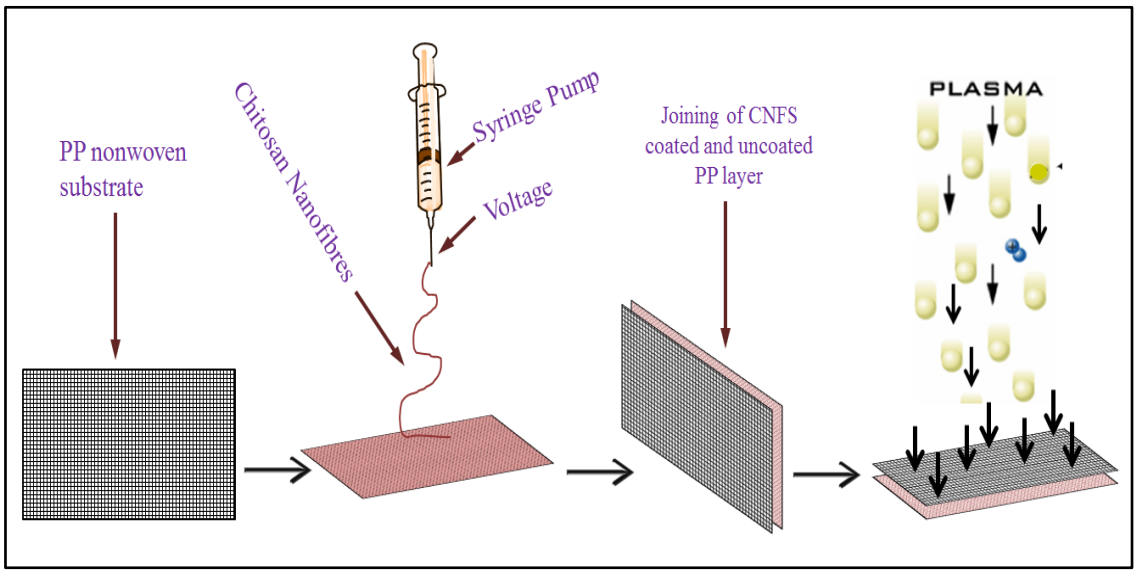

Figure 3.4: Schematic diagram of development of CSNF coated PP respiratory filter

3.4 Characterization

Surface morphology, fibre diameter (100 fibres each sample), and pore size distribution (100 pores each sample) of PP nonwoven substrate and chitosan nanofibres were analysed by using TESCAN MIRA3 (GMU VP Analytical FESEM) electron microscope as shown in Figure 3.5. Nanofibre add on (gsm) was calculated by weighing the sample before and after coating. Fourier transmission infrared spectroscopy (FTIR) was performed on NICOLET 5700121 spectrophotometer. FTIR peaks before and after coating were recorded to confirm the presence of chitosan after nanofibre coating on PP nonwoven substrate.

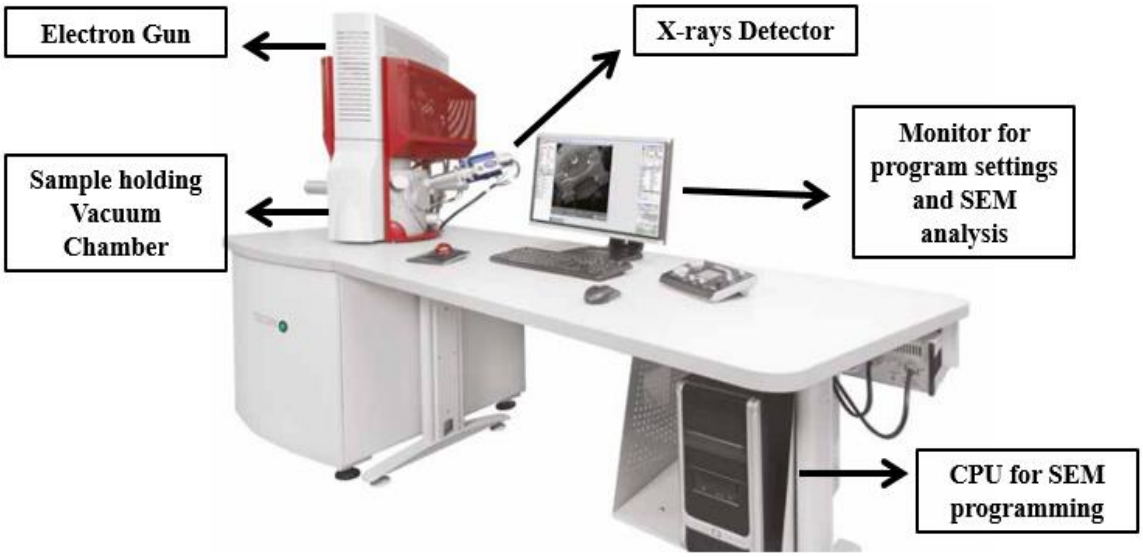

Figure 3.5. TESCAN MIRA3 (GMU VP Analytical FESEM) scanning electron microscope

3.4.1 Filtration efficiency testing

Filtration efficiency test was performed on the PALAS Promo 2000 system manufactured by PALAS particle technology, Germany as shown in Figure 3.7. The schematic diagram for the filtration efficiency process is shown in Figure 3.6.

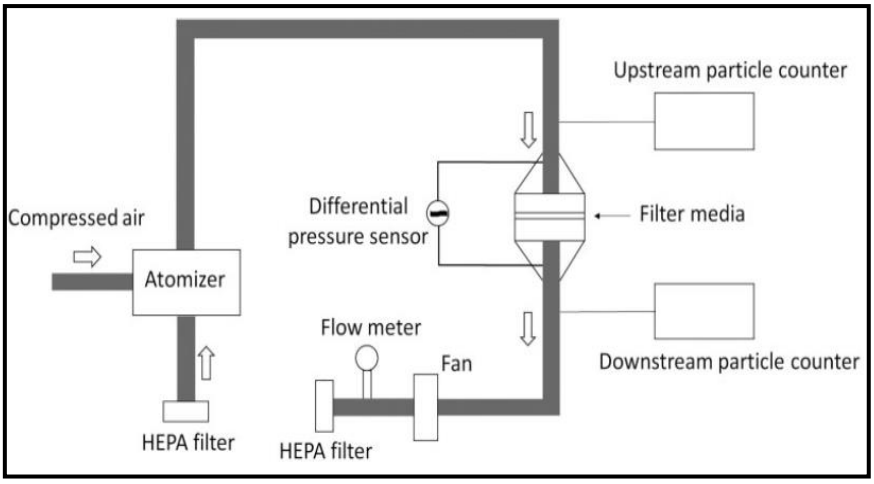

Figure 3.6: Respiratory Filter performance evaluation set-up [7]

Environmental aerosol ranges from 100 nm to 2.5 µm were used for the filtration efficiency evaluation because this diameter range of cotton dust particle found in a textile environment responsible for the byssinosis in textile workers. Flow rate is very important with respect to filtration efficiency. There are different flow rates, 30 l/min and 85 l/min, were reported in the literature, according to different types of working conditions for filtration performance analysis. The first represents work with normal intensity and the second used for heavy workload conditions [8]. All the samples were tested on flow rate 85 l/min as per NIOSH test condition under extreme work circumstances [9]**.** Each sample was mounted on the sample holder of the machine and particle penetration was evaluated upstream and downstream of the sample penetration. Filtration efficiency calculation was done as per the following equation 3.1.

$$\eta = \frac{n2-n1}{n2} \tag{3.1}$$

η is filtration efficiency while n1 and n2 are the aerosol concentrations on downstream and upstream of the filter respectively.

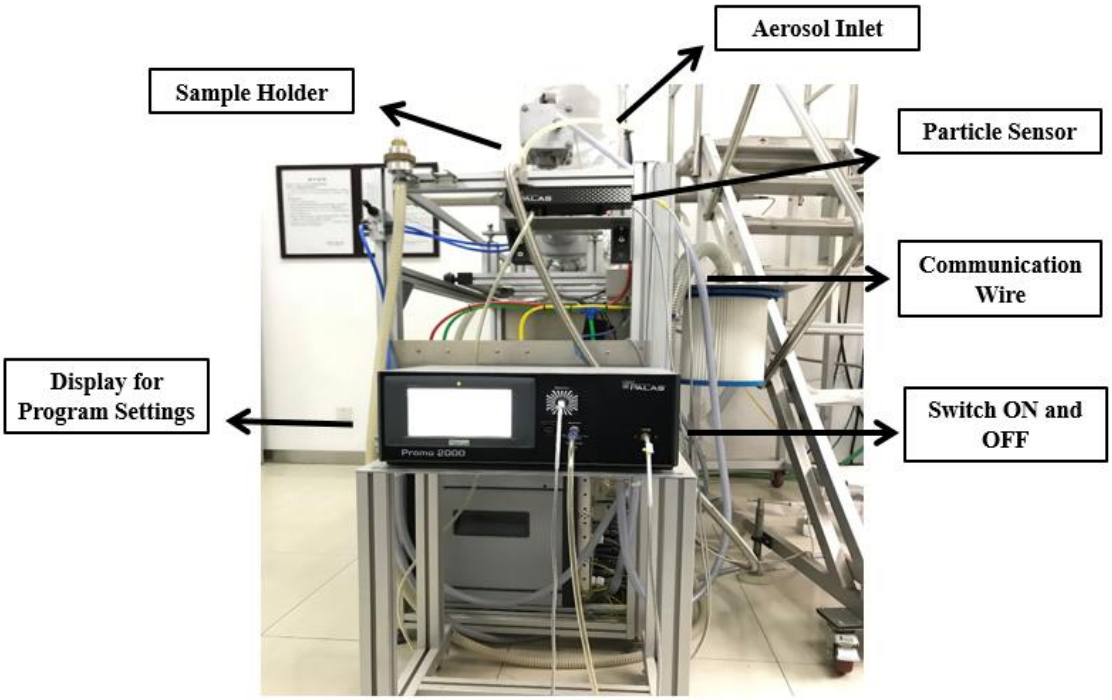

Figure 3.7: PALAS Promo 2000 system for filtration efficiency analysis

3.4.2 Pressure drop and quality factor calculation

Pressure drop and quality factor are very important for the evaluation of filter media and directly related to the ease of breathability [10]. Pressure drop was measured by using the SDLATLAS air permeability tester and calculated by using equation 3.2. On the basis of filtration efficiency and pressure drop results, quality factor (Q) was calculated by using the following equation 3.3.

$$\Delta P = P1 - P2 \tag{3.2}$$

$$Q = \frac{-\ln(1-^{\eta})}{\Delta P} \tag{3.3}$$

P is the fractional aerosol penetration while ΔP is the pressure drop. P1 and P2 are upstream and downstream air pressure respectively, while Q denotes the overall quality factor of the filter [7].

3.4.3 Water contact angle test

Plasma surface activation on plastics normally decays with time due to environmental contaminations and thermodynamic reorientation of polar groups towards the bulk of the surface [11]. Decay of plasma surface modification is also important in terms of storage after the manufacturing of filter material and will also provide information about the time based effectiveness of treatment. Therefore, decays of plasma treatment on the outer layer of 50 GSM CSNF coated PP substrate was analysed by using water contact angle tests. The selected sample was tested on the same day of plasma treatment and after 15, 30, and 60 days of plasma treatment to measure the decay.

Water contact angle test was performed by using KRUSS DSA100 drop shape analyser (DSA) instrument as shown in Figure 3.8. Drop shape analysis (DSA) involves image analysis of the shadow image of a sessile drop to measure the contact angle on the surface. Fitted camera in the instrument records the image of the drop on the surface and transfers to the drop shape analysis software. Then, the contact angle is measured from the baseline of drop on the sample surface with the help of DSA software.

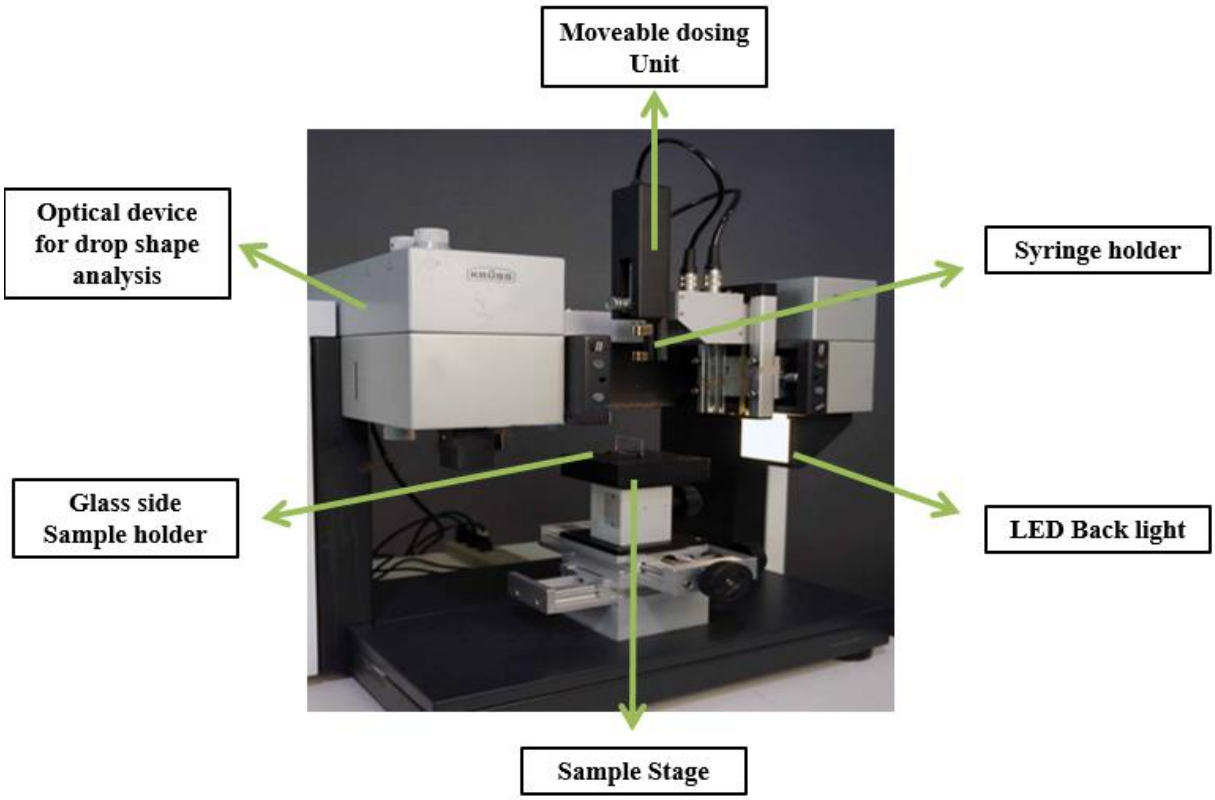

Figure 3.8: KRUSS DSA100 drop shape analyser (DSA) for water contact angle test

3.4.4 Anti-bacterial efficiency of the filter

The anti-bacterial property of the coated chitosan nanofibre (CSNF) was evaluated by following ASTM E2149-13a, 2013. Biosafety level 1 Pantoea agglomerans (Formerly *Enterobacter agglomerans*) gram negative bacterial strains were selected for the test. According to literature, Enterobacter agglomerans were found to be the most abundant form of Pantoea in cotton dust [12]**.** *Pantoea agglomerans* (AATCC-27155, formerly *Enterobacter agglomerans*) were purchased from LGS Standards, Teddington, UK. As per the above mentioned testing standard, chitosan nanofibres (0.2g) were immersed in 10ml dilute bacterial suspension (10^5 CFU/ml) by using sterilised tube with a 1:50 ratio. After mixing, the tube was

placed in an incubator at 37°C temperature for 12 to 24 hours. One test sample of bacterial suspension (without CSNF) was also prepared for the comparison of results. After incubation, every sample was serial diluted 10 times with a ratio of 1 to 10. The diluted samples were spread on agar plates and further incubated for 24 hours at 37 °C for the counting of survived bacterial colonies. This test was conducted three times. Antibacterial efficiency as a function of reduction in bacterial growth (R) was calculated by using equation 3.4.

$$R(\%) = [(A - B) \div A] \times 100 \quad (3.4)$$

Where A donates the number of grown bacteria in control sample, B represents the grown bacteria in test sample. Furthermore, performance of filtration efficiency was explained against the extended incubation time 12h and 24h. The purpose of extended time selection is related to the working condition and reusable possibility of the developed filter material in textile sector. In textile spinning mills, normal working shift time varies from 8h to 12h per day and workers are meant to use the provided mask for multiple shifts. Therefore, extended test incubation time was selected due to specified use of the filter material in textile environment.

References

[1] P. B. Malafaya, G. A. Silva, and R. L. Reis, "Natural-origin polymers as carriers and scaffolds for biomolecules and cell delivery in tissue engineering applications," *Adv. Drug Deliv. Rev.*, vol. 59, no. 4–5, pp. 207–233, 2007.

[2] K. Kurita, "Chitin and chitosan: Functional biopolymers from marine crustaceans," *Mar. Biotechnol.*, vol. 8, no. 3, pp. 203–226, 2006.

[3] M. Arkoun, F. Daigle, M. C. Heuzey, and A. Ajji, "Mechanism of action of electrospun chitosan-based nanofibres against meat spoilage and pathogenic bacteria," *Molecules*, vol. 22, no. 4, 2017.

[4] "Spunbonded Polypropylene," *techtex*. [Online]. Available: http://www.techtex.co.uk/industrial/products/non-woven/spunbonded-polypropylene. [Accessed: 23-Jul-2017].

[5] W. W. F. Leung, C. H. Hung, and P. T. Yuen, "Effect of face velocity, nanofibre packing density and thickness on filtration performance of filters with nanofibres coated on a substrate," *Sep. Purif. Technol.*, vol. 71, no. 1, pp. 30–37, 2010.

[6] M. Tang, J. Hu, Y. Liang, and D. Y. H. Pui, "Pressure drop, penetration and quality factor of filter paper containing nanofibres," *Text. Res. J.*, vol. 87, no. 4, pp. 498–508, 2017.

[7] V. V. Kadam, L. Wang, and R. Padhye, "Electrospun nanofibre materials to filter air pollutants – A review," *J. Ind. Text.*, vol. 47, no. 8, pp. 2253–2280, 2018.

[8] R. M. Eninger, T. Honda, A. Adhikari, H. Heinonen-Tanski, T. Reponen, and S. A. Grinshpun, "Filter performance of N99 and N95 facepiece respirators against viruses

and ultrafine particles," *Ann. Occup. Hyg.*, vol. 52, no. 5, pp. 385–396, 2008.

[9] J. P. Eshbaugh, P. D. Gardner, A. W. Richardson, and K. C. Hofacre, "N95 and P100 Respirator Filter Efficiency Under High Constant and Cyclic Flow," *J. Occup. Environ. Hyg.*, vol. 6, no. 1, pp. 52–61, 2008.

[10] S. Sundarrajan, K. L. Tan, S. H. Lim, and S. Ramakrishna, "Electrospun nanofibres for air filtration applications," *Procedia Eng.*, vol. 75, pp. 159–163, 2014.

[11] R. A. Jelil, *A review of low-temperature plasma treatment of textile materials*, vol. 50, no. 18. 2015.

[12] M. D. Ragnar Rylander, "Bacterial Toxins and Etiology of Byssinosis," *Chest*, vol. 79, no. 4, 1981.

Chapter 4: Process optimisation of chitosan nanofibres production

Muhammad Tauseef Khawar, Hugh Gong, Jiashen Li

Abstract

Chitosan (CS) is an important biomaterial due to its various application in filtration, wound dressings, tissue engineering and as a natural antimicrobial agent. Therefore, the electrospinning process optimisation was carried out with the aim to produce chitosan nanofibres with the maximum chitosan concentration for filtration application. Polyethylene oxide (PEO) was used as a co-spinning agent and glacial acetic acid was used as a solvent during electrospinning. Surface morphology and fibre diameter analysis were carried out by using scanning electron microscopy (SEM). Results illustrated that smooth nanofibre production was achieved from solutions with 1% to 3.5% chitosan. When the concentration of chitosan was 4% or above, nanofibres could not be produced due to high viscosity and high surface tension of the solution. Furthermore, fibre diameter analysis illustrated that higher applied voltage and longer working distance resulted in finer nanofibres.

Keywords: Chitosan, filtration, electrospinning, concentration, fibre diameter, nanofibres

4.1 Introduction

The electrospinning is an effective process for the production of nanofibres. This technology is a combination of electrospray and solution dry spinning [1]. In the electrospinning process, high voltage is applied between the needle tip of the polymer containing a syringe and the collector, which induces a charge in the polymer solution. Applied high voltage in the polymer enables the deformation of the spherical droplet shape of the polymer to a conical shape [2]. When the electrostatic repulsion force value increases from the value of polymer surface tension, a charged fine polymer jet ejects from the Taylor cone and is collected on the opposite pole of the electric field. During traveling from the tip to the collector, the solvent evaporates [3]. This method of fine fibre production enables high surface area, high aspect ratio and interconnected porous structure in the resultant membrane [4][5]. Due to their versatility, developed electrospun nanofibres are commercially beneficial in the field of air filtration [6], drug delivery, tissue engineering, and wound healing [7][8][9]. There are many natural and synthetic polymers which are spinnable by using electrospinning and are used in various applications.

Chitosan is a natural polymer and an abundantly occurring amino polysaccharide of cationic nature. Chitosan is produced from the deacetylation of chitin [10]. The main sources of chitin are skeletal materials of sea creatures, including crabs, prawns, lobsters, shrimps, and cephalopods [11]. It is also nontoxic, biodegradable, and biocompatible. Various studies have shown that chitosan possesses anti-microbial effects against bacteria, fungi, and viruses [12][13]. Chitosan can be converted into fibre form by using electrospinning. Due to its high viscosity and surface tension, it is being electrospun by using different co-spinning polymers. The blending of chitosan can be with alginate, collagen, poly (ethylene oxide), starch, silk

fibroin, poly (vinyl alcohol) [14][15][16]. Poly (L-lactic acid) membrane coated with chitosan can be used for water filtration by removing copper ion [17].

Chitosan based nanofibrous membrane was also reported for antibacterial water filtration application[18]. Polycaprolactone was used as a co-spinning agent and fibres were produced with percentages of chitosan from 25% to 75%. Results showed that 25% of chitosan supported membrane showed excellent filtration performance against 300nm particulates. Production of chitosan nanofibre with polyethylene dioxide (PEO) as a co-spinning agent by using 0.5M acetic acid as a solvent was also reported [19]. Results indicated the smooth production of nanofibres up to 5 wt% of chitosan with 20 wt% PEO. Furthermore, poly (vinyl alcohol-co-ethylene) nanofibrous membrane was produced with chitosan and graphene oxide coating to make multicomponent structure which showed inactivation of E. coli and S.aureus bacteria up to 99.5% [20]. The antibacterial property of chitosan nanofibres with PEO as a co-spinning agent was also investigated by Arkoun et al [21]. Their nanofibrous membrane exhibited good antibacterial property against different gram positive and gram negative bacterial species, and they recommended the chitosan nanofibrous membrane as a bacterial disruptor and perforator for the application in food packaging. Although many researchers have produced chitosan nanofibres with a combination of PEO but the achieved flow rate was reported up to 0.5ml/hour and the concentration of PEO was also reported to be very high. There is a lack of detailed process optimisation of chitosan electrospun nanofibres with a high flow rate up to 1ml/hour of low molecular weight chitosan.

In this study, a range of weight percentages of low molecular weight chitosan (1%, 2%, 3%, 4%, 5%, 6%, and 7%) solutions was prepared in 50% glacial acetic acid for the development of chitosan nanofibres by using a fixed 3 wt% of PEO. The effect of these process parameters on the surface morphology and fibre diameter were studied.

4.2 Experimental

4.2.1 Materials

Low molecular weight chitosan (Mw = 50,000-190,000 Da) was purchased from Sigma Aldrich. The degree of deacetylation of the supplied chitosan was 75-85%. Polyethylene oxide (PEO) was used as co-spinning for smooth nanofibres production. PEO (co-spinning agent) was purchased in powder form also from Sigma Aldrich. The molecular weight of PEO was 600 KDa. Glacial acetic acid (Mw = 60 Da) was also purchased from Sigma Aldrich and used as a solvent for the electrospinning process. Deionized water was used for the dilution of glacial acetic acid concentration up to 50%.

4.2.2 Solution Preparation for Electrospinning

Chitosan powder of the appropriate amount (1g to 7g) was dissolved in a solvent containing 50% (v/v) glacial acetic acid (as shown in Table 4.1) by continuous magnetic stirring for 24 hours to obtain 1% to 7% (w/v) chitosan solution. PEO (3g) was also dissolved in a solvent containing 50% (v/v) glacial acetic acid separately by overnight magnetic stirring. After that, a blend of each chitosan solution and PEO solution was prepared with 8:2 ratio respectively by four hours of continuous mixing. Every sample of chitosan solution were prepared with the addition of co-spinning agent PEO. As an example, 8 parts of the 1% (w/v) chitosan solution is mixed with 2 parts of 3% (w/v) PEO solution to obtain the solution for electrospinning of sample N1 TO N4 in Table 4.1. This means that the final electrospinning solution contains 0.8% (w/v) of chitosan and 0.6% (w/v) PEO. However, in all the prepared samples percentage contribution of PEO remained 0.6% due to its fixed solution ratio, while chitosan percentages were increased with increase of solution percentage. The solubility of chitosan in glacial acetic acid enables the process to be non-toxic and eco-friendly with respect to solvent usage.

Table 4.1: Electrospinning process optimisation plan with different % of chitosan

Chitosan Electrospinning Process Optimisation				
Sample ID	**Chitosan Solution (%*)**	**Spinning Solution of Chitosan (%*)**	**Voltage (kV)**	**Working Distance (cm)**
N1	1	0.8	15	15
N2	1	0.8	15	10
N3	1	0.8	20	15
N4	1	0.8	20	10
N5	2	1.6	15	15
N6	2	1.6	15	10
N7	2	1.6	20	15
N8	2	1.6	20	10
N9	3	2.4	15	15
N10	3	2.4	15	10
N11	3	2.4	20	15
N12	3	2.4	20	10
N13	4	3.2	15	15
N14	4	3.2	15	10
N15	4	3.2	20	15
N16	4	3.2	20	10
N17	5	4	15	15
N18	5	4	15	10
N19	5	4	20	15
N20	5	4	20	10
N21	6	4.8	15	15
N22	6	4.8	15	10
N23	6	4.8	20	15
N24	6	4.8	20	10
N25	7	5.6	15	15
N26	7	5.6	15	10
N27	7	5.6	20	15
N28	7	5.6	20	10

*Note: The % in the table refers to % of chitosan in the solution

4.2.3 Electrospinning Parameters

Chitosan (CS) nanofibres were produced by using electrospinning and collected on a rotating drum collector as shown in Figure 4.1. Each blended CS:PEO solution was poured in a 20 ml syringe and mounted on the pump with a tight grip holder. The syringe was connected with a 19-gauge blunt tip needle. 1 mL/hour flow rate and 15kV to 20 kV voltages were applied for the production of nanofibres. The distance between the needle tip and the PP substrate mounted collector was maintained at 10 cm. Sample identification of different % solution of chitosan and process parameters for electrospinning are shown in Table 4.1. All the experiments were performed in atmospheric condition (22±1 °C, 42-45% RH). Electrospinning process for each combination of CS/PEO solution was repeated thrice.

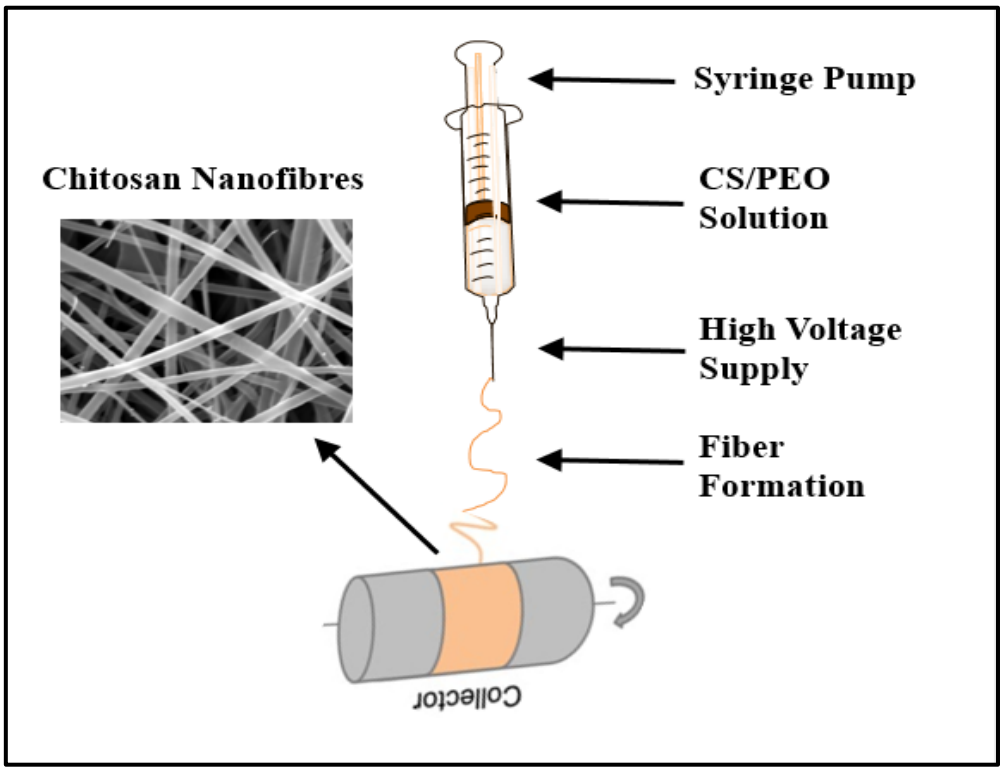

Figure 4.1: Electrospinning setup for the production of chitosan nanofibres

4.2.4 Characterization

The surface morphology of electrospun chitosan-based nanofibres (CSNF) was evaluated by using high performance field emission scanning electron microscope (TESCAN MIRA3 GMU VP Analytical FESEM). Image analysis was performed at 15kv voltage. The average fibre diameter (100 fibres each sample), was examined by using ImageJ computer software. Randomly chosen three hundred nanofibres in each CS/PEO combination (as shown in Table 4.1) were selected for the quantification of surface morphology.

4.3 Results and Discussion

All the combinations of different concentrations of chitosan were electrospun as per Table 4.1 process parameters. The results of all the samples are given in Table 4.2 and graphically shown in Figure 4.2.

Table 4.2: Electrospinning results of all combinations of different % solutions of chitosan

Electrospinning results of different % solutions of chitosan							
Sample ID	**% Solution of chitosan**	**Voltage (kV)**	**Working Distance (cm)**	**Fibre Formation Results**	**Remarks**	**Average Fibre Diameter (nm)**	**Standard Deviation (SD)**
N1	1	15	15	Fibres	Smooth Production	130	54
N2	1	15	10	Fibres	Smooth Production	163	61
N3	1	20	15	Fibres	Smooth Production	91	19
N4	1	20	10	Fibres	Smooth Production	115	43
N5	2	15	15	Fibres	Smooth Production	172	31

N6	2	15	10	Fibres	Smooth Production	207	53
N7	2	20	15	Fibres	Smooth Production	135	27
N8	2	20	10	Fibres	Smooth Production	155	53
N9	3	15	15	Fibres	Smooth Production	185	28
N10	3	15	10	Fibres	Smooth Production	227	53
N11	3	20	15	Fibres	Smooth Production	154	23
N12	3	20	10	Fibres	Smooth Production	175	46
N13	4	15	15	No Fibre	Solution wastage	N/A	N/A
N14	4	15	10	Beaded Fibres	Solution wastage	N/A	N/A
N15	4	20	15	No Fibre	Solution wastage	N/A	N/A
N16	4	20	10	No Fibre	Solution wastage	N/A	N/A
N17	5	15	15	No Fibre	Solution wastage	N/A	N/A
N18	5	15	10	No Fibre	Solution wastage	N/A	N/A
N19	5	20	15	No Fibre	Solution wastage	N/A	N/A
N20	5	20	10	No Fibre	Solution wastage	N/A	N/A
N21	6	15	15	No Fibre	Solution wastage	N/A	N/A
N22	6	15	10	No Fibre	Solution wastage	N/A	N/A
N23	6	20	15	No Fibre	Solution wastage	N/A	N/A
N24	6	20	10	No Fibre	Solution wastage	N/A	N/A
N25	7	15	15	No Fibre	Solution wastage	N/A	N/A
N26	7	15	10	No Fibre	Solution wastage	N/A	N/A
N27	7	20	15	No Fibre	Solution wastage	N/A	N/A
N28	7	20	10	No Fibre	Solution wastage	N/A	N/A

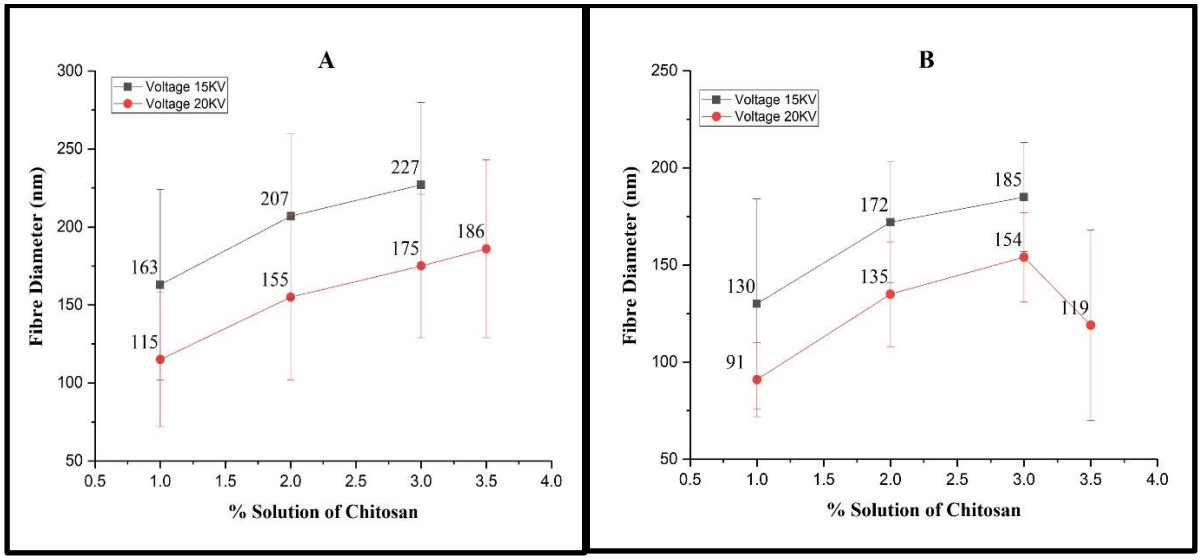

Figure 4.2: Impact of voltage and working distance on nanofibre diameter (A) voltage impact on fibre diamter at 10cm working distance, (B) votage impact on fibre diameter at 15cm working distance

4.3.1 (1%) Chitosan containing Nanofibres

Experimental results of 1% solution of chitosan nanofibres on two different working distance and high voltages are shown in Table 4.2 with samples from N1 to N4. All four samples showed smooth chitosan nanofibres without beads. Figure 4.3 shows the surface morphology of samples N1 and N2 which were produced at 15kv voltage while keeping the working distance at 15cm and 10cm respectively. Results indicate that the average fibre diameter for sample N1 was 130nm, while the maximum and minimum fibre diameter was 56nm and 267nm respectively. In the case of sample N2, the average fibre diameter remained around 163nm, while the maximum and minimum fibre diameter was 66nm and 286nm respectively. Sample N1 showed thinner fibre than sample N2, due to longer working distance.

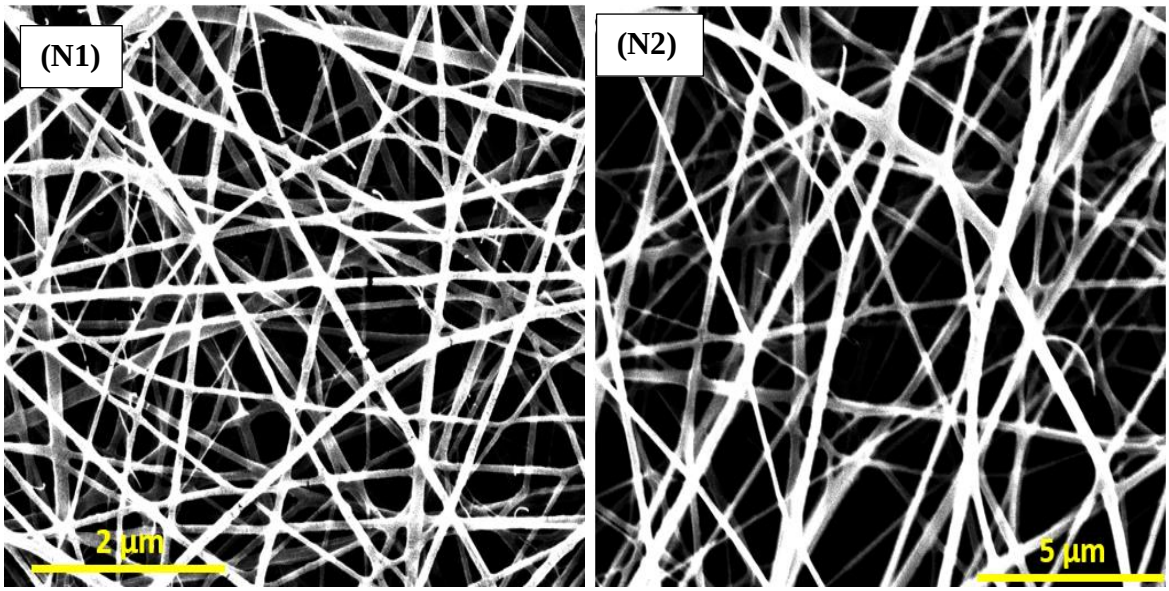

Figure 4.3: SEM image of 1% chitosan containing nanofibres at 15kv voltage with (N1) working distance 15cm, (N2) working distnace 10cm

Figure 4.4 shows the surface morphology of samples N3 and N4 which were produced at 20kv voltage while keeping the working distance at 15cm and 10cm respectively. Chitosan nanofibres produced from both samples are uniform and bead free. The average fibre diameter for sample N3 was 91nm, while the maximum and minimum fibre diameter was 28nm and 137nm respectively. In case of sample N4, the average fibre diameters were 115nm, while the maximum and minimum fibre diameter value remained at 55nm and 235nm respectively. Sample N3 also showed thinner fibre than the sample N4, due to a longer working distance.

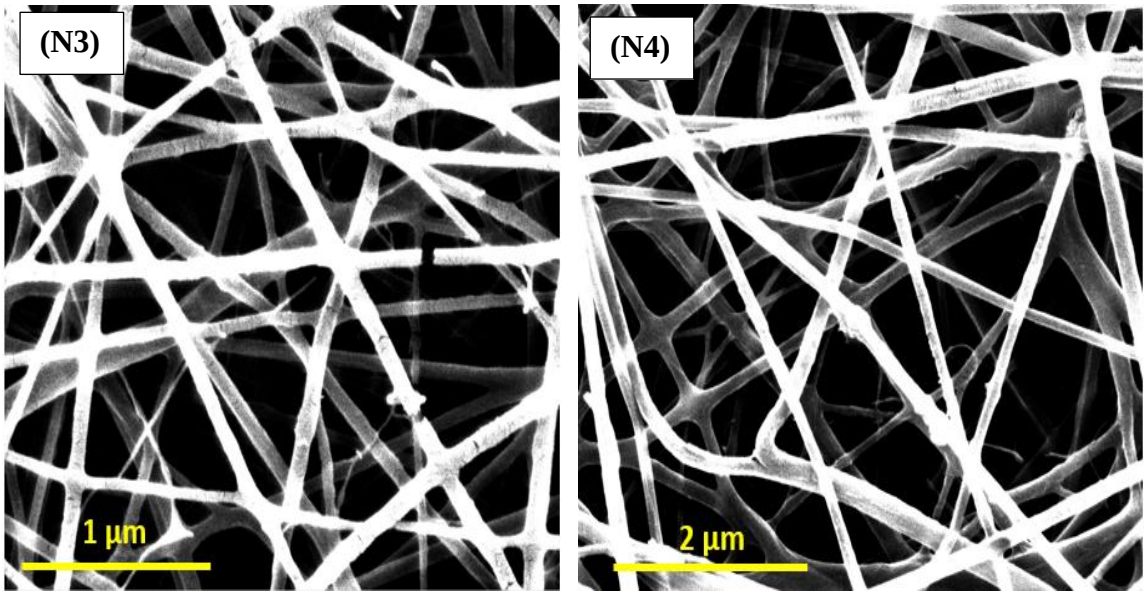

Figure 4.4: SEM image of 1% chitosan containing nanofibres at 20kv voltage with (N3) working distance 15cm, (N4) working distnace 10cm

In general, long working distance promotes higher draft in the polymer jet during electrospinning. However, bending instability (whipping instability) of the jet in the presence of an electric field is also very important in this phenomenon. Therefore, longer working distance accounts for higher whipping instability of the jet and is responsible for the reduction of the diameter of resultant fibre due to the acceleration and higher stretching before the fibre deposition on collector [22]. As a result fibre diameter reduces with the increase of working distance, as shown by the thinner fibres of samples N1 and N3 compared with those of samples N2 and N4.

Apart from the working distance, applied voltage is also very important to study regarding nanofibres morphology. Results showed that the average fibre diameter of chitosan nanofibres was also reduced with the increase of applied voltage from 15kv to 20kv, with the same working distance as reported in Table 4.2 and Figure 4.2. The average fibre diameter for samples N1 and N3 remained at 183nm and 71nm having applied voltage 15kv and 20kv

respectively. Similarly, sample N2 and N4 also showed same results pattern with the increase of applied voltage respectively. Hence it can be seen that applied electric field has inverse impact on fibre diameter and fibre diameter reduces with the increase of higher voltage, due to higher stretch induced in the polymer jet. Applied higher voltage generally determines the strength of the electric field, the amount of charge carried by the polymer jet and the strength of the interaction between the jet and applied electric field. A higher voltage will lead to higher stretching of the polymer jet and thinner fibre formation [23]..

4.3.2 (2%) Chitosan containing Nanofibres

Experimental results of 2% concentration of chitosan nanofibres on two different working distances and high voltages are shown in Table 4.2 and Figure 4.2 with sample identification from N5 to N8. All four samples showed uniform production of chitosan nanofibres without beads formation. Figure 4.5 shows the surface morphology of sample N5 and N6 at 15kv applied voltage while keeping the path length 15cm and 10cm respectively. Results illustrated that the average fibre diameter value for sample N5 was 172nm, while maximum and minimum fibre diameter value achieved 69nm and 315nm respectively. In the case of sample N6, average fibre diameters value reported 207nm, while maximum and minimum fibre diameter value achieved 78nm and 321nm respectively. However, sample N5 showed finer fibre production as compared to sample N6, due to longer working distance.

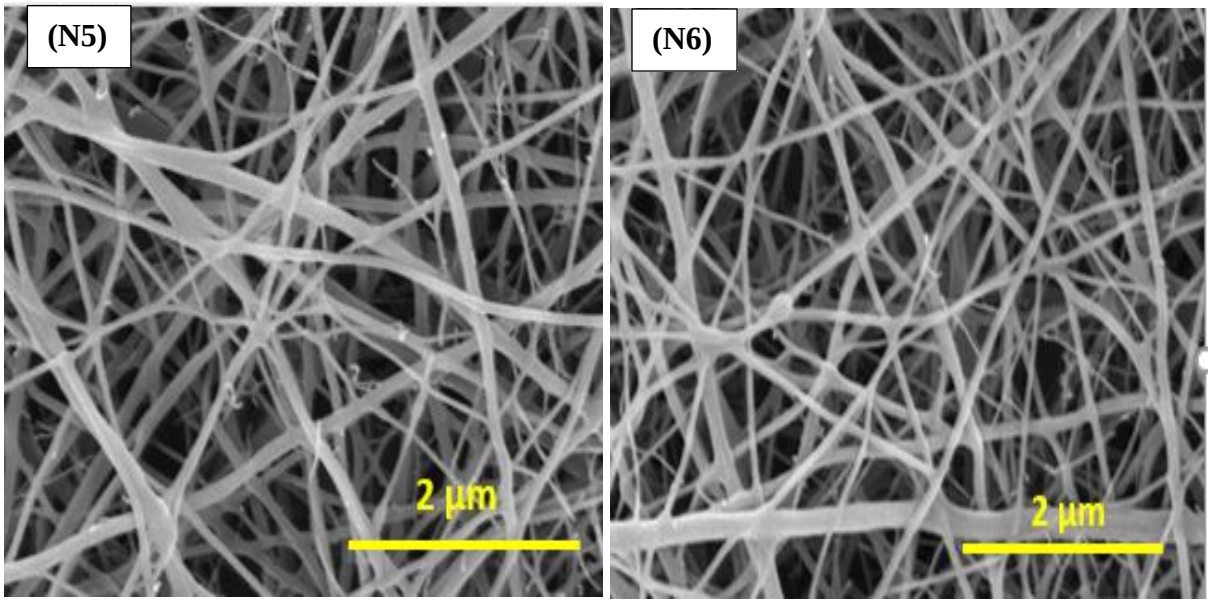

Figure 4.5: SEM image of 2% chitosan containing nanofibres at 15kv voltage with (N5) working distance 15cm, (N6) working distnace 10cm

Surface morphology of sample N7 and N8 is showed in Figure 4.6, which were fabricated at 20kv voltage while keeping the working distance 15cm and 10cm respectively. Both samples of chitosan reported smooth and uniform production of nanofibres as shown in Figure 4.6. Results indicated that the average fibre diameter value for sample N7 was 135nm while maximum and minimum fibre diameter value achieved 57nm and 296nm respectively as reported in Table 4.2 and Figure 4.2. In the case of sample N8, average fibre diameters value recorded 155nm, while maximum and minimum fibre diameter value remained 63nm and 305nm respectively. Comparatively, sample N7 also showed finer diameter fibre production from sample N8 due to the impact of path length.

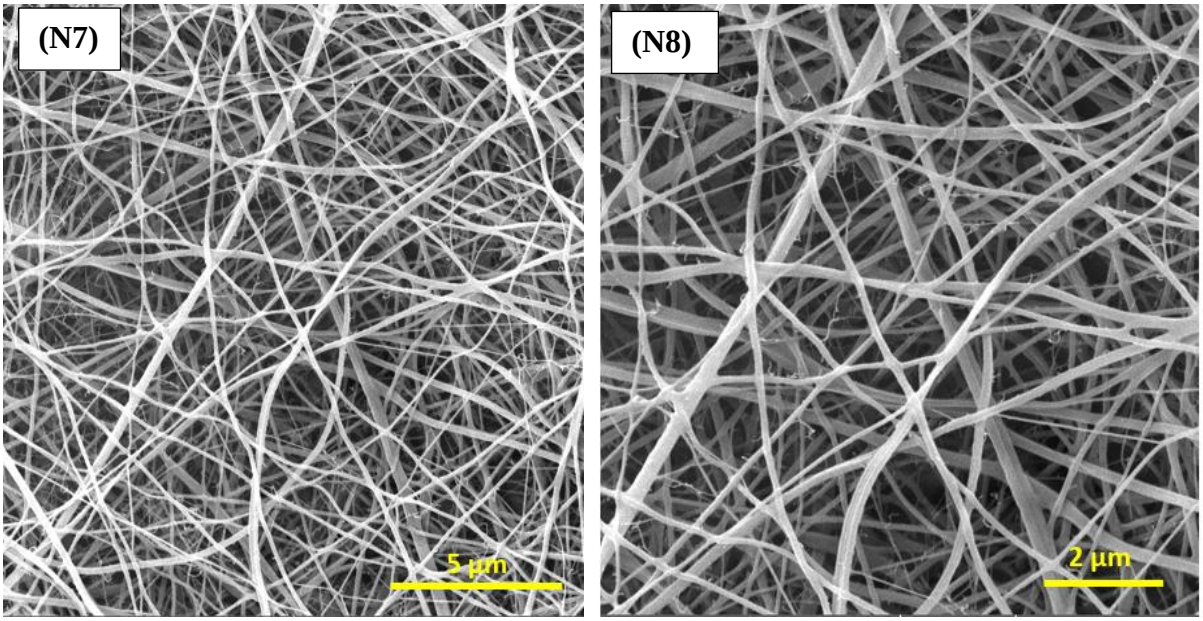

Figure 4.6: SEM image of 2% chitosan containing nanofibres at 20kv voltage with (N7) working distance 15cm, (N8) working distnace 10cm

As explained in section 4.3.1, working distance plays an important role in the finer fibre production. Longer path length and whipping instability lead to higher stretch and elongation of the polymer jet during the acceleration from tip to the collector. As a resultant, fibre diameter reduces with the increase of working distance. Conclusively, the same theory applies here in all four samples of 2% chitosan concentrated nanofibres and as a resultant, fibre diameter reduced with the increase of working distance. In addition to tip to collector path length, a higher value of applied voltage also reduced the diameter of developed nanofibres. Results showed that the average fibre diameter of chitosan nanofibres was also reduced with the increase of applied voltage from 15kv to 20kv, having the same working distance as reported in Table 4.2 and Figure 4.2. Average fibre diameter for sample N5 and N7 remained 172nm and 135nm having applied voltage 15kv and 20kv respectively. Similarly, sample N6 and N8 also showed similar results with the increase of applied voltage. According to literature, polymer jet stretching of the polymer jet and will favour thinner fibre formation due to the

strong electric field [23]. Therefore, the same theory applied here in all samples of 2% chitosan concentrated fabricated nanofibres.

4.3.3 (3%) Chitosan containing Nanofibres

Experimental results of 3% concentrated chitosan nanofibres are shown in Table 4.2 and Figure 4.2 with sample identification from N9 to N12. All four samples showed a smooth production of chitosan nanofibres. Figure 4.7 shows the surface morphology of sample N9 and N10 which were produced at 15kv voltage while keeping the working distance 15cm and 10cm respectively. Furthermore, the average fibre diameter value for sample N9 was 185nm, while maximum and minimum fibre diameter value achieved 72nm and 317nm respectively.

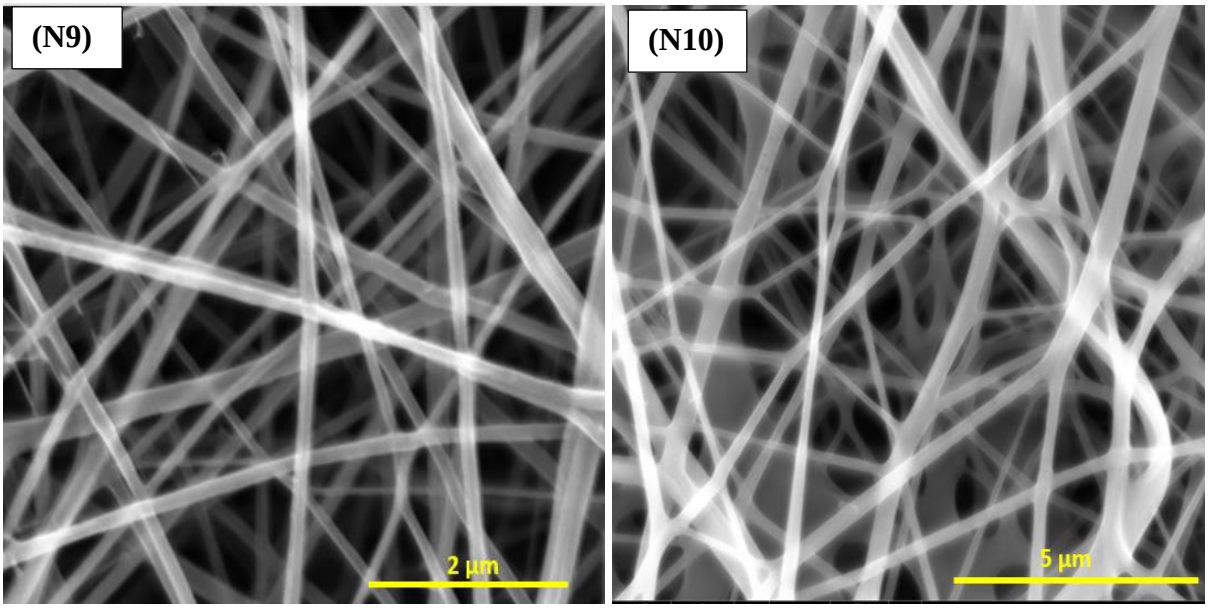

Figure 4.7: SEM image of 3% chitosan containing nanofibres at 15kv voltage with (N9) working distance 15cm, (N10) working distnace 10cm

In case of sample N10, average fibre diameters value remained 227nm, while maximum and minimum fibre diameter value achieved 80nm and 325m respectively. However, sample N9

showed thinner fibre production from sample N10, due to prolonged working distance during electrospinning.

Figure 4.8 shows the surface morphology of sample N11 and N13 which were produced at 20kv voltage while keeping the working distance 15cm and 10cm respectively. Results indicated that the average fibre diameter value for sample N11 was 154nm, while maximum and minimum fibre diameter value achieved 61nm and 302nm respectively. In the case of sample N12, average fibre diameters value recorded 175nm, while maximum and minimum fibre diameter value remained 66nm and 327nm respectively. Comparatively, sample N11 also showed thinner fibre production from sample N12, due to longer path length from tip to the collector.

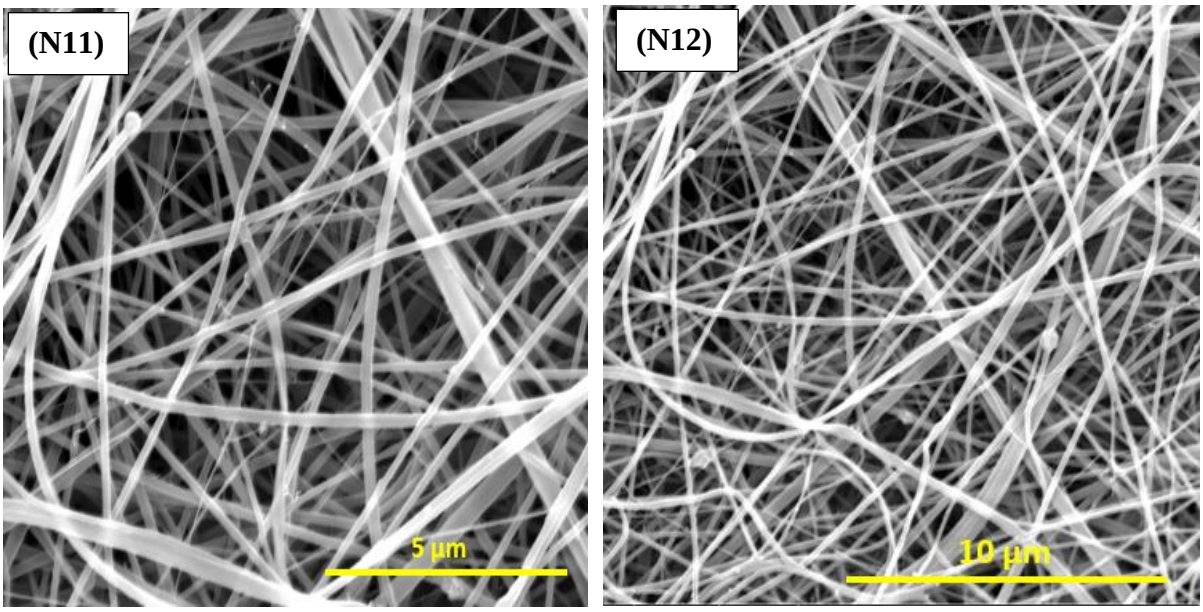

Figure 4.8: SEM image of 3% chitosan containing nanofibres at 20kv voltage with (N11) working distance 15cm, (N12) working distnace 10cm

Results also showed that the average fibre diameter of chitosan nanofibres was also reduced with the increase of applied voltage from 15kv to 20kv, having the same working distance as reported in Table 4.2 and Figure 4.2. Average fibre diameter for sample N9 and N11 remained

185nm and 154nm having applied voltage 15kv and 20kv respectively. Similarly, sample N10 and N12 also showed similar results with the increase of applied voltage. Impact of working distance and applied high voltage already explained in sections 4.3.1 and 4.3.2 and similar reasons of finer fibre production applied in all samples of 3% chitosan concentrated samples.

4.3.4 (4% to 7%) Chitosan containing nanofibres

Results of nanofibre production for all the samples of different concentrations of chitosan are reported in Table 4.2 and Figure 4.2. Results showed that nanofibre production remained smooth from 1% to 3% solution of chitosan. However, fibre production was not achieved at 4% and above chitosan concentrations due to gel formation of the prepared solution for electrospinning. At higher concentration, solution wastage was higher and the electrospinning process was unsuccessful due to the cohesive nature and higher viscosity of chitosan solution. Furthermore, the higher concentration of chitosan increases the amount of strong hydrogen bonding between $–NH_2$ and $–OH_2$ groups of chitosan molecules and hinders the flow of polymer solution which yields the unspinnable results. Therefore, higher voltage above 20kv with adjustments in working distance, solvent and co-spinning agent concentrations were required to further investigate the possibility of nanofibre production for 4% and above chitosan concentrations.

However, the experimental plan was modified to investigate the possibility of nanofibres production at 3.5% solution concentration of chitosan by keeping the process parameters same as per Table 4.2 and Figure 4.2. Detailed process parameters of 3.5% chitosan concentrated samples are shown in Table 4.3 and results of nanofibre production are explained in Table 4.4.

Table 4.3: Electrospinning process parameters for 3.5% chitosan concentration nanofibres production

Sample ID	Chitosan Solution (%*)	Spinning Solution of Chitosan (%*)	Voltage	Working Distance (cm)
N29	3.5	2.8%	15	15
N30	3.5	2.8%	15	10
N31	3.5	2.8%	20	15
N32	3.5	2.8%	20	10

*Note: The % in the table refers to % of chitosan in the solution

4.3.5 (3.5%) Chitosan containing Nanofibres

Experimental results of 3.5% concentrated chitosan nanofibres are shown in Table 4.4 with sample identification from N29 to N32. The surface morphology of CSNF was analysed using SEM images as shown in Figure 4.8 & 4.9.

Table 4.4: Electrospinning results of 3.5% chitosan concentration nanofibres

Sample ID	% Solution of chitosan	Voltage (kV)	Working Distance (cm)	Fibre Formation Results	Remarks	Average Fibre Diameter (nm)	Standard Deviation (SD)
N29	3.5	15	15	No Fibre	Solution wastage	N/A	N/A
N30	3.5	15	10	No Fibre	Solution wastage	N/A	N/A
N31	3.5	20	15	Fibres	Low Production and solution waste	119	49
N32	3.5	20	10	Fibres	Smooth Production	186	57

In the case of sample N29 and N30, fibre production remained unsuccessful and solution wastage was higher due to higher surface tension. The applied voltage for both samples was 15kv, which hindered to cope with the surface tension of the prepared solution due to the higher concentration of chitosan molecules. Furthermore, longer working distance also prevented the fibre production for sample N29. Therefore, higher voltage and shorter path length were required to fabricate the 3.5% chitosan concentrated solution.

Figure 4.9 shows the surface morphology of sample N31 which was electrospun at 20kv voltage and 15cm working distance. Results indicated that the average fibre diameter value for sample N31 was 119nm, while maximum and minimum fibre diameter value achieved 59nm and 296nm respectively. Produced nanofibres were smooth and uniform. However, solution wastage was also observed due to high flow rate and longer working distance and fibre productivity also remained low. At the same flow rate, working distance plays an important ole towards produced electrify field at same applied voltage. Longer path length weakens the strength of the applied electric field, which is required to cope surface tension of polymer solution for the acceleration and deposition of a jet in the form of fibre. Therefore, due to greater working distance, the applied electric field was not sufficient to electrospun the supplied quantity of chitosan solution. As a resultant, solution wastage was also observed parallel to chitosan nanofibre production.

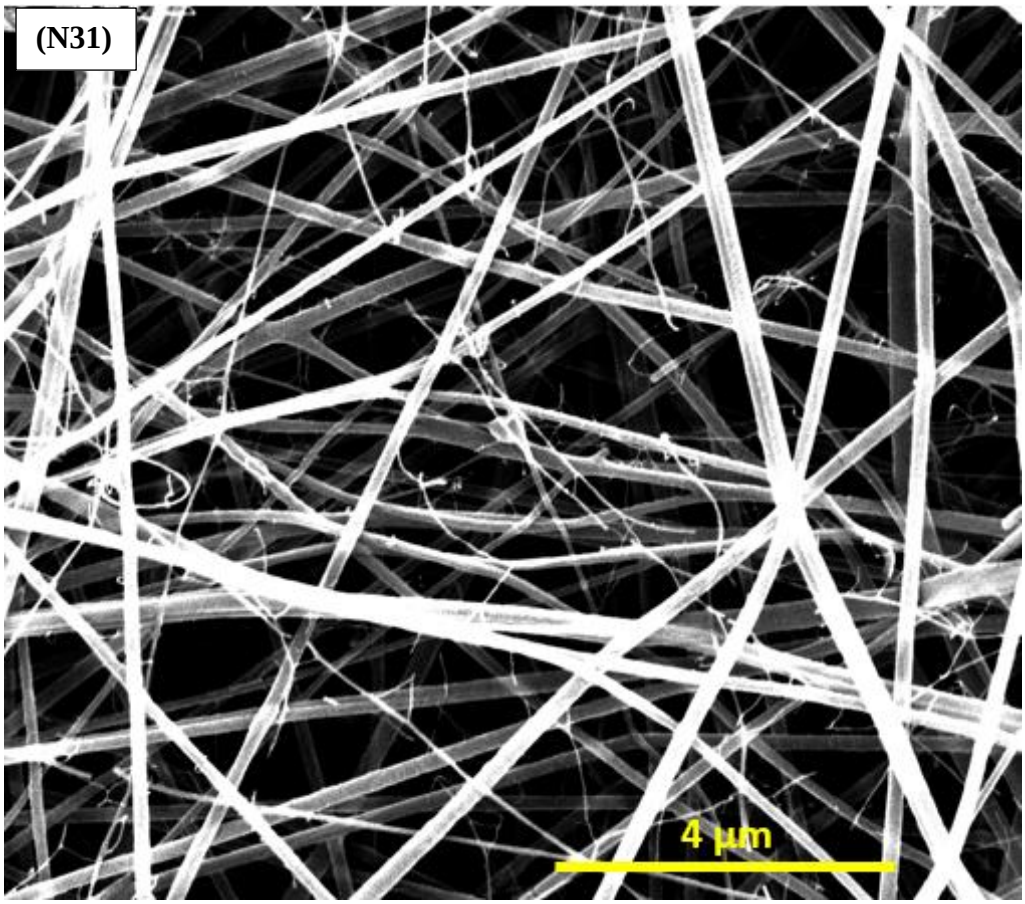

Figure 4.9: SEM image of 3.5% chitosan containing nanofibres at 20kv voltage with 15cm working distance

The surface morphology of sample N32 is shown in Figure 4.10. In the case of sample N32, produced nanofibres are smooth and beads free. The fibre diameter distribution histogram is also shown in Figure 4.11. The diameter of CSNF ranges from 43 nm to 336 nm with an average of 186 nm. Furthermore, fibre productivity was also improved due to the short working distance of 10cm and greater strength of the applied electric field at 20kv voltage. Therefore, nanofibres were successfully produced with a wide range of fibre diameter and the higher concentration of chitosan which was desirable to investigate the antibacterial property against gram negative bacterial species. Furthermore, Addition of these fine nanofibres will be helpful to develop

respiratory filters having higher surface area and better filtration performance to cope with the possible causes of byssinosis disease in textile workers.

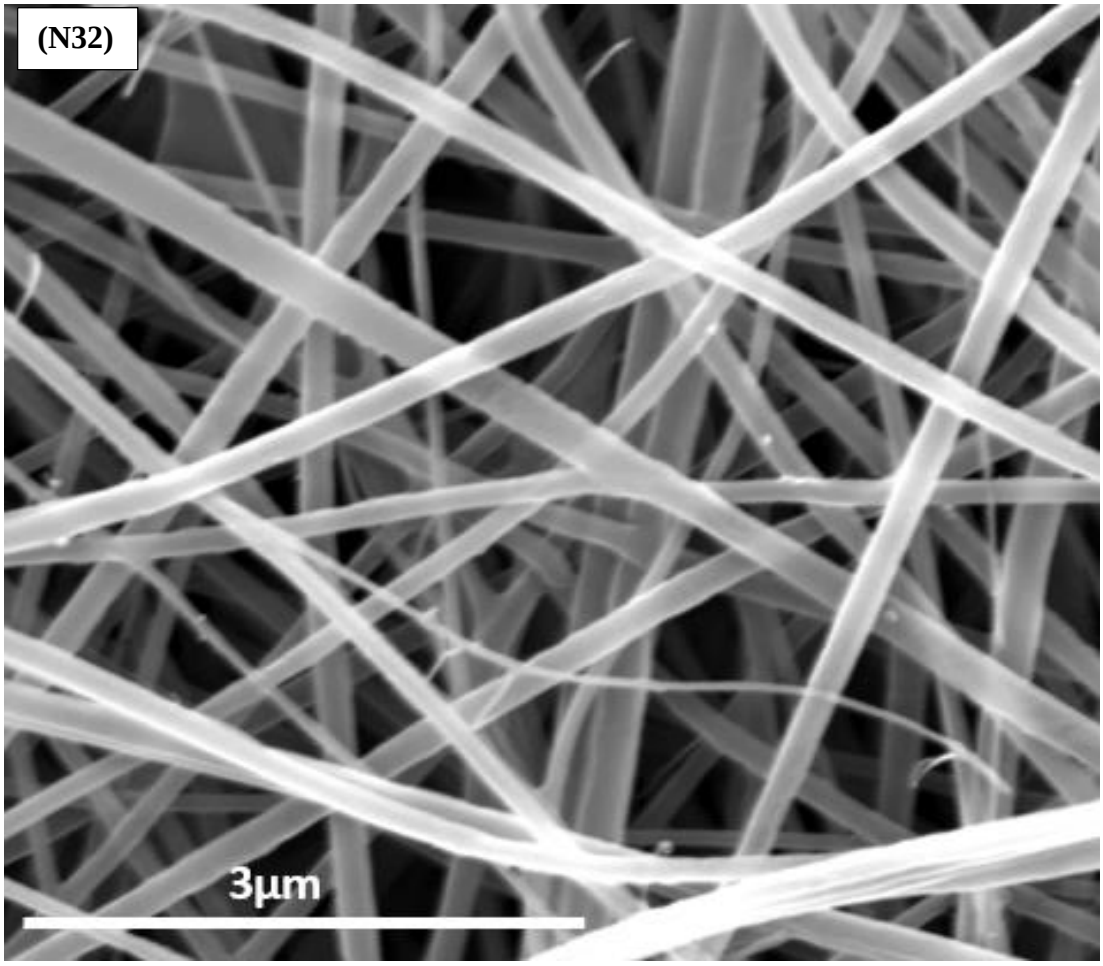

Figure 4.10: SEM image of 3.5% chitosan containing nanofibres at 20kv voltage with 10cm working distance

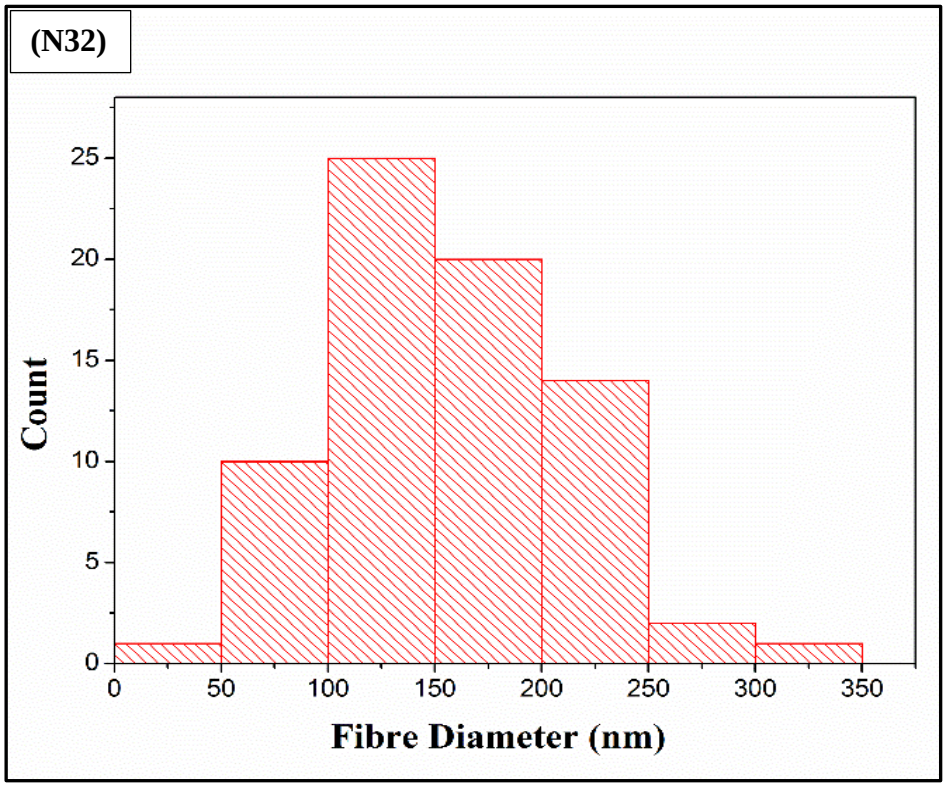

Figure 4.11: Fibre diameter (nm) histogram of 3.5% chitosan containing nanofibres at 20kv voltage with 10cm working distance

4.4 Conclusion

In this study, the process optimization of chitosan nanofibre production was investigated. Chitosan containing nanofibres were electrospun by using 50% glacial acetic as a solvent and 3% PEO solution as a co-spinning agent. Higher applied voltage and longer working distance developed finer diameter nanofibres in all the samples. However, fibre production was achieved only up to 3% concentration of chitosan. Solutions with 4% and above the concentration of chitosan could not produce nanofibres due to high viscosity and high surface tension of solutions. In order to achieve the maximum chitosan concentration, 3.5% chitosan was also investigated. It was shown that smooth nanofibre production was possible with a 3.5% concentration of chitosan by applying 10cm working distance and 20kv voltage while keeping

the other parameters constant. These highly chitosan concentrated nanofibres will be further utilized to develop composite materials for the respiratory filter.

Acknowledgement

I acknowledge the financial support of Punjab Education Endowment Fund (PEEF) for awarding a student grant to pursue my PhD. The author also thankful to University of Manchester and Xian Polytechnic University, China, for providing all research and characterisation facilities.

References:

[1] D. J. Lockwood, "Overview of the Electrospinning," in *Electrospun Nanofibres for Energy and Environmental Applications*, B. Ding and J. Yu, Eds. Springer-Verlag Berlin, 2014, p. 6.

[2] D. J. Lockwood, "Basic Principles," in *Electrospun Nanofibres for Energy and Environmental Applications*, B. Ding and J. Yu, Eds. Springer-Verlag Berlin, 2014, pp. 8–9.

[3] X. Geng, O. H. Kwon, and J. Jang, "Electrospinning of chitosan dissolved in concentrated acetic acid solution," *Biomaterials*, vol. 26, no. 27, pp. 5427–5432, 2005.

[4] H. Homayoni, S. A. H. Ravandi, and M. Valizadeh, "Electrospinning of chitosan nanofibres: Processing optimization," *Carbohydr. Polym.*, vol. 77, no. 3, pp. 656–661, 2009.

[5] M. Cao, F. Gu, C. Rao, J. Fu, and P. Zhao, "Improving the electrospinning process of fabricating nanofibrous membranes to filter PM2.5," *Sci. Total Environ.*, vol. 666, pp. 1011–1021, 2019.

[6] V. Kadam, I. L. Kyratzis, Y. B. Truong, J. Schutz, and L. Wang, "2019 Electrospun bilayer nanomembrane with hierarchical placement of bead-on-string and fibres for low resistance

respiratory air filtration.pdf," *Sep. Purif. Technol.*, vol. 224, no. 1, pp. 247–254, 2019.

[7] M. Liu, X. P. Duan, Y. M. Li, D. P. Yang, and Y. Z. Long, "Electrospun nanofibres for wound healing," *Mater. Sci. Eng. C*, vol. 76, pp. 1413–1423, 2017.

[8] K. Sun and Z. H. Li, "Preparations, properties and applications of chitosan based nanofibres fabricated by electrospinning," *Express Polym. Lett.*, vol. 5, no. 4, pp. 342–361, 2011.

[9] U. Habiba *et al.*, "Effect of deacetylation on property of electrospun chitosan/PVA nanofibrous membrane and removal of methyl orange, FE(III) nad Cr(VI) ions.pdf," *Carbohydr. Polym.*, vol. 177, pp. 32–39, 2017.

[10] K. Kurita, "Chitin and chitosan: Functional biopolymers from marine crustaceans," *Mar. Biotechnol.*, vol. 8, no. 3, pp. 203–226, 2006.

[11] P. B. Malafaya, G. A. Silva, and R. L. Reis, "Natural-origin polymers as carriers and scaffolds for biomolecules and cell delivery in tissue engineering applications," *Adv. Drug Deliv. Rev.*, vol. 59, no. 4–5, pp. 207–233, 2007.

[12] K. M. Vårum, M. M. Myhr, R. J. N. Hjerde, and O. Smidsrød, "In vitro degradation rates of partially N-acetylated chitosans in human serum," *Carbohydr. Res.*, vol. 299, no. 1–2, pp. 99–101, 1997.

[13] P. J. VandeVord, H. W. T. Matthew, S. P. DeSilva, L. Mayton, B. Wu, and P. H. Wooley, "Evaluation of the biocompatibility of a chitosan scaffold in mice," *J. Biomed. Mater. Res.*, vol. 59, no. 3, pp. 585–590, 2002.

[14] C. V Stevens, "Chitosan as Antimicrobial Agent : Applications and Mode of Action Chitosan as Antimicrobial Agent : Applications and Mode of," vol. 4, no. SEPTEMBER, 2003.

[15] H. Sashiwa and S. I. Aiba, "Chemically modified chitin and chitosan as biomaterials," *Prog. Polym. Sci.*, vol. 29, no. 9, pp. 887–908, 2004.

[16] E. a El-hefian, M. M. Nasef, and A. H. Yahaya, "Chitosan Physical Forms : A Short Review,"

Aust. J. Basic Appl. Sci., vol. 5, no. 5, pp. 670–677, 2011.

[17] Q. Zia *et al.*, "Porous poly(L–lactic acid)/chitosan nanofibres for copper ion adsorption," *Carbohydr. Polym.*, vol. 227, no. September 2019, p. 115343, 2020.

[18] A. Cooper, R. Oldinski, H. Ma, J. D. Bryers, and M. Zhang, "Chitosan-based nanofibrous membranes for antibacterial filter applications," *Carbohydr. Polym.*, vol. 92, no. 1, pp. 254–259, 2013.

[19] S. M. Lemma, F. Bossard, and M. Rinaudo, "Preparation of pure and stable chitosan nanofibres by electrospinning in the presence of poly(ethylene oxide)," *Int. J. Mol. Sci.*, vol. 17, no. 11, 2016.

[20] K. Liu *et al.*, "Concurrent filtration and inactivation of bacteria using poly(vinyl alcohol-co-ethylene) nanofibrous membrane facilely modified using chitosan and graphene oxide," *Environ. Sci. Nano*, vol. 4, no. 2, pp. 385–395, 2017.

[21] M. Arkoun, F. Daigle, M. C. Heuzey, and A. Ajji, "Antibacterial electrospun chitosan-based nanofibres: A bacterial membrane perforator," *Food Sci. Nutr.*, no. January, pp. 1–10, 2017.

[22] J. Xue, T. Wu, Y. Dai, and Y. Xia, "Electrospinning and electrospun nanofibres: Methods, materials, and applications," *Chem. Rev.*, vol. 119, no. 8, pp. 5298–5415, 2019.

[23] J. Hu, X. Wang, B. Ding, J. Lin, J. Yu, and G. Sun, "One-step electro-spinning/netting technique for controllably preparing polyurethane nano-fibre/net," *Macromol. Rapid Commun.*, vol. 32, no. 21, pp. 1729–1734, 2011.

Chapter 5: Chitosan nanofibrous respiratory filter for byssinosis prevention

Muhammad Tauseef Khawar, Jiashen Li, Hugh Gong,

Abstract

Byssinosis is a chronic obstructive pulmonary disease very common in textile cotton workers due to inhalation of fine cotton dust and gram negative bacteria. A three layer composite respiratory filter was developed for byssinosis prevention by using the combination of polypropylene (PP) based meltblown layers and chitosan nanofibres (CSNF). Filtration efficiency against fine particulates ranges from 100 nm to 2.5 µm and anti-bacterial activity against *Pantoea agglomerans* (Biosafety level 1, *Enterobacter agglomerans*) were investigated. Chitosan nanofibres were produced by using the electrospinning process and were sandwiched between two PP layers to improve the overall surface area of the filter as well as providing a protective barrier against bacterial pathogens. The filter sample with just 2 hour's CSNF coating showed more than 99% filtration efficiency with a low pressure drop of 71.6 Pa and a high quality factor value 0.082. The antibacterial performance of CSNF layers achieved up to 91% against the *Pantoea agglomerans*. Finally, results concluded that the developed respiratory filter can potentially reduce byssinosis in textile workers.

Keywords: Byssinosis, chronic obstructive pulmonary disease**,** Polypropylene Chitosan, Filtration Efficiency, Antibacterial

5.1 Introduction

Personal protective equipment is critical for the prevention of respiratory diseases such as byssinosis and asthma. Byssinosis, considered as environmental lung disease, is defined as a narrowing of the airways caused by inhaling cotton, flax, or hemp particles [1]**.** It may cause wheezing and tightness in the chest, and it is an occupational chronic obstructive pulmonary disease (COPD) [1]**.** COPD Standard Collaboration Group reported that COPD is the fourth leading cause of death worldwide. It is estimated that there are currently 900,000 diagnosed cases, and an estimated 2 million people are thought to have the disease but remain undiagnosed [2]. In a comprehensive review on long term respiratory health effects in textile workers, it was reported that over 60 million people worldwide work in the textile or clothing industry, are exposed to the risk of chronic lung diseases, in particular COPD, in their workplaces, which leads to the considerable potential cost. It was also reported that the costs of occupational COPD from 2002 could amount to $5.0 billion for the USA annually [3].

Raw cotton contains bacterial contamination from the crop, mainly gram negative bacteria, and their endotoxins. In addition to cotton dust, these bacteria and their endotoxins become part of the working environment in textile spinning mills, and transfer to the inhaler employee during work [4]. After inhalation, these contaminations cause the tightening of airways and inflammation in the lungs [5]. Preparatory processes of yarn manufacturing in textile spinning mills are very dusty and produce a lot of fine cotton dust that can be inhaled by employees. All men and women working in such departments (especially card room and blow room) interact with cotton dust and the risk of being affected by byssinosis [6].

Cotton dust is categorized into three types, micro dust, breathable dust, and fine particulates. Micro, breathable and fine particulates of cotton have size ranges 15-50 µm, 2.5-15 µm, and 0.1-2.5 µm respectively. Fine dust is the most dangerous and easily inhalable due to the very

fine particle size [7]. There are three types of rod shape gram negative bacteria which are normally found in cotton dust, i.e. *Enterobacter Agglomerans*, Pseudomonas Syringae, and Agrobacterium (spp.). *Enterobacter Agglomerans* are the most abundant of these pathogens [8]. Inhalation of all these aerosol particles is dangerous for the workers and has a strong possibility of leading to byssinotic symptoms. Dust and endotoxin exposure control (e.g. using face masks and other measures) is the best way to reduce the risk of byssinosis [5].

Air filtration technology is very effective to control pollution for the protection of different types of disease [9]. Nanofibres play an important role in the development of respiratory filters because of their large surface area [10]. Thanks to the larger surface for a given mass of filter media, it becomes possible to capture pollutants having a size range of 100 nm to 500 nm. Electrospinning is very common for the production of nanofibres [11]. Electrospun fibres can achieve surface area from 1 m^2/g to 35 m^2/g. Electrospinning allows better functionality enrichment up to fibre level, fine pore size distribution and high filtration efficiency.

Polypropylene (PP) is being used in filtration applications worldwide. Spunbonded and melt-blown layers of PP are considered an important base for both gas and liquid filtration products. Due to its hydrophobicity and compatibility with a variety of chemicals, PP is used for the filtration of non-aqueous chemicals and other solvents [12]. Chitosan is being used widely due to its affordability, versatility, and anti-microbial property [13]. It has good defensive potential against microbes, toxins, viruses, and fungi, etc.

Chitosan is being used in food packaging to kill the bacterial contaminations, which enables the longer shelf life of the packed food [14]**.** Chitosan nanofibrous membranes find application as perforators in food packaging for the protection of foodborne pathogens. Recently, chitosan-coated biochar-nanosilver composite was developed for the purification of drinking water due to its antibacterial property [15]. It was observed from the literature that the chitosan

nanofibrous membrane has applications in filtration, tissue engineering, wound dressing, and drug delivery due to its antibacterial property, nontoxicity, biodegradability, and biocompatibility [16]–[18].

In this study, we developed a sandwich structured composite of two PP layers and a chitosan nanofibres layer for the development of respiratory filter. The upper layer is composed of PP and serves as a barrier for large dust particles and the bottom layer serves as supporting material for the chitosan nanofibres. Chitosan nanofibres were produced with the help of electrospinning, and polyethylene oxide (PEO) was used as a co-spinning agent of chitosan for smooth nanofibre production [19]. The barrier performance of prepared respiratory filters against the factors of byssinosis disease was examined. The barrier performance parameters, including filtration efficiency (η), pressure drop (ΔP), and quality factor (Q), against fine dust particles with a size range from 100 nm to 2.5 µm were discussed and the antibacterial performance of the CSNF layer was also evaluated to conclude the effectiveness of filter against byssinosis. To the best of my knowledge, there is current; no literature available on this type of preventive solution for byssinosis.

5.2 Experimental

5.2.1 Materials

Low molecular weight chitosan (Mw = 50,000-190,000 Da) was purchased from Sigma Aldrich. The degree of deacetylation of the supplied chitosan was 75-85%. PEO (co-spinning agent) was purchased in powder form also from Sigma Aldrich. The molecular weight of PEO was 600 KDa. Meltblown PP nonwoven substrate was supplied by Jiangxi Haorui Industry, Jiangxi province, China. The areal density of the nonwoven substrate was 25 g/m^2. Glacial

acetic acid (Mw = 60 Da) was also purchased from Sigma Aldrich and used as a solvent for the electrospinning process. Deionized water was used for the dilution of glacial acetic acid.

5.2.2 Solution Preparation for Electrospinning

Chitosan (3.5%, w/v) was dissolved in solvent of 50% (v/v) glacial acetic acid by continuous magnetic stirring for 24 hours. PEO (3%, w/v) was also dissolved in glacial acetic acid 50% (v/v) separately by overnight magnetic stirring. After that, the solution of chitosan and PEO blend was prepared with an 80/20 ratio by four hours of continuous mixing. The solubility of chitosan in glacial acetic acid enables the process to be non-toxic and eco-friendly with respect to solvent usage.

5.2.3 Preparation of respiratory filter with nanofibre coating

Chitosan (CS) nanofibres were produced by electrospinning and directly coated on the PP nonwoven substrate which was wrapped on the rotating drum collector as shown in Figure 5.1. Blended CS:PEO solution was poured in a 20 ml syringe which is mounted on the pump with a tight grip holder. The syringe was connected with a 19-gauge blunt tip needle. The electrospinning process parameters were 1 mL/hour flow rate and 20 kV voltage. The distance between the needle tip and the PP substrate mounted collector was maintained at 10 cm. All the experiments were performed under the atmospheric condition of 22±2 °C and relative humidity 42±2%.

The surface area and pore size distribution of the filter is dependent on the amount of nanofibre and the fibre distribution on the PP substrate. However, greater amounts of nanofibre coating lead to a higher pressure drop and poorer quality factor of the resultant respiratory filter [20].

The filter performance needs to be optimised by controlling the nanofibre coating density, which can be carried out by controlling the coating times (2h, 4h, 6h, and 8h). After coating, the PP substrate was removed from the collector and placed in a fume cupboard for 12 hours to ensure the complete removal of volatile solvent from the nanofibre coating. Subsequently, the samples were dried in a hot air oven. A PP meltblown nonwoven was then placed on the nanofibre coated PP substrate to make a multi-layer structure as shown in Figure 5.1. The process was repeated three times for each sample category.

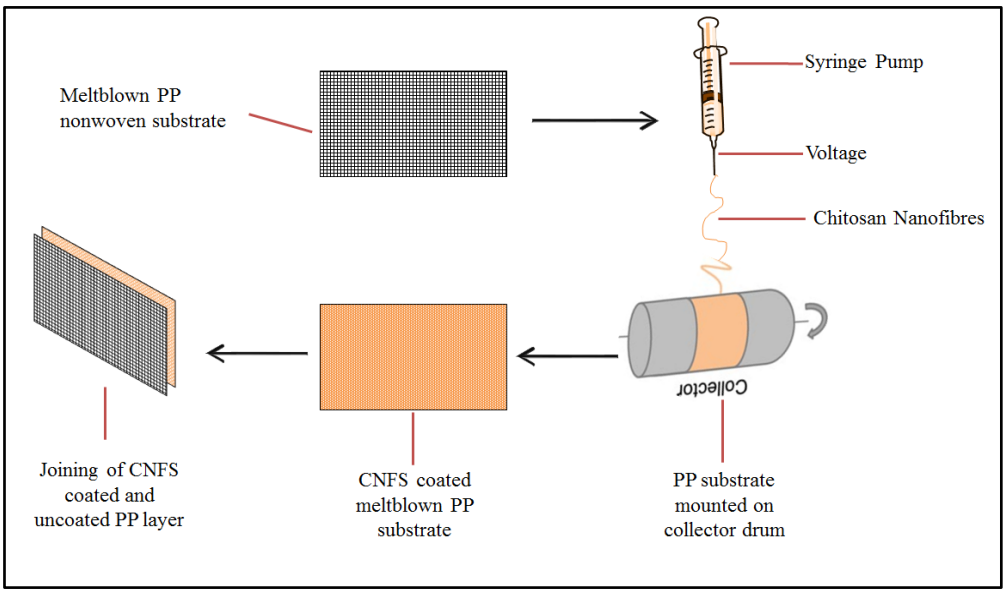

Figure 5.1: Schematic diagram of development of CSNF coated PP respiratory filter.

5.2.4 Characterization

The surface morphology, fibre diameter (100 fibres each sample), and pore size distribution (100 pores each sample) of the PP nonwoven substrate and chitosan nanofibres were analysed by using TESCAN MIRA3 (GMU VP Analytical FESEM) electron microscope. Nanofibre add-on was calculated by weighing the sample before and after coating. Fourier transmission

infrared spectroscopy (FTIR) was performed on NICOLET 5700121 spectrophotometer. FTIR peaks before and after coating were recorded to examine the presence of chitosan in the coated PP nonwoven substrate.

5.2.5 Filtration efficiency testing

Filtration efficiency was tested on the PALAS Promo 2000 system manufactured by PALAS Particle Technology, Germany. Environmental aerosols ranging from 100 nm to 2.5 µm were used for the filtration efficiency evaluation because the cotton dust particles found in the textile environment responsible for the byssinosis in textile workers are within the same range. Flow rate is very important with respect to filtration efficiency. In general two flow rates, 30 l/min and 85 l/min, are reported to replicate different types of working conditions. The first represents working with normal intensity and the second for heavy workload conditions [21]. In this research, all the samples were tested using a flow rate 85 l/min as per NIOSH test condition under extreme work circumstances [22]**.** The sample was mounted on the sample holder of the machine and the particle quantity was evaluated upstream and downstream of the filter sample. Filtration efficiency was calculated using equation 5.1.

$$\eta = \frac{n2-n1}{n2} \tag{5.1}$$

Where η is the filtration efficiency, n1 and n2 are the aerosol concentrations downstream and upstream of the filter respectively.

5.2.6 Pressure drop and quality factor calculation

Pressure drop and quality factor are very important for the evaluation of filter media and directly relate to the breathability [23]. Pressure drop was measured by using the SDL ATLAS air permeability tester and calculated by using equation 5.2. On the basis of filtration efficiency and pressure drop results, quality factor (Q) was calculated by using equation 5.3.

$$\Delta P = P1 - P2 \tag{5.2}$$

$$Q = \frac{-\ln(1-\eta)}{\Delta P} \tag{5.3}$$

Where ΔP is pressure drop, P1 and P2 are the upstream and downstream air pressure respectively, and Q denotes the overall quality factor of the filter [9].

5.2.7 Antibacterial Testing

The anti-bacterial property of the coated chitosan nanofibre (CSNF) was evaluated by following ASTM E2149-13a, 2013. Biosafety level 1 Pantoea agglomerans (Formerly *Enterobacter agglomerans*) gram negative bacterial strains were selected for the test. According to literature, *Enterobacter agglomerans* were found to be the most abundant form of Pantoea in cotton dust [8]**.** *Pantoea agglomerans* (AATCC-27155, formerly *Enterobacter agglomerans* were purchased from LGS Standards, Teddington, UK. As per the above mentioned testing standard, chitosan nanofibres (0.2g) were immersed in 10ml dilute bacterial suspension (10^5 CFU/ml) by using sterilised tube with a 1:50 ratio. After mixing, the tube was placed in an incubator at 37°C temperature for 12 to 24 hours. One test sample of bacterial suspension (without CSNF) was also prepared for the comparison of results. After incubation, every sample was serially diluted up to 10 times with a ratio of 1 to 10. The diluted samples were spread on agar plates and further incubated overnight at 37°C for the counting of survived

bacterial colonies. This test was conducted three times. Antibacterial efficiency as a function of reduction in bacterial growth (R) was calculated by using equation 5.4.

$$R(\%) = [(A - B) \div A] \times 100 \quad (5.4)$$

Where A donates the number of grown bacteria in control sample, B represents the grown bacteria in test sample. The purpose of extended time selection is related to the working condition and reusable possibility of the developed filter material in textile sector. In textile spinning mills, normal working shift time varies from 8h to 12h per day and workers are meant to use the provided mask for multiple shifts. Therefore, extended test incubation time was selected due to specified use of the filter material in textile environment.

5.3 Results and Discussion

5.3.1 Characterisation of chitosan nanofibres

The surface morphology of CSNF was analysed using SEM images. The nanofibres are smooth and bead free as shown in Figure 5.2(a). The fibre diameter distribution is also shown in Figure 5.2(b).

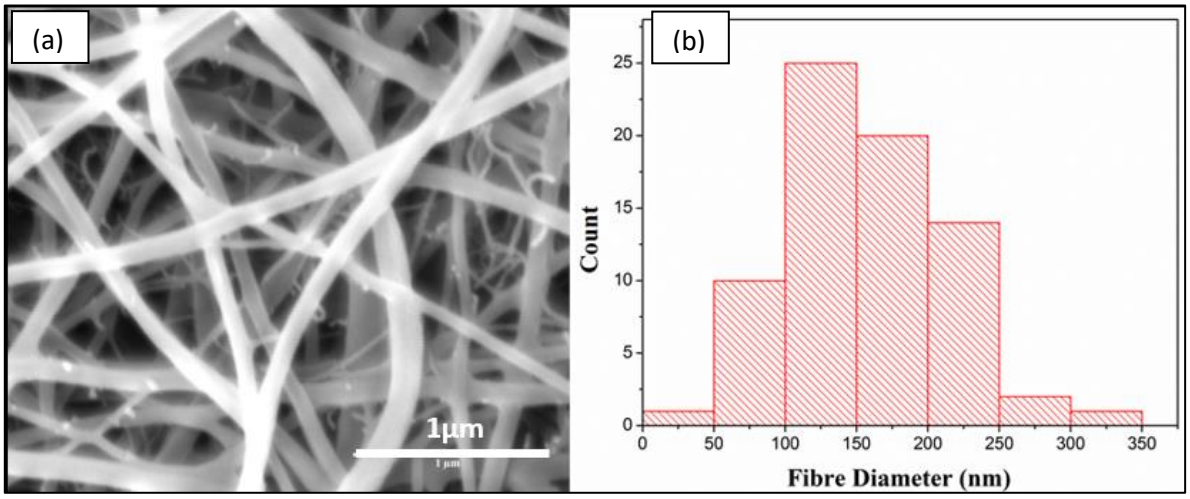

Figure 5.2: (a): SEM image of chitosan nanofibres (b): Histogram of chitosan nanofibres diameter (nm).

The diameter of CSNF ranges from 43 nm to 336 nm with an average of 186 nm. The addition of these fine nanofibres increases the overall surface area of the resultant filter, which leads to improved filtration efficiency. Furthermore, small diameter nanofibres provide better aerodynamic slip in the filter which can prevent the collision of air molecules with nanofibres [24]**.** The slip of air molecules can lead to lower pressure drop for more effective breathing.

Pore size distribution is also a very important factor for respiratory filters [25]. Narrower pore size distribution provides better filtration efficiency but increases the pressure drop which remains a challenging factor to control [26]**.** The pore size distribution of PP meltblown substrate before CSNF coating and after CSNF coating was analyzed with the help of FESEM images as shown in Figure 5.3. The results show that the pore size ranges from 1.4 µm to 10.4 µm and 54 nm to 329 nm for the PP meltblown substrate before and after CSNF coating, respectively. However, the average pore size was 4.7 µm and 153 nm before and after CSNF coating respectively. As a result of the CSNF coating, there is a significant reduction of pore size with an increased surface area in the developed filter.

Four different respiratory filter samples were produced by using four coating times (2h, 4h, 6h, and 8h respectively). The addition of CSNF on each sample was measured by weighing the sample before and after coating. As expected, the amount of nanofibres increases linearly with the increase of coating time, as shown in Figure 5.4.

FTIR spectrums of PP substrate, pure chitosan (CS) and CSNF coated PP substrate (CSNFPP) are shown in Figure 5.5 (a, b, and c). The peaks between 2800-3000 cm^{-1} are attributed to C-H stretching vibrations while peaks at 1376 cm^{-1} and 1457 cm^{-1} indicate $–CH_2$ and $–CH_3$ bending vibration in pure PP samples [27]. In the case of CS, peaks at 1541 cm^{-1} and 1511 cm^{-1} represent the N-H group while the peak at 2918 cm^{-1} shows C-H stretch [28]. The presence of amine

groups in the CSNFPP spectrum confirms that CSNF is effectively coated on the PP meltblown substrate.

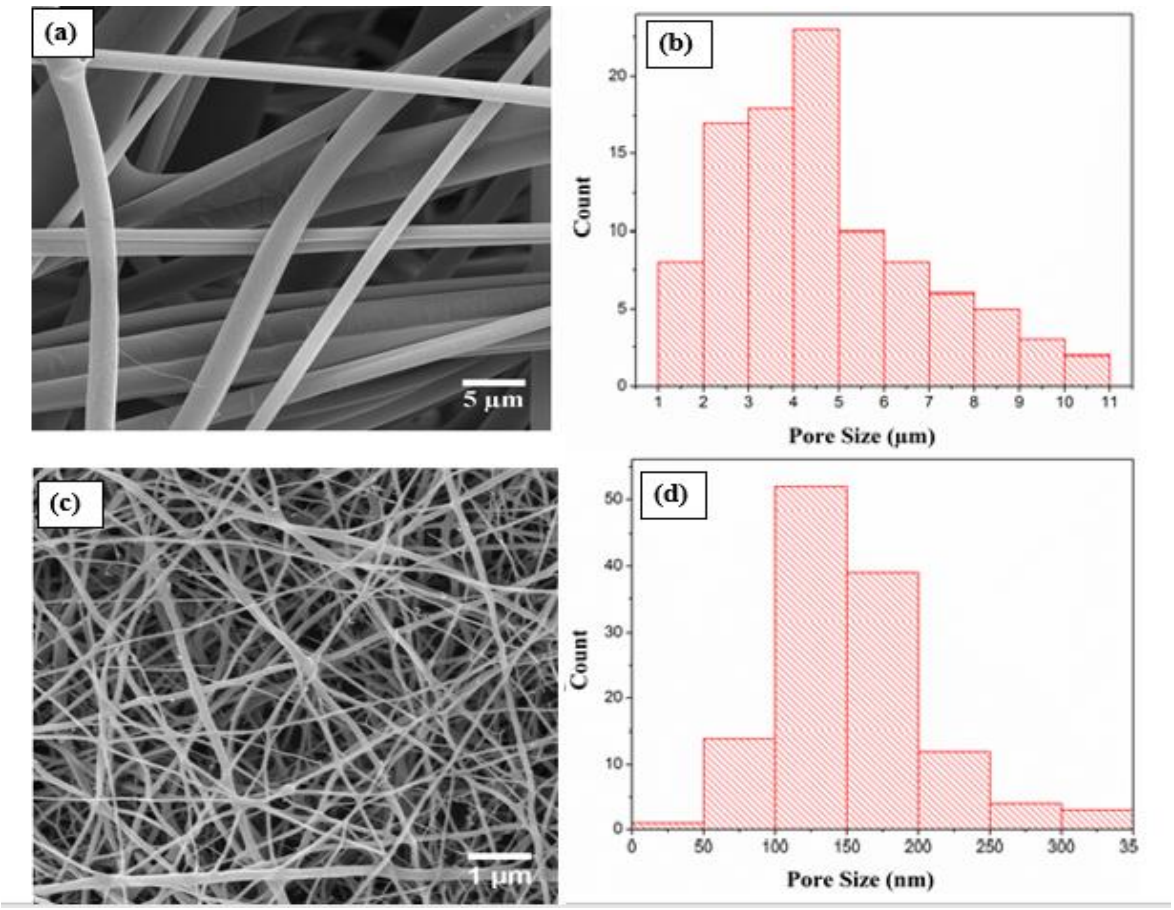

Figure 5.3: SEM image of meltblown pp substrate (a): before nanofibre coating and (c): after CSNF coating, Fibre diameter distribution of PP substrate (b): before CSNF coating and (d): after CSNF coating.

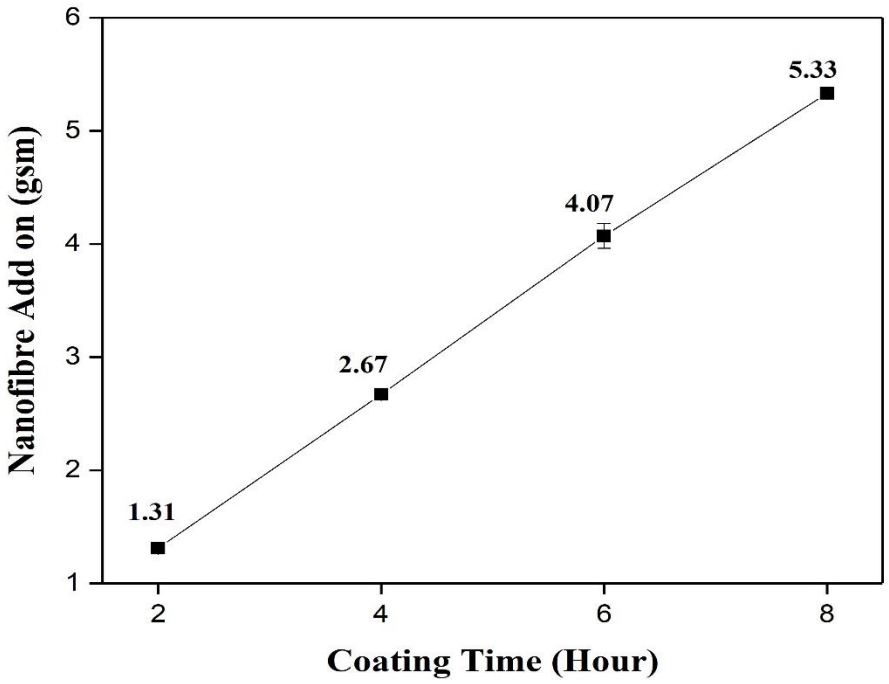

Figure 5.4: Addition of CSNF (gsm) on PP meltblown substrate at different time intervals.

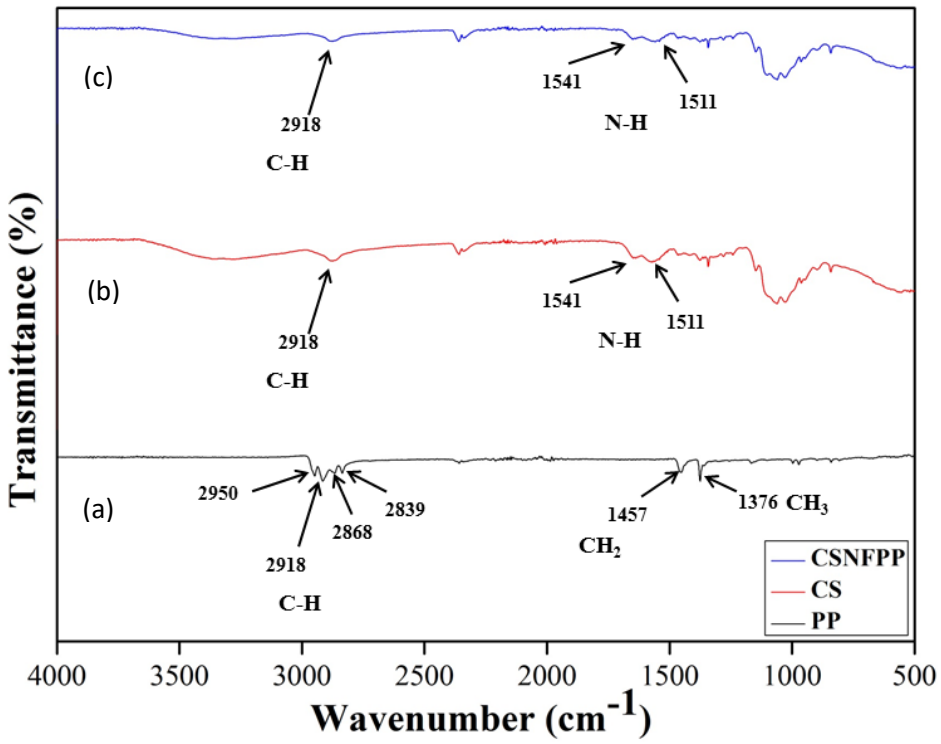

Figure 5. 5: FTIR of (a): PP substrate (b) pure chitosan (c) CSNF coated PP substrate.

5.3.2 Filtration performance

Filtration performance results are explained in following sections and statistical data is shown in Table A-1.

5.3.2.1 Filtration efficiency analysis

The filtration efficiency of all four respiratory filters was investigated over a particle size range from 100 nm to 2.5 μm. The filtration efficiencies are displayed in Figure 5.6. Experimental results show that filtration efficiency increases from 99.72% to 99.99% with the increase of CSNF coating time. The increasing trend is observed significantly from 2h to 6h coating time but not for 8h. However, more than 99% of filtration efficiency is achieved at only two-hour coating sample. An increasing trend of filter performance is attributed to the formation of the CSNF layer on the PP substrate which enhanced the surface area and reduced the pore size. Furthermore, the higher surface area of the filter increases the possibility of particle deposition on the fibre surface and decreases the diffusion of particulate matters, which significantly improves the filtration efficiency [29].

Pore size distribution is also important with respect to filtration efficiency and pressure drop. Generally, the addition of nanofibres produces three types of pores, namely closed pores, blind pores, and through pores, in the filter structure. Closed pores and blind pores terminate inside the structure and are not suitable for air filtration while pores provide the air passage and are very important for air filtration [30]. However, with an excessive coating of nanofibres, closed and blind pores increase and through pores decrease, which leads to higher filtration efficiency but also higher pressure drop. Based on this analysis, the increase of filtration efficiency with the addition of CSNF can be attributed to the higher surface area and fine pore size distribution.

All the samples show high filtration efficiency but the optimum sample can only be decided by considering pressure drop and quality factor.

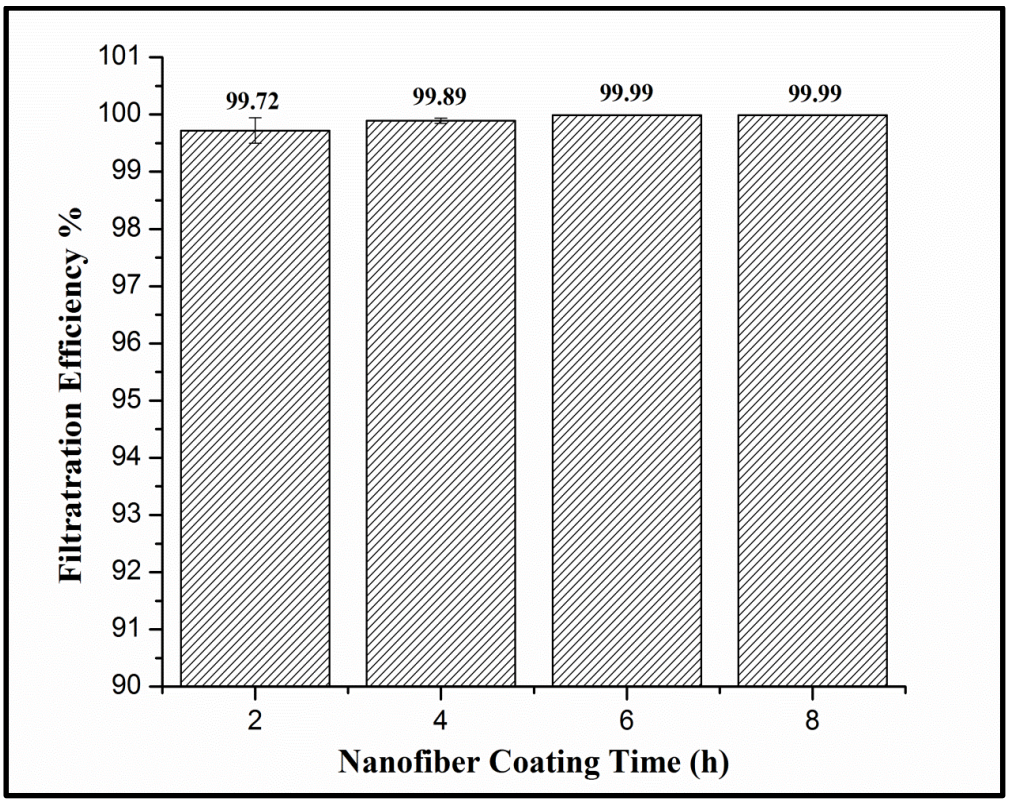

Figure 5.6: Filtration efficiency results of chitosan nanofibre coated PP respiratory filter.

5.3.2.2 Pressure drop analysis

Figure 5.7 illustrates the pressure drop for all the samples. The results show that pressure drop increases significantly (from 72 Pa to 935 Pa) with the increase of CSNF coating. The significant increase of pressure drop after the CSNF coating is due to the reduction of pore size diameter and increase of surface area. Furthermore, the thickness of the nanofibre layer depends on the coating time**,** which directly affects the pressure drop and adversely affects the air permeability of the filter [31].

According to the European standard for air filtration FFP2 (EN 149:2001), the maximum pressure drop should not exceed 250 Pa for fine particulate filters. Therefore, the first samples (with 2h coating) meet the standard while the samples with 4h, 6h and 8h coating have too high pressure drops. It can thus be concluded that 2h coated sample is acceptable as respiratory filters. Samples with coating times beyond 2 hours show excellent filtration efficiency but have too high pressure drops.

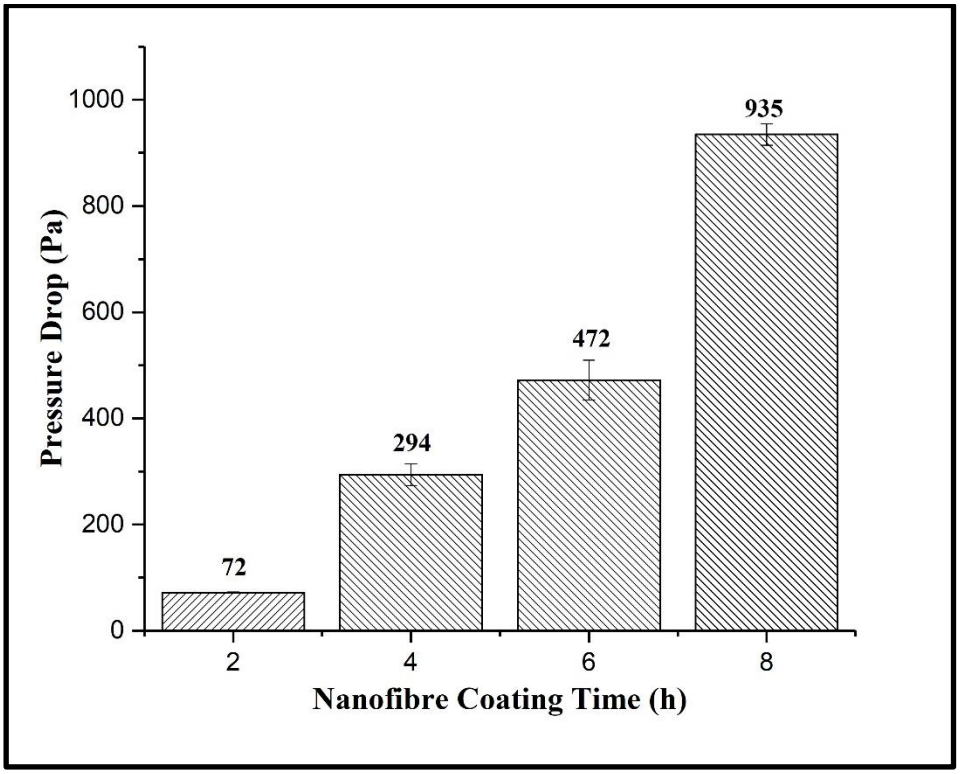

Figure 5.7: Pressure drop (ΔP) results of different chitosan nanofibre coated PP respiratory filter.

5.3.2.3 Quality factor analysis

The quality factor is calculated by using Equation 5.3. The results show that quality factor decreases with the increase of coating time. Sample 1 (2h coating time) shows a higher quality factor due to the higher filtration efficiency with a lower pressure drop, while the quality factor

of 4h, 6h, and 8h coated samples are lower comparatively due to the higher pressure drop. A higher quality factor value is the key factor for better overall filtration performance of respiratory filters. These results can be attributed to the fine diameter of CSNF, the high packing density of CSNF and fine pore sizes [32].

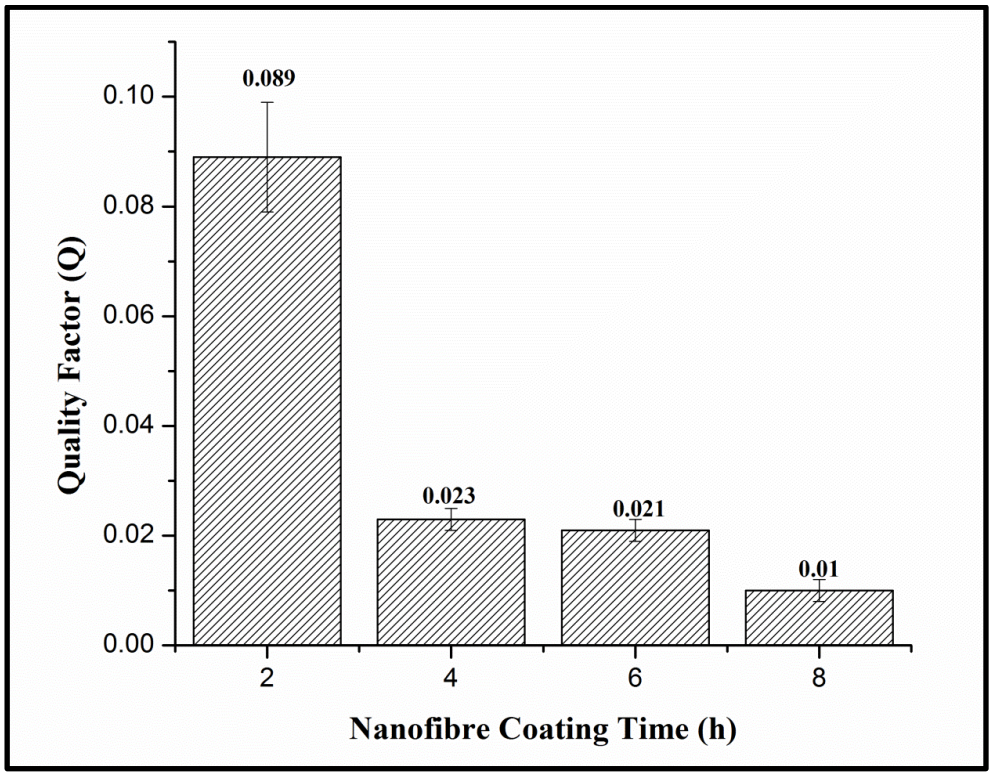

Figure 5.8: Quality factor (Q) results of different chitosan nanofibre coated PP respiratory filter.

On the basis of all the above results, it can be concluded that the sample with 2 hours coating is best suited for the use as respiratory filter.

5.3.2.4 Antibacterial activity of chitosan nanofibres

Quantitative antibacterial property of CSNF layer was investigated by using class 1 Pantoea agglomerans (*Enterobacter agglomerans*, gram negative) bacterial strains due to their

abundant presence in the textile working environment. The results are shown in Figure 5.9 and Table A-2. CSNF exhibits good antibacterial activity against tested bacterial species. Antibacterial activity of CSNF was up to 91% and prohibited the growth of Pantoea agglomerans effectively. Furthermore, the bactericidal activity of CSNF increases from 76% to 91% with the increase of interaction time from 12 hours to 24 hours. The protonation of chitosan amine group ($-NH_3^+$) is activated under acidic conditions [33]. Protonated chitosan interacts with negatively charged cell membranes and ruptures the cell wall to stop the growth of gram negative bacterial species. This mechanism is responsible for the antibacterial ability of chitosan.

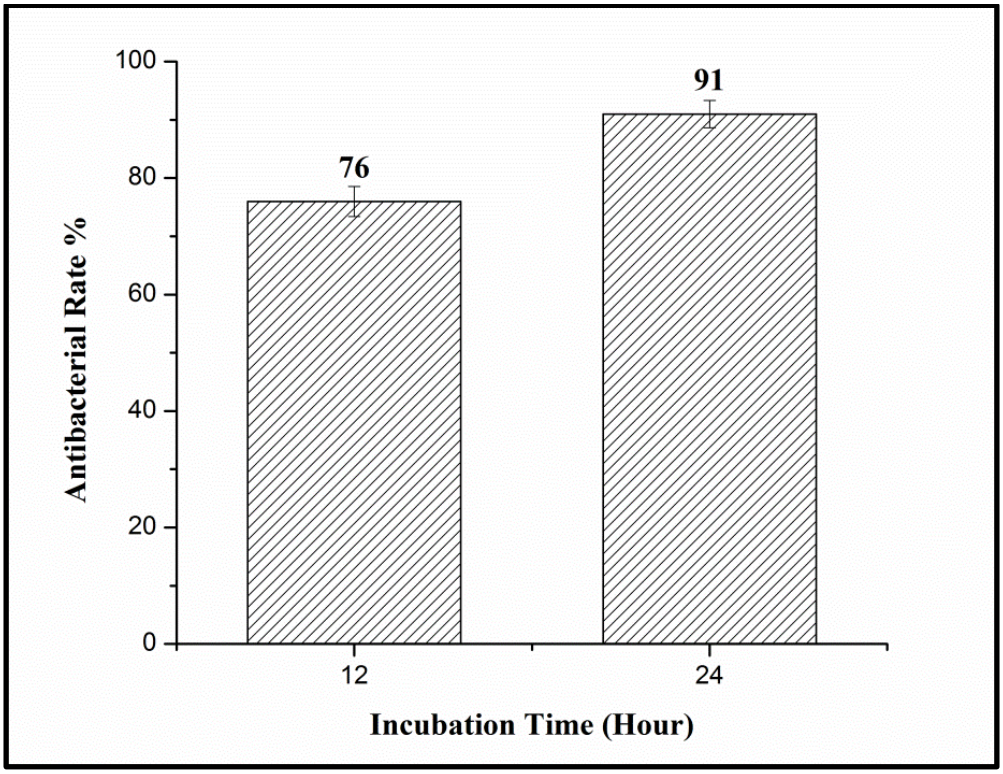

Figure 5.9. Antibacterial activity results of CSNF nanofibres against biosafety level 1, Pantoea agglomerans (*Enterobacter agglomerans*).

The increase of antibacterial activity with time is attributed to the interaction and adhesion of NH_3^+ functional groups of chitosan with the outer cell wall of the bacterial species. It can be concluded from the results that CSNF has effective antibacterial ability against the targeted bacterial pathogen.

5.4 Conclusions

Chitosan nanofibrous coated PP three layer composite filter material was fabricated for applications to reduce byssinosis in textile cotton workers. Filtration efficiency was evaluated against targeted environmental particulate size, ranging from 100 nm to 2.5 μm. Filtration efficiency increased with the increase of the coating time of CSNF while pressure drop also increased. However, samples with 2h CSNF coating time showed high filtration efficiency of 99.27%, low pressure drop of 71.6 Pa, and higher quality factor among all the samples. In addition to filtration efficiency, the antibacterial activity of CSNF against Pantoea agglomerans (*Enterobacter agglomerans*, Biosafety level 1, gram negative) bacterial strains was investigated. Quantitative analysis showed that CSNF has up to 91% antibacterial efficiency against the targeted pathogens. Furthermore, the highest recorded filtration efficiency with a combination of lower pressure drop value and higher antibacterial activity proved better filtration performance as compared to previously recorded researches. On the basis of results, it can be concluded that the fabricated PP respiratory filter with a 2 hour CSNF coating time offers a combination of high filtration efficiency, low pressure drop, and good antibacterial property, thus filters made from such material can effectively prevent byssinosis in textile cotton workers.

Declaration of competing interest

The authors declare that they have no known competing financial interests or personal relationships that could have appeared to influence the above reported work.

Acknowledgement

The authors acknowledge the financial support of Punjab Education Endowment Fund (PEEF). The authors are also thankful to Xian Polytechnic University, China, for providing some of the characterisation facilities.

References:

[1] U.S. National Library of Medicine, "Byssinosis," 2017. [Online]. Available: https://medlineplus.gov/ency/article/001089.htm. [Accessed: 01-Sep-2019].

[2] D. Fishwick *et al.*, "Occupational chronic obstructive pulmonary disease: A standard of care," *Occup. Med. (Chic. Ill).*, vol. 65, no. 4, pp. 270–282, 2015.

[3] P. S. Lai and D. C. Christiani, "Long Term Respiratory Health Effects in Textile Workers," *Curr Opin Pulm Med. J.*, vol. 19, no. 2, pp. 152–157, 2014.

[4] R. Rylander and M. Lundholm, "Bacterial contamination of cotton and cotton dust and effects on the lung.," *Br. J. Ind. Med.*, vol. 35, no. 3, pp. 204–207, 1978.

[5] M. A. Lara, "Byssinosis," *MSD Manual Consumer Version*, 2018. [Online]. Available: https://www.msdmanuals.com/home/lung-and-airway-disorders/environmental-lung-diseases/byssinosis. [Accessed: 01-Sep-2019].

[6] R. S. F. Schilling, J. P. W. Hughes, I. Dingwall-Fordyce, and J. C. Gilson, "an Epidemiological Study of Byssinosis Among Lancashre Cotton Workers," *Brit. J. Ind. Med,*

vol. 12, 1955.

[7] B. Dangi and A. Bhise, “Cotton dust exposure: Analysis of pulmonary function and respiratory symptoms,” *Lung India*, vol. 34, no. 2, p. 144, 2017.

[8] M. D. Ragnar Rylander, “Bacterial Toxins and Etiology of Byssinosis,” *Chest*, vol. 79, no. 4, 1981.

[9] V. V. Kadam, L. Wang, and R. Padhye, “Electrospun nanofibre materials to filter air pollutants – A review,” *J. Ind. Text.*, vol. 47, no. 8, pp. 2253–2280, 2018.

[10] Y. C. Ahn *et al.*, “Development of high efficiency nanofilters made of nanofibres,” *Curr. Appl. Phys.*, vol. 6, no. 6 SPEC. ISS., pp. 1030–1035, 2006.

[11] Y. Si, X. Tang, J. Yu, and B. Ding, “Electrospun Nanofibres for Energy and Environmental Applications,” *Nanostructure Sci. Technol.*, no. DOI 10.1007/978-3-642-54160-5__1, p. 525, 2014.

[12] “Polypropylene Membranes,” *SterliTech*, 2019. [Online]. Available: https://www.sterlitech.com/polypropylene-membrane-filters.html. [Accessed: 01-Sep-2019].

[13] M. Kong, X. G. Chen, K. Xing, and H. J. Park, “Antimicrobial properties of chitosan and mode of action: A state of the art review,” *Int. J. Food Microbiol.*, vol. 144, no. 1, pp. 51–63, 2010.

[14] M. Arkoun, F. Daigle, M. C. Heuzey, and A. Ajji, “Mechanism of action of electrospun chitosan-based nanofibres against meat spoilage and pathogenic bacteria,” *Molecules*, vol. 22, no. 4, 2017.

[15] Z. Hu, L. Zhang, L. Zhong, Y. Zhou, J. Xue, and Y. Li, “Preparation of an antibacterial chitosan-coated biochar-nanosilver composite for drinking water purification,” *Carbohydr. Polym.*, vol. 219, no. January, pp. 290–297, 2019.

[16] K. Sun and Z. H. Li, “Preparations, properties and applications of chitosan based nanofibres

fabricated by electrospinning," *Express Polym. Lett.*, vol. 5, no. 4, pp. 342–361, 2011.

[17] U. Habiba, T. A. Siddique, T. C. Joo, A. Salleh, B. C. Ang, and A. M. Afifi, "Synthesis of chitosan/polyvinyl alcohol/zeolite composite for removal of methyl orange, Congo red and chromium(VI) by flocculation/adsorption," *Carbohydr. Polym.*, vol. 157, pp. 1568–1576, 2017.

[18] U. Habiba *et al.*, "Effect of deacetylation on property of electrospun chitosan/PVA nanofibrous membrane and removal of methyl orange, FE(III) nad Cr(VI) ions.pdf," *Carbohydr. Polym.*, vol. 177, pp. 32–39, 2017.

[19] S. M. Lemma, F. Bossard, and M. Rinaudo, "Preparation of pure and stable chitosan nanofibres by electrospinning in the presence of poly(ethylene oxide)," *Int. J. Mol. Sci.*, vol. 17, no. 11, 2016.

[20] M. Tang, J. Hu, Y. Liang, and D. Y. H. Pui, "Pressure drop, penetration and quality factor of filter paper containing nanofibres," *Text. Res. J.*, vol. 87, no. 4, pp. 498–508, 2017.

[21] R. M. Eninger, T. Honda, A. Adhikari, H. Heinonen-Tanski, T. Reponen, and S. A. Grinshpun, "Filter performance of N99 and N95 facepiece respirators against viruses and ultrafine particles," *Ann. Occup. Hyg.*, vol. 52, no. 5, pp. 385–396, 2008.

[22] J. P. Eshbaugh, P. D. Gardner, A. W. Richardson, and K. C. Hofacre, "N95 and P100 Respirator Filter Efficiency Under High Constant and Cyclic Flow," *J. Occup. Environ. Hyg.*, vol. 6, no. 1, pp. 52–61, 2008.

[23] S. Sundarrajan, K. L. Tan, S. H. Lim, and S. Ramakrishna, "Electrospun nanofibres for air filtration applications," *Procedia Eng.*, vol. 75, pp. 159–163, 2014.

[24] H. Wan *et al.*, "Hierarchically structured polysulfone/titania fibrous membranes with enhanced air filtration performance," *J. Colloid Interface Sci.*, vol. 417, pp. 18–26, 2014.

[25] X. Liu, H. Shen, and X. Nie, "Study on the filtration performance of the baghouse filters for

ultra-low emission as a function of filter pore size and fibre diameter," *Int. J. Environ. Res. Public Health*, vol. 16, no. 2, pp. 1–19, 2019.

[26] W. Sambaer, M. Zatloukal, and D. Kimmer, "3D air filtration modeling for nanofibre based filters in the ultrafine particle size range," *Chemical Engineering Science*, vol. 82. pp. 299–311, 2012.

[27] K. S. Chun, S. Husseinsyah, and H. Osman, "Utilization of cocoa pod husk as filler in polypropylene biocomposites: Effect of maleated polypropylene," *J. Thermoplast. Compos. Mater.*, vol. 28, no. 11, pp. 1507–1521, 2015.

[28] A. Razzaz, S. Ghorban, L. Hosayni, M. Irani, and M. Aliabadi, "Chitosan nanofibres functionalized by TiO2 nanoparticles for the removal of heavy metal ions," *Journal of the Taiwan Institute of Chemical Engineers*, vol. 58. pp. 333–343, 2016.

[29] A. Podgórski, A. Bałazy, and L. Gradoń, "Application of nanofibres to improve the filtration efficiency of the most penetrating aerosol particles in fibrous filters," *Chem. Eng. Sci.*, vol. 61, no. 20, pp. 6804–6815, 2006.

[30] A. Patanaik, V. Jacobs, and R. D. Anandjiwala, "Performance evaluation of electrospun nanofibrous membrane," *J. Memb. Sci.*, vol. 352, no. 1–2, pp. 136–142, 2010.

[31] M. A. Hassan, B. Y. Yeom, A. Wilkie, B. Pourdeyhimi, and S. A. Khan, "Fabrication of nanofibre meltblown membranes and their filtration properties," *J. Memb. Sci.*, vol. 427, pp. 336–344, 2013.

[32] N. Wang *et al.*, "Multilevel structured polyacrylonitrile/silica nanofibrous membranes for high-performance air filtration," *Sep. Purif. Technol.*, vol. 126, pp. 44–51, 2014.

[33] R. C. Goy, S. T. B. Morais, and O. B. G. Assis, "Evaluation of the antimicrobial activity of chitosan and its quaternized derivative on E. Coli and S. aureus growth," *Brazilian J. Pharmacogn.*, vol. 26, no. 1, pp. 122–127, 2016.

Chapter 6: Effect of low pressure plasma surface modification on filtration performance of chitosan nanofibrous respiratory filter

Muhammad Tauseef Khawar, Jiashen Li, Hugh Gong,

Abstract

Low pressure drop is highly desirable for respiratory filters. Surface activation plays an important role to enhance the filtration performance of respiratory filters. In this study, a three layer composite respiratory filter was developed by using the combination of polypropylene (PP) nonwoven layers and chitosan nanofibres (CSNF) with variable coating time (h) during the electrospinning process. To study the impact of surface activation on filtration performance, the outer surface of all the samples were modified by using low pressure plasma treatment. Filtration performance testing was conducted to determine the filtration efficiency (%), pressure drop (Pa), and quality factor (Q) results, before and after the surface treatment. The maximum values of filtration efficiency and quality factor achieved were 99.99% and 0.068 respectively. The lowest value of the pressure drop was 16.12 Pa. All the low pressure plasma treated samples showed higher filtration efficiency and quality factor compared to untreated samples due to more effective capturing mechanism. However, pressure drop results indicated no significant difference. Furthermore, the decay of plasma treatment impact was analysed by using drop shape analysis method to measure the water contact angle on the surface of the samples. Results showed a gradual decrease in surface modification impact and surface of treated samples changed from hydrophilic to hydrophobic with the passage of time.

Keywords: Filtration performance, Quality factor, Surface activation, Polypropylene, Low pressure plasma, Nanofibres, Respiratory filter

6.1 Introduction

Many people in the world is facing the threats of asthma, nausea, skin irritation, high blood pressure, cancer, and birth defects due to increasing air pollution. Air filtration technology is very effective to mitigate pollution and protect people from a variety of diseases [1]. A respiratory filter is a type of protective clothing to protect the wearer from the inhalation of hazardous substances like airborne particles, dust, mist, and pathogens [2]. There are many types of filters available for respiratory protection with specified functionality. The selection of the right respirator for the required job is t important for better protection efficiency [3]. The capturing mechanism of the filter is also very important for the protection efficiency and is totally dependent on the nature of pollutants and the material of the filter. The filtration mechanism is categorized in diffusion, interception, intermolecular interaction, straining, inertial impaction, gravitation, and electrostatic interaction of the particle on the substrate [4]. Among these mechanisms, diffusion and interception are the most important with respect to filtration protection efficiency. Particles having a diameter below 500 nm can be captured or diffused by Brownian diffusion due to their random motion. [5]

The electrospinning technique is very common for the production of nanofibrous filters by using different types of polymers on the basis of functionality [6]. These types of filtration media contain one or more layers of nanofibres on the conventional fibre web, increasing the surface area more effectively [7]. Due to the higher surface of the filter media, it becomes possible to capture pollutants having size ranges from 100nm to 500nm. A lot of nanofibres

based membranes have been developed by using different types of polymers [8]. Electrospun nanofibre can achieve higher surface areas ranging from 1 m^2/g to 35 m^2/g and better functionality enrichment up to fibre level. The nanofibrous membrane can also achieve even pore size distribution with good interconnectivity and high filtration efficiency [9]. However, achieving low process energy costs and high productivity remains a challenge. [10]

Chitosan is being used all over the world due to its affordability, versatility, and anti-microbial activity [11]–[13]. It has good defensive potential against the microbes, toxins, viruses, and fungi etc. Application of chitosan in filtration application is increasing day by day due to its biocompatibility, good electrospun possibility, better porosity, [14] and excellent anti-bacterial properties. [15]

Higher filtration efficiency with lower pressure drop value is still challenging by using a nanofibrous layer. Researchers have used a combination of mechanical and electrostatic capturing mechanisms to get higher filtration efficiency while maintaining pressure drop [16], [17]. The electrostatic mechanisms can be induced on the surface of the respiratory filter by using atmospheric plasma or coronas. Surface modification by using atmospheric corona is an efficient source of unipolar charge application on the polymer surface. Corona charged surface significantly enhanced the filtration efficiency of the respiratory filter [18]. However, there are limitations of uniformity of plasma treatment due to the chemical effects of reagent gases, which are usually found in ambient air in atmospheric conditions [19]. While low pressure (LP) plasma techniques are non-thermodynamic-equilibrium processes which modify the surface chemistry of any solid polymer compound with the help of ionized gas items under low vacuum condition ranging from 10^{-3} - 1 Torr [20]. A range of properties can be achieved regarding chemical composition and surface morphology of the polymers such as wet stability, metal adhesion, dyeability, chemical inertness, lubricity, and biocompatibility. Conventional

low-pressure plasma is operated under vacuum or low pressure of a few Pa which prevents the surface from chemical effects and ensures the uniformity of treatment [21]. There is a paucity of published scientific literature relating to the impact of low pressure plasma surface modification on filtration performance.

In this study, a sandwich structured composite was developed by using two PP (polypropylene) layers and a chitosan nanofibres coating layer. The top PP layer was surfaced modified by using low pressure plasma treatment and served as a barrier for large dust particles. The bottom PP layer served as supporting material for the coated chitosan nanofibres. Chitosan nanofibres were produced with electrospinning, and polyethylene oxide (PEO) was used as the co-spinning agent [22]. The prepared respiratory filter was characterised for filtration efficiency (η), pressure drop (Pa) and quality factor (Q), against fine dust particles with a size range from 100 nm to 2.5 µm. Furthermore, the impact of low pressure plasma surface modification on the filtration performance of all the developed filters is reported. The decay of plasma treatment was also studied by using water contact angle test after 15, 30 and 60 days to find out the effectiveness period of treatment on developed filter material which is very important towards the storage and use of filter material after development.

6.2 Experimental

6.2.1 Materials

Different PP nonwoven substrates were purchased with a range of areal density (g/m^2) as shown in Table 6.1. Average fibre diameter and pore size information were calculated by ImageJ from SEM images of all three substrates which are shown in figures A-1, A-2 and A-3. Low molecular weight chitosan (Mw = 50,000-190,000 Da) was purchased from Sigma

Aldrich. Degree of deacetylation of the supplied chitosan was 75-85%. PEO (co-spinning agent) was purchased in powder form from Sigma Aldrich. The molecular weight of PEO was 600 KDa. Glacial acetic acid (Mw = 60 Da) was also purchased from Sigma Aldrich and used as a solvent for the electrospinning process. Deionized water was used for the dilution of glacial acetic acid.

Table 6.1: PP nonwoven substrate details

Sr. #	GSM	Supplier	Average Fibre Diameter (µm)	Average Pore Size (µm)
1	50 (Meltblown)	Jiangxi Haorui Industry China	2.56	2.08 ± 0.62
2	70 (Spunbonded)	KBT Ltd Birmingham	23	10.08 ± 4.64
3	100 (Spunbonded)	Veijun Nonwoven China	34	16.81 ± 4.54

6.2.2 Solution Preparation for Electrospinning

Chitosan (3.5%, w/v) was dissolved in 50% (v/v) glacial acetic acid by continuous magnetic stirring for 24 hours. PEO (3%, w/v) was also dissolved in 50% (v/v) glacial acetic acid separately by overnight magnetic stirring. After that, a blend of chitosan and PEO solution was prepared with an 80/20 ratio respectively by four hours of continuous mixing. The Solubility of chitosan in glacial acetic acid enables the process to be non-toxic and eco-friendly with respect to solvent usage.

6.2.3 Preparation of respiratory filters with nanofibre coating

Chitosan (CS) nanofibres were produced by using the electrospinning method and directly coated on the PP nonwoven substrates (Table 6.1) by wrapping them on the rotating drum collector as shown in Figure 1. Blended CS:PEO solution was poured in a 20 ml syringe and mounted on the pump with a tight grip holder. The syringe was connected with a 19-gauge blunt tip needle. The Combination of optimal parameters including, 1 mL/hour flow rate and 20 kV voltage were applied for the production of nanofibres. Distance between the needle tip and the PP substrate mounted collector was maintained at 10 cm. All the experiments were performed in (22±1 °C) and relative humidity was 42-45% under the atmospheric condition.

The surface area and pore size distribution of the filter is dependent to the number of nanofibres and their uniform dispersion on the collecting PP substrate. However, excessive nanofibre coating can lead to high pressure drop and poor quality factor of the resultant respiratory filter [23]**.** Optimisation of nanofibre coating was carried out by varying the coating times (2h, 4h, 6h, and 8h) as shown in Table 6.2. Thus, four different nanofibres coated PP substrate samples were produced in each category of Table 6.1. After the coating, each PP substrate was removed from the collector and placed in a fume cupboard for 12 hours to ensure the complete removal of volatile solvent from the coated nanofibres. Subsequently, all twelve samples were dried in a hot air oven. After that, an uncoated PP layer was placed on the top of nanofibre holding PP substrate to make a multi-layer structure of respiratory filter as shown in Figure 6.1. The whole process was repeated thrice for each sample of Table 6.2.

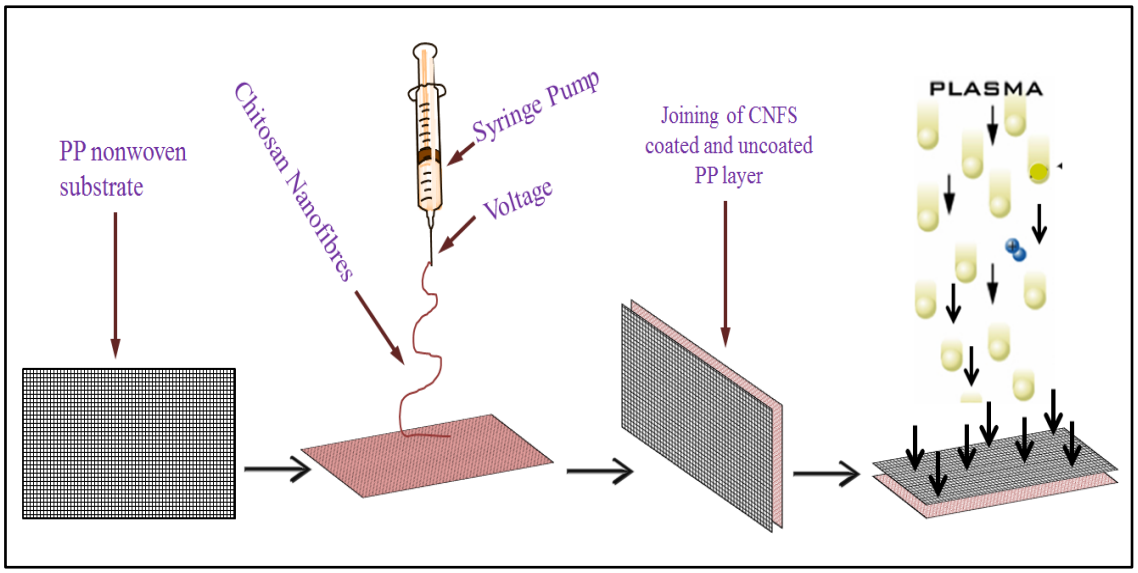

Figure 6.1: Schematic diagram of development of CSNF coated PP respiratory filter

Table 6.2: Sample description of each PP nonwoven category after Nanofibre Coating

Sr. #	Description	Nanofibre Coating Time (h)
Sample 1	50 GSM (Meltblown)	2
Sample 2		4
Sample 3		6
Sample 4		8
Sample 5	70 GSM (Spunbonded)	2
Sample 6		4
Sample 7		6
Sample 8		8
Sample 9	100 GSM (Spunbonded)	2
Sample 10		4
Sample 11		6
Sample 12		8

6.2.4 Plasma Surface Modification

All the developed respiratory filter samples were surface modified by using Low pressure plasma machine made of by Diener Electronic as shown in Figure 6.2. Oxygen (O_2) was used as a source of plasma generation, and the plasma treatment time was five minutes for each sample. After the plasma treatment, each sample was placed in an air-tight polybag to avoid further surface reactions. The purpose of low pressure plasma treatment is to increase the surface energy of the outer layer of the respiratory for a more effective capturing mechanism which will help to reduce the pressure drop by keeping the same surface area. Figure 6.1 shows the whole procedure of filter sample development and plasma surface modification.

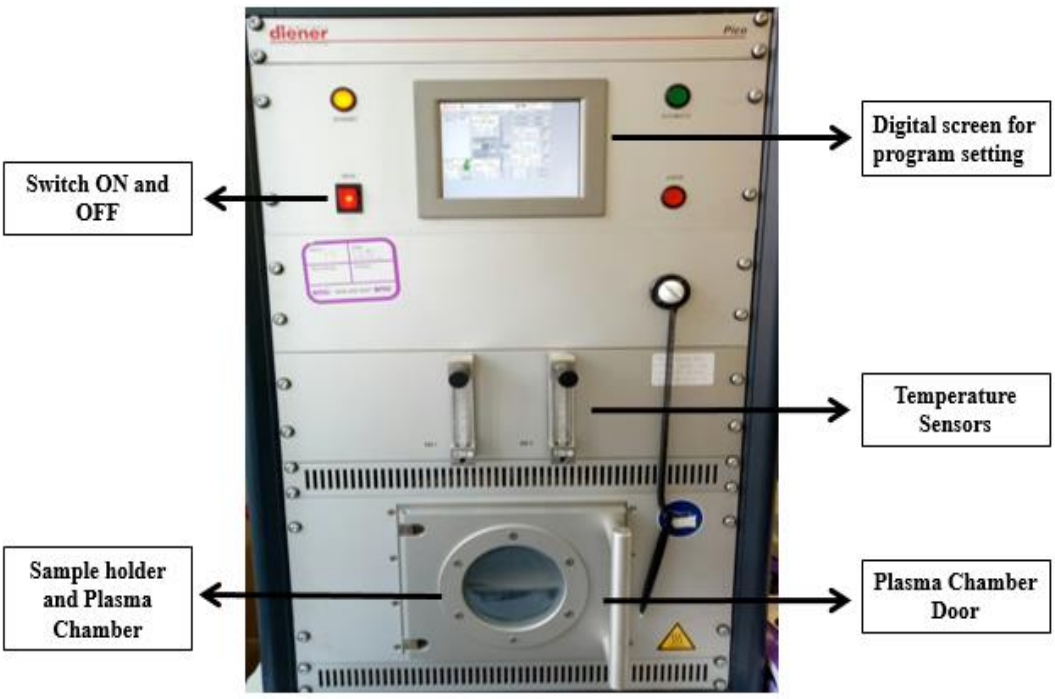

Figure 6.2: Low pressure plasma surface modification machine

6.2.5 Characterization

Surface morphology, fibre diameter (100 fibres each sample), and pore size distribution (100 pores each sample) of PP nonwoven substrate and chitosan nanofibres were analysed by using TESCAN MIRA3 (GMU VP Analytical FESEM). Nanofibre add-on (g) was calculated by

weighing the sample before and after coating. Fourier transmission infrared spectroscopy (FTIR) was performed on NICOLET 5700121 spectrophotometer. FTIR peaks before and after coating were recorded to ensure the presence of chitosan after nanofibre coating on PP nonwoven substrate.

6.2.6 Filtration efficiency testing

The filtration efficiency test was performed on the PALAS Promo 2000 system manufactured by PALAS Particle Technology, Germany. Environmental aerosol ranging from 100 nm to 2.5 µm were used for the filtration efficiency evaluation because this diameter range of cotton dust particles is found in a textile environment responsible for the byssinosis in textile workers. The flow rate during testing is very important with respect to filtration efficiency. There are two standard flow rates, 30 l/min and 85 l/min, corresponding to different types of working conditions. The first represents work with normal intensity and the second for heavy workload conditions [24]. All the samples were tested on flow rate 85 l/min as per NIOSH test condition under extreme work circumstances [25]**.** Each sample was mounted on the sample holder of the machine and aerosol particle penetration was evaluated upstream and downstream of the sample penetration. Filtration efficiency calculation was done as per the following equation 6.1.

$$\eta = \frac{n2-n1}{n2} \tag{6.1}$$

η is filtration efficiency while n1 and n2 are the aerosol concentrations on downstream and upstream of the filter respectively. [27]

6.2.7 Pressure drop and quality factor calculation

Pressure drop and quality factor are very important for the evaluation of filter media and directly related to ease of breathability [26]. Pressure drop was measured by using the SDLATLAS air permeability tester and calculated by using equation 6.2. On the basis of filtration efficiency and pressure drop results, quality factor (Q) was calculated by using the following equation 6.3.

$$\Delta P = P1 - P2 \tag{6.2}$$

$$\mathrm{Q} = \frac{-\ln(1-^{\eta})}{\Delta P} \tag{6.3}$$

P is the fractional aerosol penetration while ΔP is pressure drop. P1 and P2 are the upstream and downstream air pressure respectively, while Q denotes the overall quality factor of the filter. [27]

6.2.8 Water contact angle test

Plasma surface activation on plastics normally decays with time due to environmental contaminations and thermodynamic reorientation of polar groups towards the bulk of the surface [28]. Decay of plasma surface modification is also important in terms of storage after the manufacturing of filter material and will also provide information about the time based effectiveness period of treatment. Therefore, the decay of plasma treatment on the outer layer of 50 GSM CSNF coated PP substrate was analysed by using water contact angle test [is this common? why the water contact angle can be used? provide reference]. Selected samples were

tested on the same day of plasma treatment and after 15, 30 and 60 days of plasma treatment to measure the decay.

The water contact angle test was performed by using the KRUSS DSA100 drop shape analyser (DSA) instrument as shown in Figure 6.3. Drop shape analysis (DSA) involves image analysis of the shadow image of a sessile drop to measure the contact angle on the surface. Fitted camera in the instrument records the image of the drop on the surface and transfer to the drop shape analysis software. Then, the contact angle is measured from the baseline of drop on the sample surface with the help of DSA software.

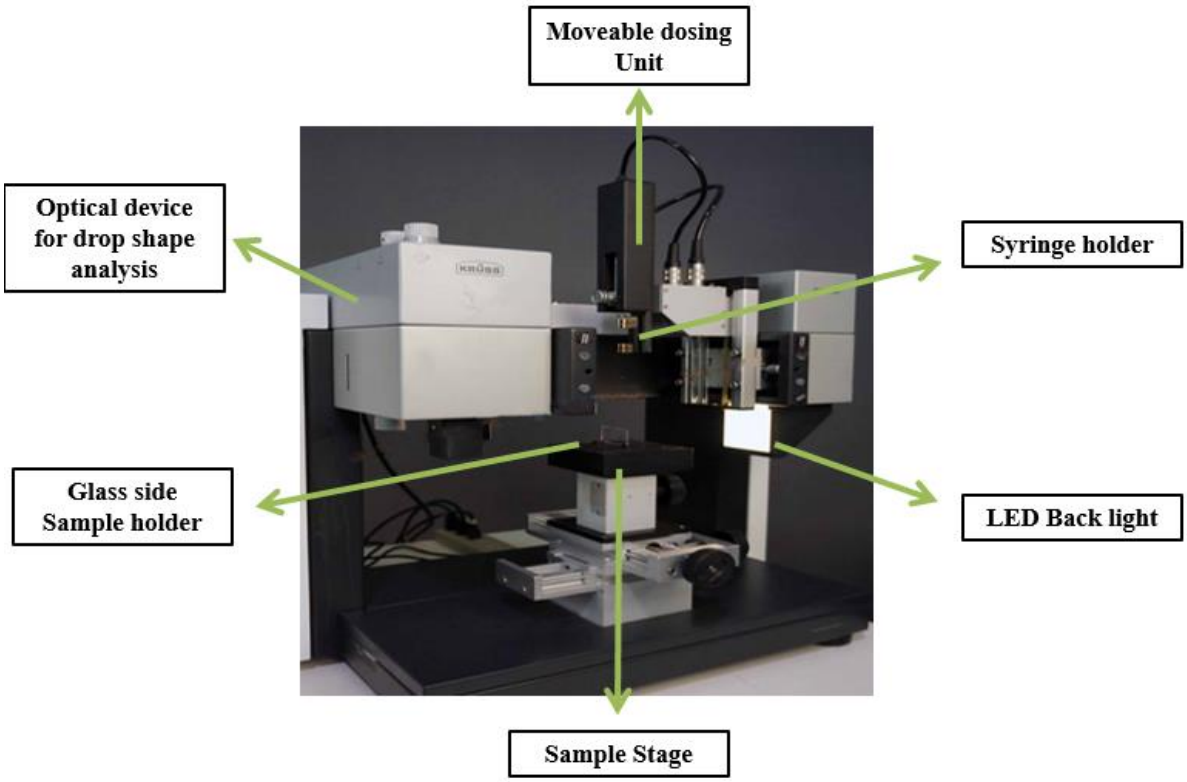

Figure 6.3: KRUSS DSA100 drop shape analyser (DSA) for water contact angle test

6.3 Results and Discussion

6.3.1 Characterisation of chitosan nanofibres

The surface morphology of CSNF was analysed using SEM images. Produced nanofibres are smooth and bead free as shown in Figure 6.4(a). Fibre diameter distribution is also shown in Figure 6.4(b). The diameter of CSNF ranges from 43 nm to 336 nm with an average of 186 nm. The addition of these fine nanofibres increases the overall surface area of the resultant filter, which leads to improving filtration efficiency. Furthermore, small diameter nanofibres provide better aerodynamic slip in the filter which can prevent the collision of air molecules with nanofibres [29]**.** Therefore, the slip of air molecules can lead to lower pressure drop for more effective breathing.

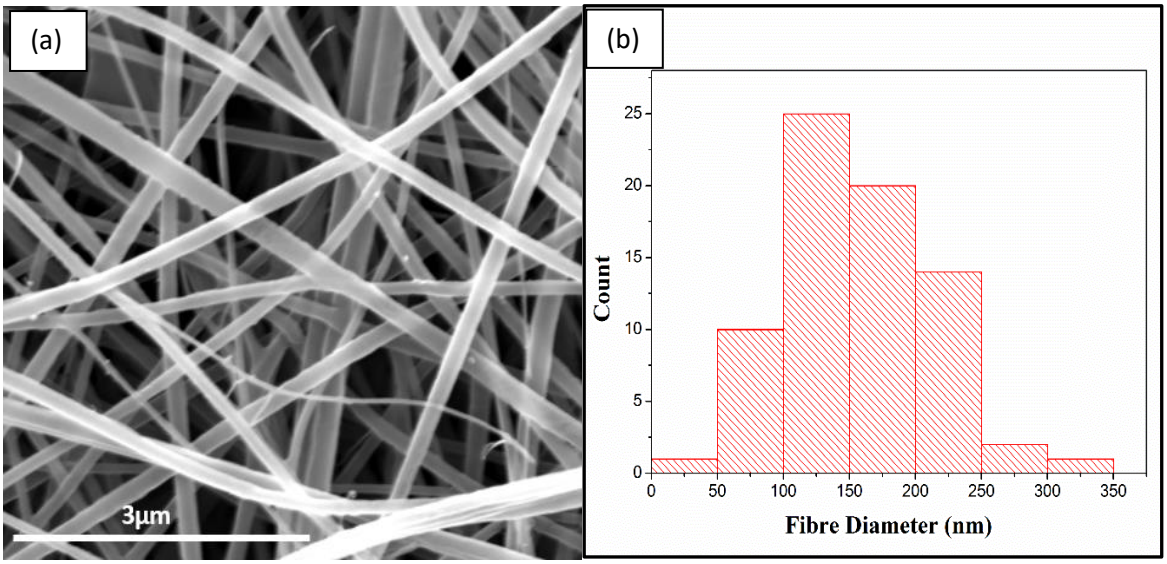

Figure 6.4: (a): SEM image of chitosan nanofibres (b): Histogram of chitosan nanofibres diameter (nm)

Pore size distribution is also a very important factor for respiratory filters. Narrower pore size distribution provides better filtration efficiency but also increases the pressure drop which

remains a challenging factor to control [30]**.** Pore size distribution is dependent on the diameter and amount of nanaofibres in a resultant filter. While the amount of nanofibres increases with coating time. Therefore, four different respiratory filter samples were produced by using four coating times (2h, 4h, 6h and 8h respectively) on each substrate as shown in Table 6.2. The addition of CSNF on each sample was measured by weighing the sample before and after coating. As expected, the amount of nanofibres increases linearly with the increase of coating time, as shown in Figure 6.5.

FTIR spectrums of PP substrate, pure chitosan (CS) and CSNF coated PP substrate (CSNFPP) are shown in Figure 6.6 (a, b and c). The peaks between 2800-3000 cm^{-1} are attributed to C-H stretching vibrations while peaks at 1376 cm^{-1} and 1457 cm^{-1} indicate $–CH_2$ and $–CH_3$ bending vibration in pure PP samples [31]. In the case of chitosan, peaks at 1541 cm^{-1} and 1511 cm^{-1} represent the N-H group while the peak at 2918 cm^{-1} shows C-H stretch [32]. The presence of amine groups in the CSNFPP spectrum confirms that CSNF is effectively coated on the PP meltblown substrate.

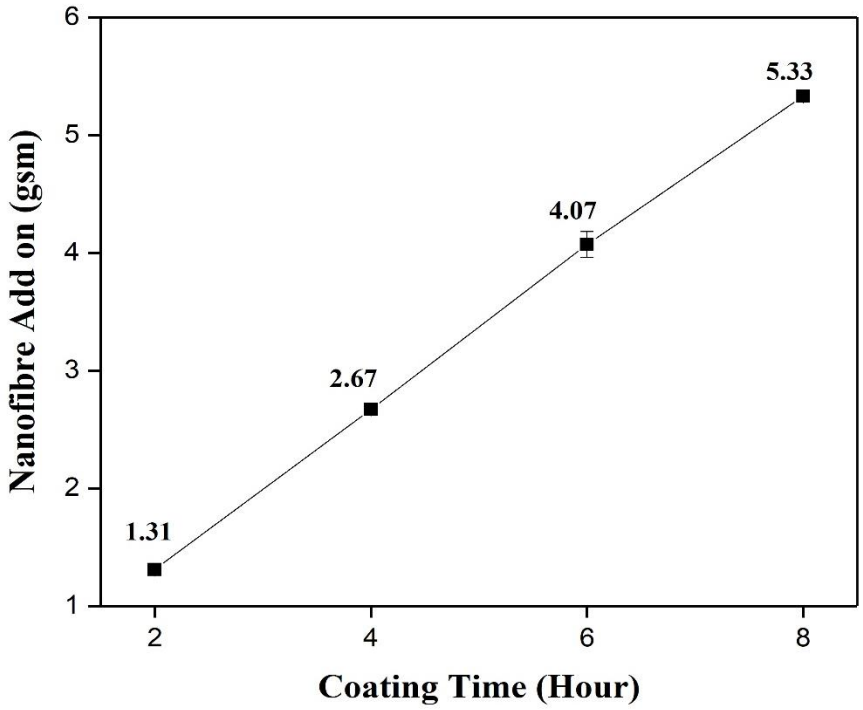

Figure 6.5: Addition of CSNF (gsm) on PP meltblown substrate at different time intervals

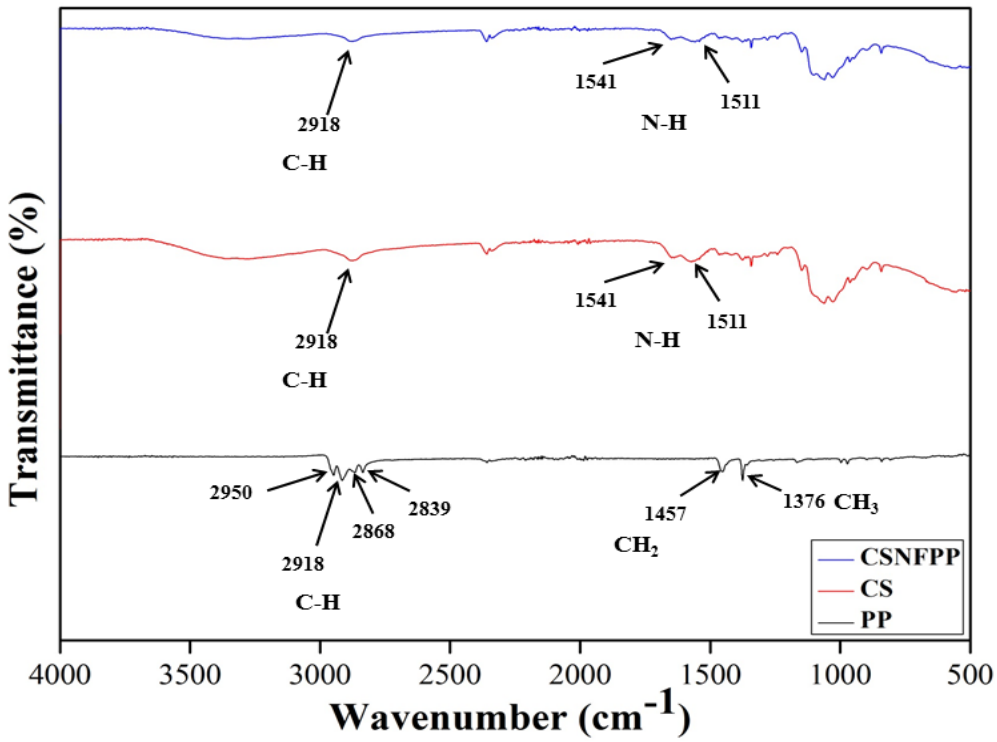

Figure 6. 6: FTIR of (a): PP substrate (b) pure chitosan (c) CSNF coated PP substrate.

6.3.2 Filtration performance of respiratory filter

Filtration performance of the respiratory filter is dependent on filtration efficiency (%), pressure drop (Pa), and quality factor (Q) of the resultant filter. Results of filtration performance are discussed in the following sections.

6.3.2.1 Filtration efficiency analysis

The test results of filtration efficiency of 50 GSM PP meltblown samples are shown in Figure 6.7. In the case of untreated samples, results showed that filtration efficiency increased from 95.48% to 99.99 with the increase of coating time of nanofibres from zero hours to 8 hours respectively. This improvement in filtration efficiency is attributed to increasing in surface area and a decrease in pore size diameter [33] due to a gradual increase in CSNF coating in each category. However, a sample with 8h coating time showed maximum filtration efficiency due to the high amount of CSNF deposition which reduced the pore size distribution even more and increased the surface area significantly as compared to other samples.

In the case of plasma treated samples with the same coating times, filtration efficiency value remained slightly higher as compared to untreated samples in each category as shown in Figure 6.7. However, impact of plasma surface modification was not significant in 50 GSM meltblown samples as they already showed higher filtration performance in untreated samples due its composition and reduced microfibre diameter in the nonwoven substrate form. Moreover, plasma treated sample with 6h CSNF coating time showed maximum filtration efficiency and value remained unchanged after a further increase in coating time. Furthermore, in comparison to the untreated sample, maximum filtration efficiency value was achieved with reduced coating time.

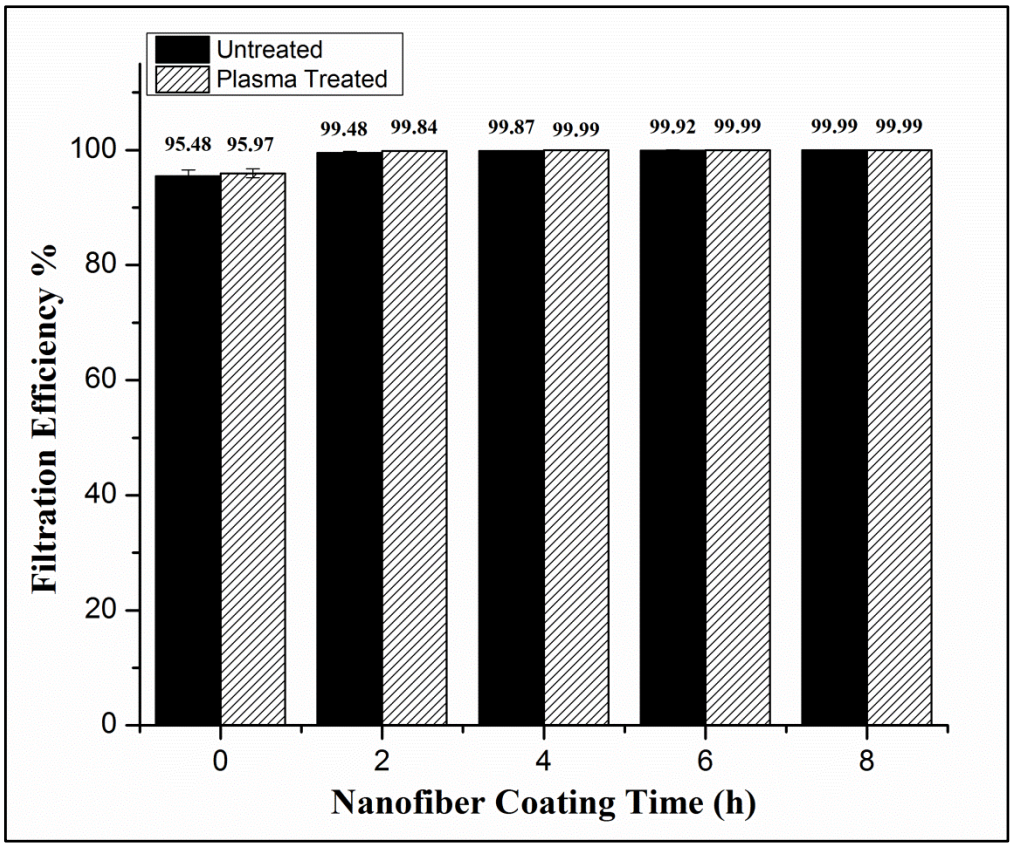

Figure 6.7: Filtration efficiency (%) results of PP 50 GSM (Meltblown) respiratory filter samples after CSNF coating and plasma surface modification

Filtration efficiency results of 70 GSM PP spunbonded samples are shown in Figure 6.8. In the case of untreated samples, results indicate that filtration efficiency increased from 7.75% to 99.95 with the increase of coating time of nanofibres from zero hours to 8 hours respectively. Sample without CSNF coating showed very poor filtration efficiency value (5.27%) due to the higher value of average fibre diameter (Table 6.1) and resultant microporous structure of spunbonded layer. However, a sample with 8h coating time showed a maximum filtration efficiency value of 99.95% due to high surface area and reduced pore size distribution induced by maximum CSNF coating as compared to other samples.

A comparison of plasma treated and untreated samples on each coating time (h) are also shown in Figure 6.6. However, plasma treated samples showed slightly higher filtration efficiency as

compared to untreated samples. These higher filtration efficiency values of plasma coated samples resulted due to surface activation and charge density formation on the outer surface of each sample. However, plasma treated sample with 8h CSNF coating time showed a maximum filtration efficiency value of 99.99%.

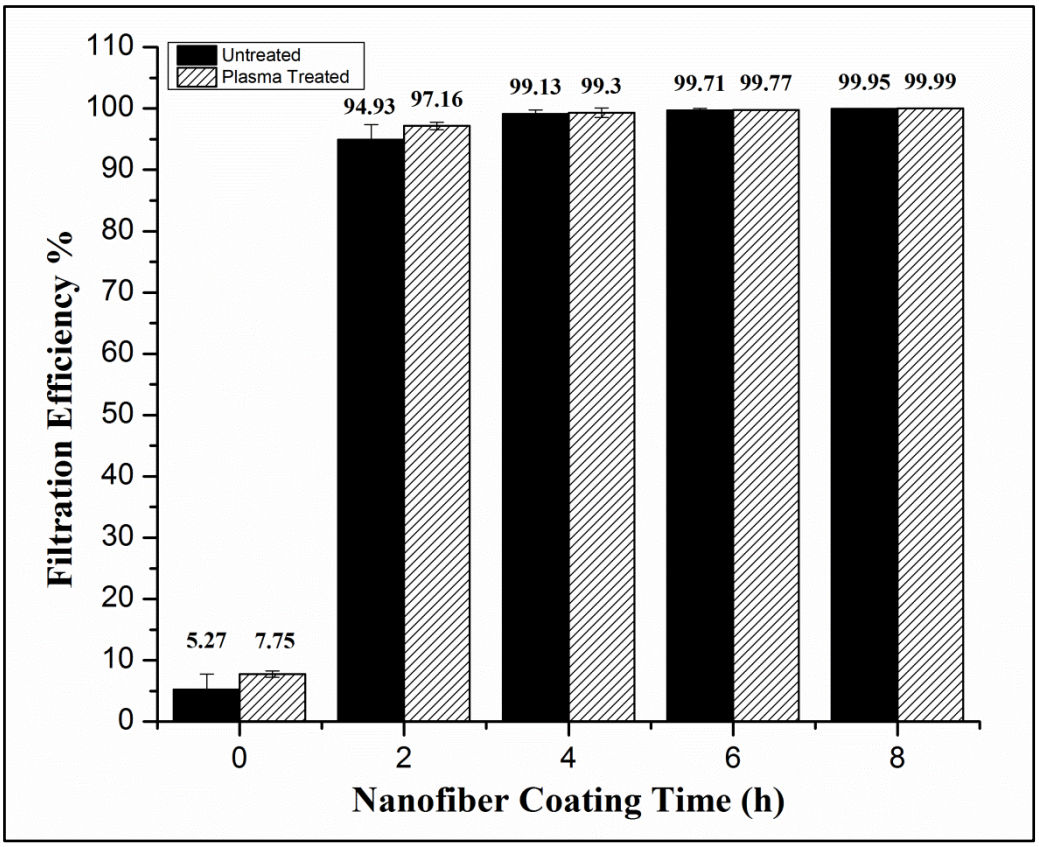

Figure 6.8: Filtration efficiency (%) results of PP 70 GSM (Spunbonded) respiratory filter samples after CSNF coating and plasma surface modification

Filtration efficiency results of 100 GSM PP spunbonded samples are shown in Figure 6.9. In the case of untreated samples, results illustrate that filtration efficiency significantly increased from 23.81% to 86.84% with the increase of coating time of nanofibres from zero hours to 8 hours respectively. Sample without CSNF coating showed very poor filtration efficiency value

(23.81%) due to higher fibre diameter value (Table 6.1) and resultant microporous structure of spunbonded layer alike 70 GSM samples. Similarly, a higher value of filtration efficiency (86.84%) was also achieved at maximum coating time (8h) due to higher surface area induced by nanofibres.

As a comparison, filtration efficiency results of plasma treated 100 GSM samples on each coating time (h) are also shown in Figure 6.8. Similarly, plasma treated samples slightly showed higher filtration efficiency from 26.55% to 89.66% with the gradual increase of CSNF coating time respectively as compared to untreated samples. However, plasma treated sample with 8h CSNF coating time showed maximum filtration efficiency value of 89.66%.

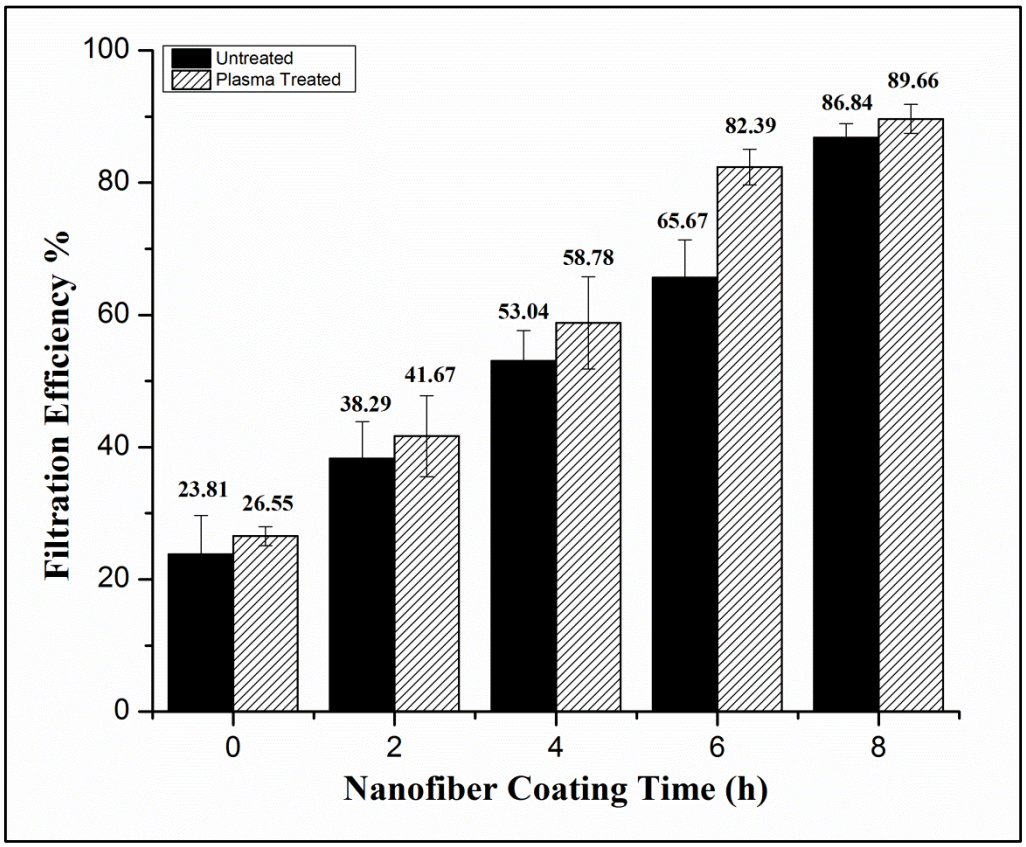

Figure 6.9: Filtration efficiency (%) results of PP 100 GSM (Spunbonded) respiratory filter samples after CSNF coating and plasma surface modification

Improvement in filtration efficiency in all the samples of three different PP substrates is attributed due to the increase in surface area and a decrease in pore size diameter with a gradual increase in CSNF coating time. It is well documented that addition of nanofibres increases the surface area, decrease the average pore size diameter and ultimately improves the overall filtration efficiency of resultant filter [8], therefore same theory applied in this scenario. Impact of plasma treatment on the outer layer of all the samples for the comparison was also elaborated earlier. All the plasma treated samples in each category also showed higher filtration efficiency in comparison to untreated ones. These higher filtration efficiency values of plasma treated samples are associated with surface activation, induced polarity and charge density formation on the outer surface of each sample. Plasma surface treatment produces energised free radicals of oxygen which directed towards the inert surface of polypropylene samples under vacuum. Bombardment of oxygen base radicals, breaks the bond between carbon and hydrogen and creates hydroxyl (-OH), carbonyl (-CO) and carboxyl (-COOH) based polar group on the surface. Therefore, charges polymer surface produced with improved wetting and adhesive properties due to formation of polar groups. These polar groups increases the overall surface energy and electrostatic attraction of PP due to induced polarity. [20]

Conclusively, results elaborated the positive impact of plasma surface modification on the filtration efficiency of all the samples due to the improved capturing mechanism by surface activation. Surface modification impact was more significant in spunbonded 70 GSM and 100 GSM nanocomposite samples and showed less significant affect in meltblown 50 GSM nanocomposite samples as they already showed higher filtration efficiency results in untreated samples due to their reduced microfibre diameter of substrate and fine pore size formation in a resultant structure

6.3.2.2 Pressure drop (Pa) analysis

Pressure drop is a very important factor for the consideration of respiratory filter performance. Higher pressure drop value creates difficulty in breathing and reduces the performance of the respiratory filter. Pressure drop results of all the samples in each category are given below.

Pressure drop results of 50 GSM PP meltblown samples are shown in Figure 6.10. In the case of the untreated sample, pressure drop value increased from 94 Pa to 4095 Pa with the increase of CSNF coating time from 2h to 8h respectively. Significant increase in pressure drop was observed by increasing the CSNF nanofibres in a resultant sample by the gradual rise of coating time (h). Furthermore, plasma treated samples also showed a gradual increase in pressure drop with the increase of CSNF coating time and pressure drop value remained from 95 Pa to 3957 Pa respectively as illustrated in Figure 6.10. However, the impact of plasma treatment on 50 GSM PP meltblown samples remained negligible in case of pressure drop and no significant difference was observed in both treated and untreated samples.

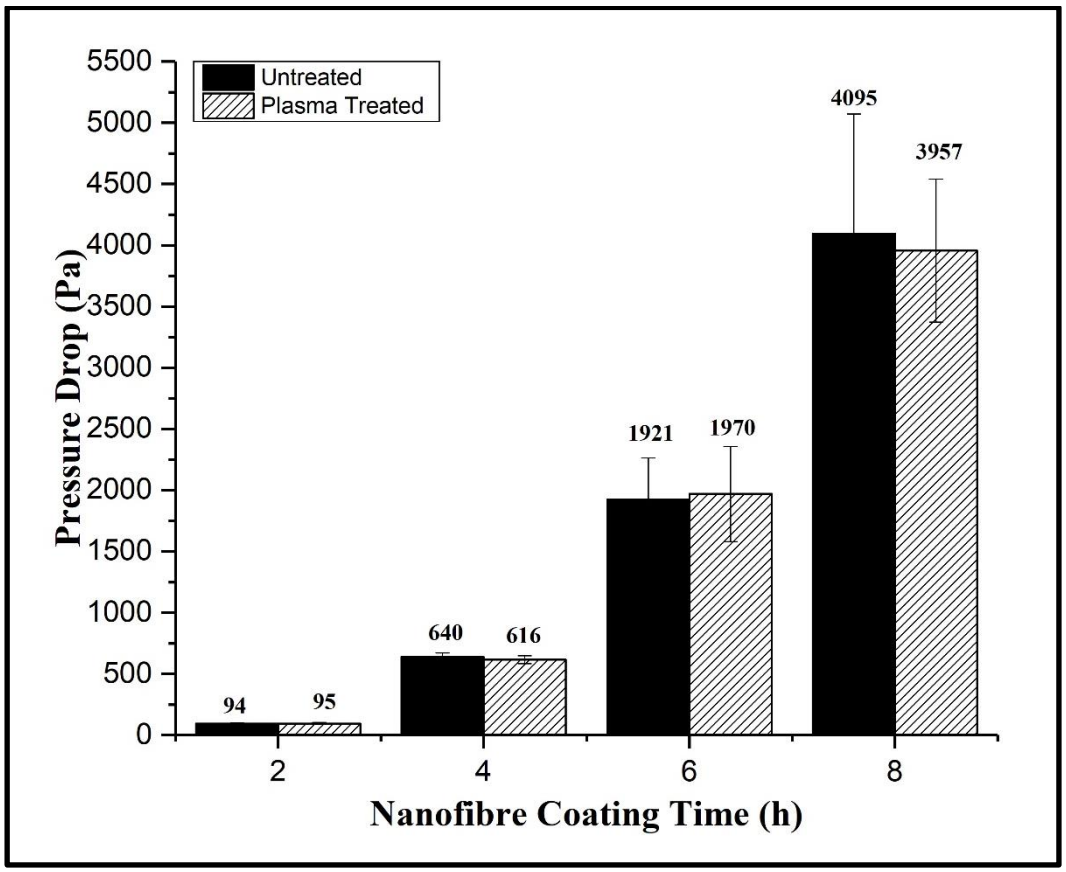

Figure 6.10: Pressure drop (Pa) results of PP 50 GSM (Meltblown) respiratory filter samples after CSNF coating and plasma surface modification

Figure 6.11 illustrates the pressure drop performance of PP 70 GSM samples after CSNF coating. Pressure drop for untreated samples increased from 81 Pa to 1645 Pa with the increase of CSNF coating time from 2h to 8h respectively. Significant increase in pressure drop was observed by increasing the nanofibrous thickness in a resultant sample by the gradual rise of coating time (h). Similarly, plasma treated samples also showed a gradual increase in pressure drop with the increase of CSNF coating time and pressure drop value remained from 82 Pa to 1623 Pa respectively as illustrated in Figure 6.10. Furthermore, the impact of plasma treatment on 70 GSM PP spunbonded samples also remained negligible in case of pressure drop and no significant difference was observed between plasma treated and untreated samples as shown in Figure 6.11.

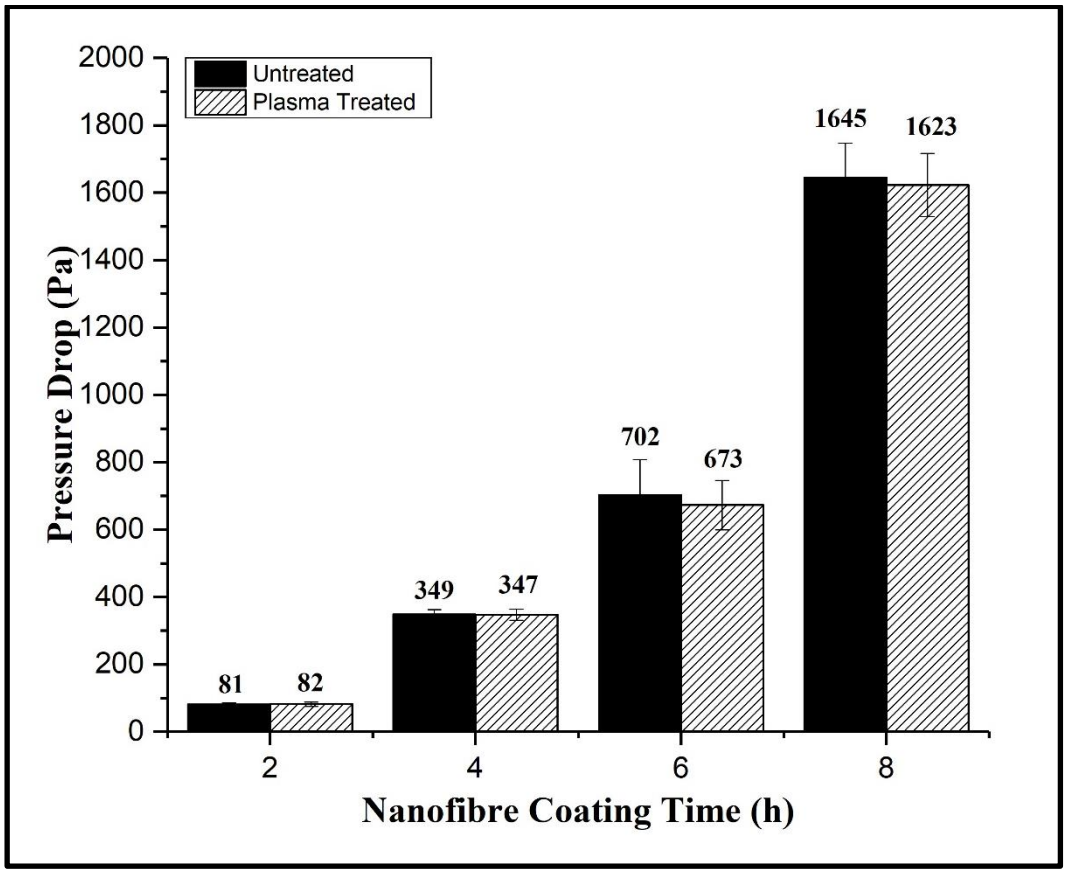

Figure 6.11: Pressure drop (Pa) results of PP 70 GSM (Spunbonded) respiratory filter samples after CSNF coating and plasma surface modification

Figure 6.12 demonstrates the pressure drop performance of PP 100 GSM spunbonded samples after CSNF coating. Pressure drop for untreated samples increased from 17 Pa to 210 Pa with the increase of CSNF coating time from 2h to 8h respectively. Similarly, plasma treated samples also showed gradual increase in pressure drop with the increase of CSNF coating time and pressure drop value remained from 16 Pa to 211 Pa respectively as illustrated in Figure 6.12. As expected, impact of plasma treatment on 100 GSM PP spunbonded samples also remained negligible in case of pressure drop as shown in Figure 6.10.

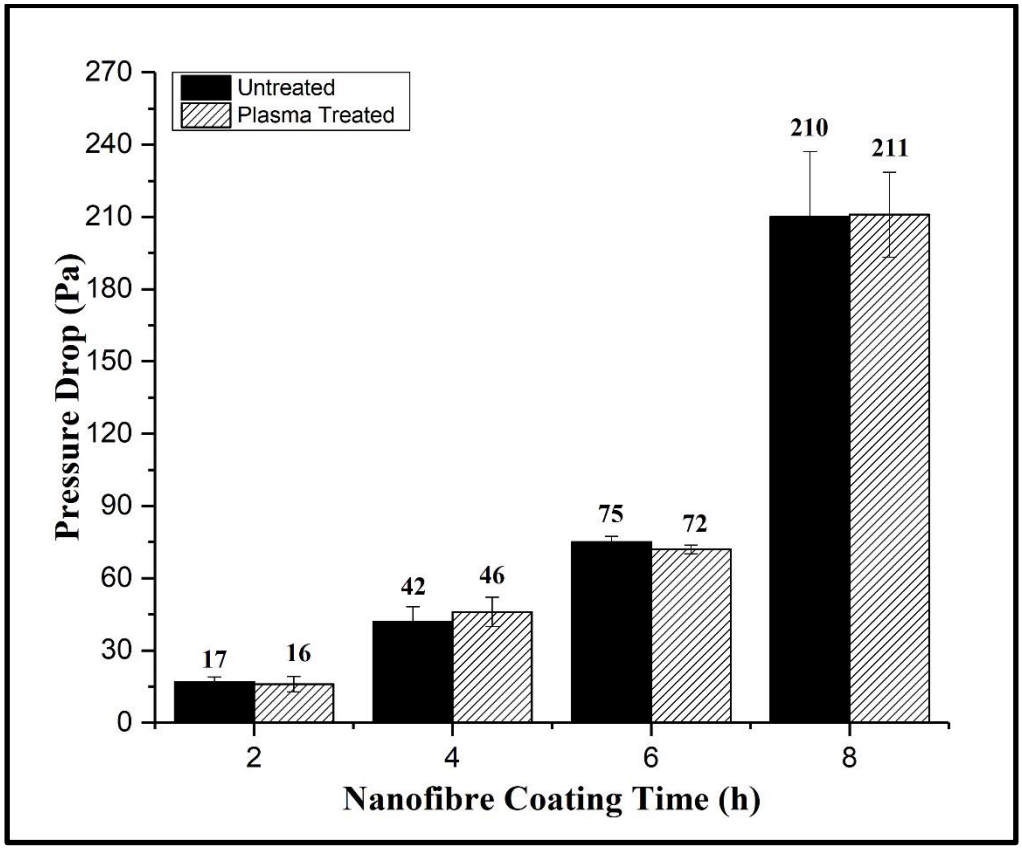

Figure 6.12: Pressure drop (Pa) results of PP 100 GSM (Spunbonded) respiratory filter samples after CSNF coating and plasma surface modification

The significant increase in pressure drop after CSNF coating is due to the reduction of pore size diameter and increase in surface area. Furthermore, the thickness of nanofibre layer depends on coating time**,** which directly affects the pressure drop and adversely affects the air permeability of the filter [34]. According to the European standard for air filtration (EN779:2012), the maximum pressure drop should not exceed 450 Pa for fine particulate filters. Therefore, all the samples in each GSM category having pressure drop value lower than 450 Pa are effective for air filtration for better performance. Furthermore, plasma surface modification showed a negligible impact on pressure drop performance in all resultant respiratory filters.

6.3.2.3 Quality factor (Q) analysis

The quality factor is also a key factor to judge the filtration performance of respiratory filters. Therefore, the quality factor of all the samples was calculated by using Equation 6.3, with the help of filtration efficiency and pressure drop data.

The quality factor results of 50 GSM (meltblown) are shown in Figure 6.13. In the case of untreated samples, the value of the quality factor decreased with the increase of coating time (h). Sample 1 (2h coating time) indicated a higher quality factor due to the higher filtration efficiency with low pressure drop value, while the quality factor of 4h, 6h, and 8h coated samples remained lower comparatively due to the higher pressure drop results. Furthermore, quality factor results for plasma treated sampled followed the pattern of the same results and showed a decline in quality factor performance with the increase in CSNF coating time (h). However, in comparison to untreated samples, plasma treated filter samples showed higher quality factor values in the first two samples (2h, 4h coating time) respectively, while value remained the same for 6h and 8h CSNF coating time as shown in Figure 6.13. Filtration performance after 2h CSNF coating increased marginally, while pressure drop increased drastically. Therefore, higher value of pressure drop decayed the quality factor results in the remaining samples.

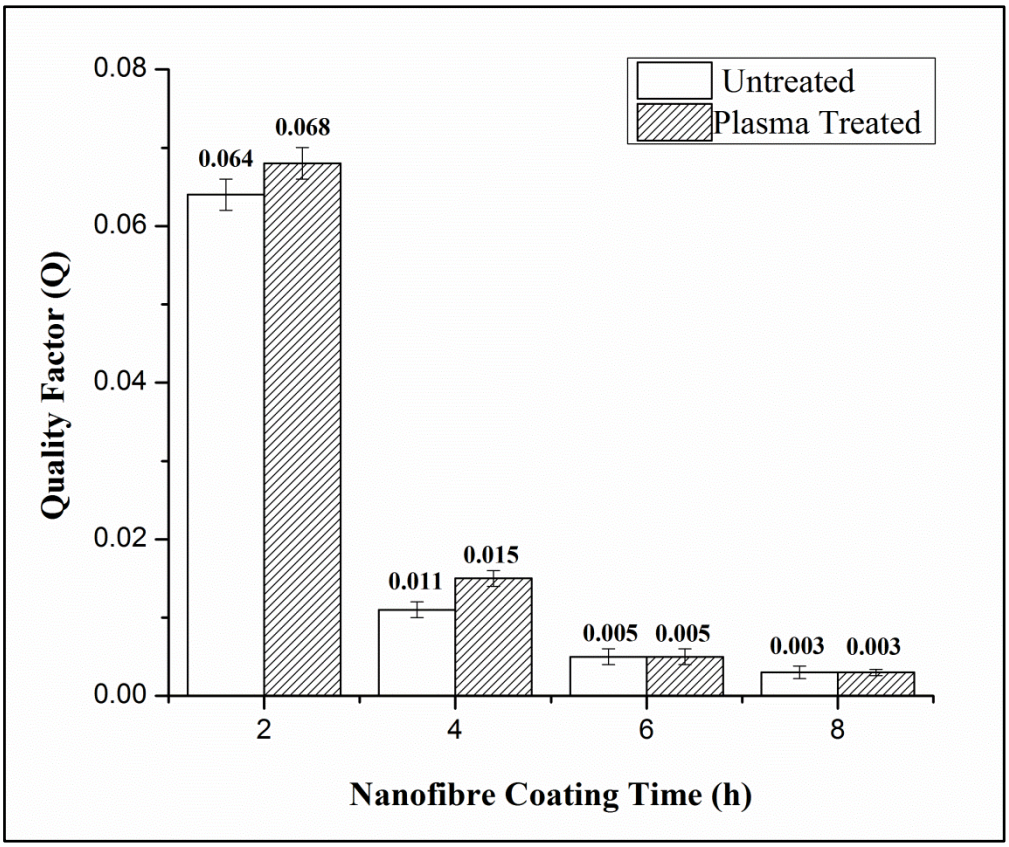

Figure 6.13: Quality factor (Q) results of PP 50 GSM (Meltblown) respiratory filter samples after CSNF coating and plasma surface modification

The quality factor results of 70 GSM (meltblown) are shown in Figure 6.14. In the case of untreated samples, the value of the quality factor followed the same pattern as 50 GSM samples and the value decreased with the increase of coating time (h). Sample 1 (2h coating time) showed a higher quality factor due to the higher filtration efficiency with lower pressure drop value, while the value decreased gradually with the increase CSNF amount in the filter. Furthermore, quality factor results for plasma treated samples followed the pattern of the same result and showed a decline in quality factor performance with the increase in CSNF coating time (h). However, in comparison to untreated samples, plasma treated filter samples showed higher quality factors respectively due to their higher filtration efficiency performance, as shown in Figure 6.14.

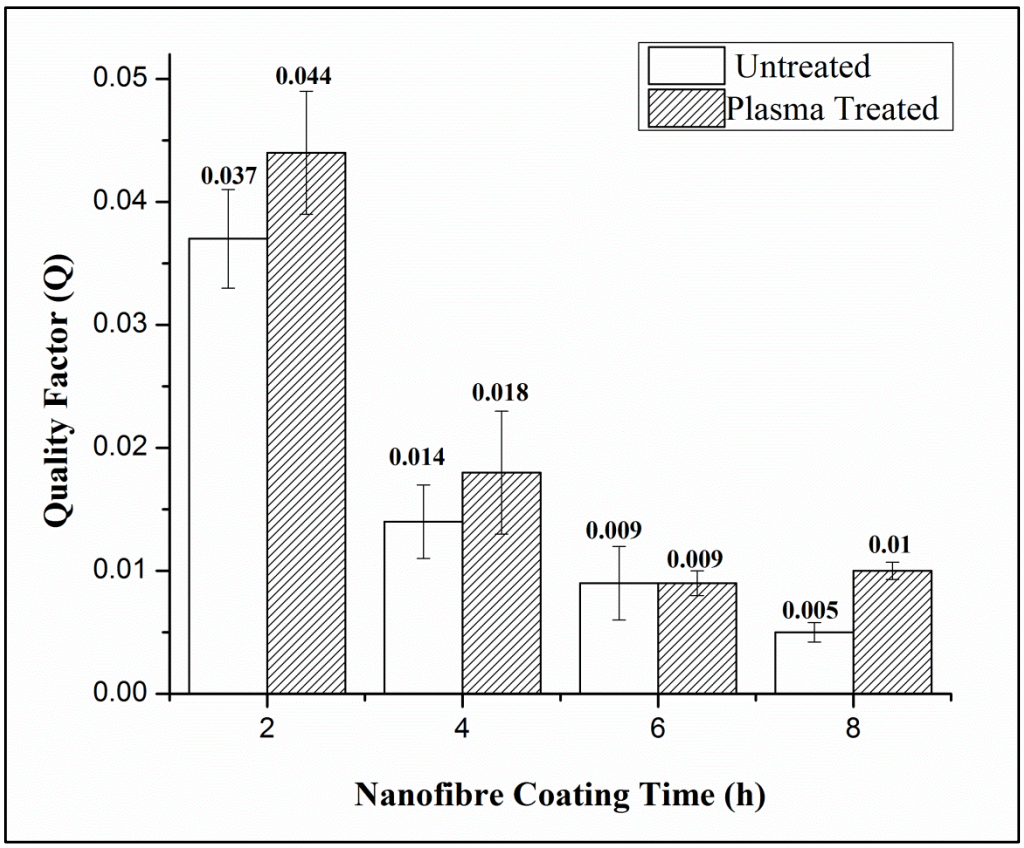

Figure 6.14 Quality factor (Q) results of PP 70 GSM (Spunbonded) respiratory filter samples after CSNF coating and plasma surface modification

Figure 6.15 illustrates the quality factor performance of 100 GSM (spunbonded) respiratory filter samples. Results demonstrated that the value of quality factor decreased with the increase of coating time (h). Furthermore, quality factor results for plasma treated samples followed the pattern of the same results and showed a decline in quality factor performance with the increase in CSNF coating time (h). However, plasma treated filter samples indicated higher quality factor results in comparison to untreated samples as shown in Figure 6.15.

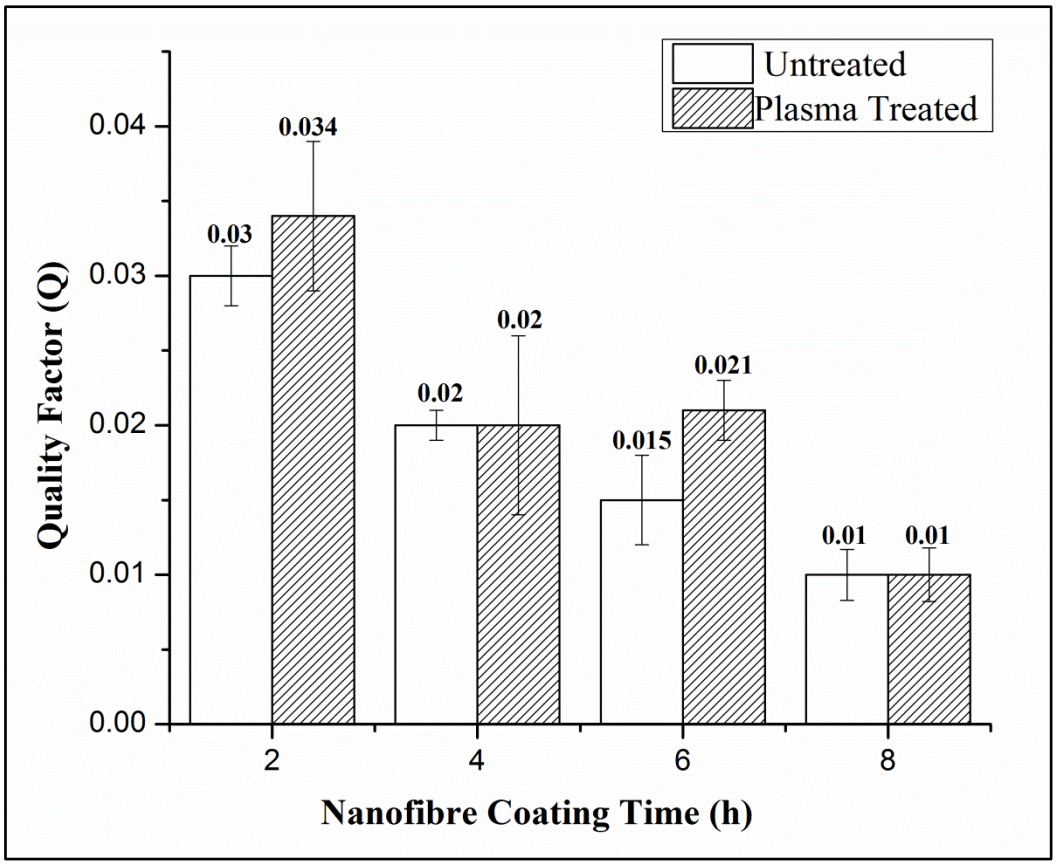

Figure 6.15: Quality factor (Q) results of PP 100 GSM (Spunbonded) respiratory filter samples after CSNF coating and plasma surface modification

A higher-quality factor value is the key factor for better overall filtration performance of respiratory filters. Conclusively, all the samples in each GSM category showed a decline in quality factor results with the increase of CSNF coating time (h). These results can be explained with the relation of coating time and thickness of nanofibrous layer in the resultant filter. The Thickness of nanofibrous layer increases with the increase of coating and governs the high packing density of nanofibres and reduces average pore size in the developed sample [35]. Furthermore, a decrease in pore size diameter increases the filtration efficiency % and also rise the pressure drop which is undesirable for better breathability of the filter. Therefore, the quality factor decreased with the increase of coating time due to higher pressure drop impact. Developed sample of 50 GSM PP meltblown layer with 2h CSNF coating time (h) and plasma

surface modification showed best filtration performance results. Sample showed 99.84% filtration efficiency with a combination of low pressure drop value 82.13 Pa and highest quality factor 0.068.

6.3.2.4 Decay of Plasma Surface modification on PP respiratory filter

The decay of plasma treatment impact on the outer layer of 50 GSM respiratory filter sample was analysed by using drop shape analysis to measure the contact angle. Figure 6.16 and 6.17 shows the results of time impact on the aging of plasma treatment. Contact angle increased from 57.05^{o} to 96.66^{o} with the increase of storage time of the filter up to 60 days. On the same day of plasma treatment, the contact angle of the sample was 57.05^{o} which indicates that the inertness of the material has modified and changed into a functionalised surface due to the formation of free radicals of oxygen [36]. After the plasma treatment, the surface of the filter was changed from hydrophobic to hydrophilic and was fully activated due to induced polar groups by the bombardment of oxygen gas plasma. Then, the sample was retested after 15 and 30 days respectively to check the impact of plasma activation on the surface. Results showed a decline in water contact angle and angle remained 66.4 ^{o} and 75.97 ^{o} respectively. However, the sample still remained in a hydrophilic range which indicates that the surface is less activated from the previous testing but gradually moving towards inertness.

After 60 days, DSA results reported that the contact angle turned to 96.66 ^{o} as shown in Figure 16. In general, a water contact angle greater than 90 ^{o} indicates that the surface of the material is hydrophobic and below than 90^{o} is referred for hydrophilic surfaces. Therefore, an increase in contact angle over 90^{o} indicates the full decay of surface activation of PP respiratory filter after 60 days. This gradual decline in contact angle is associated with the aging effect of plasma treatment due to air contamination impact, storage conditions and thermodynamic reorientation

of induced polar groups towards the bulk of the material from the surface [28]. Conclusively, plasma treatment impact was reduced with the passage of time and the surface became fully inert again after 60 days. Hence, the best results with the plasma treated PP respiratory filter can only be achieved up to 30 days in comparison to untreated samples because the surface will become hydrophobic beyond that duration due to the decay of plasma treatment with time. So, potential use of plasma treatment for better filtration performance is limited to less than 30 days, which bounds the effectiveness of product in terms of storage time and application after the surface modification and packing of filter material.

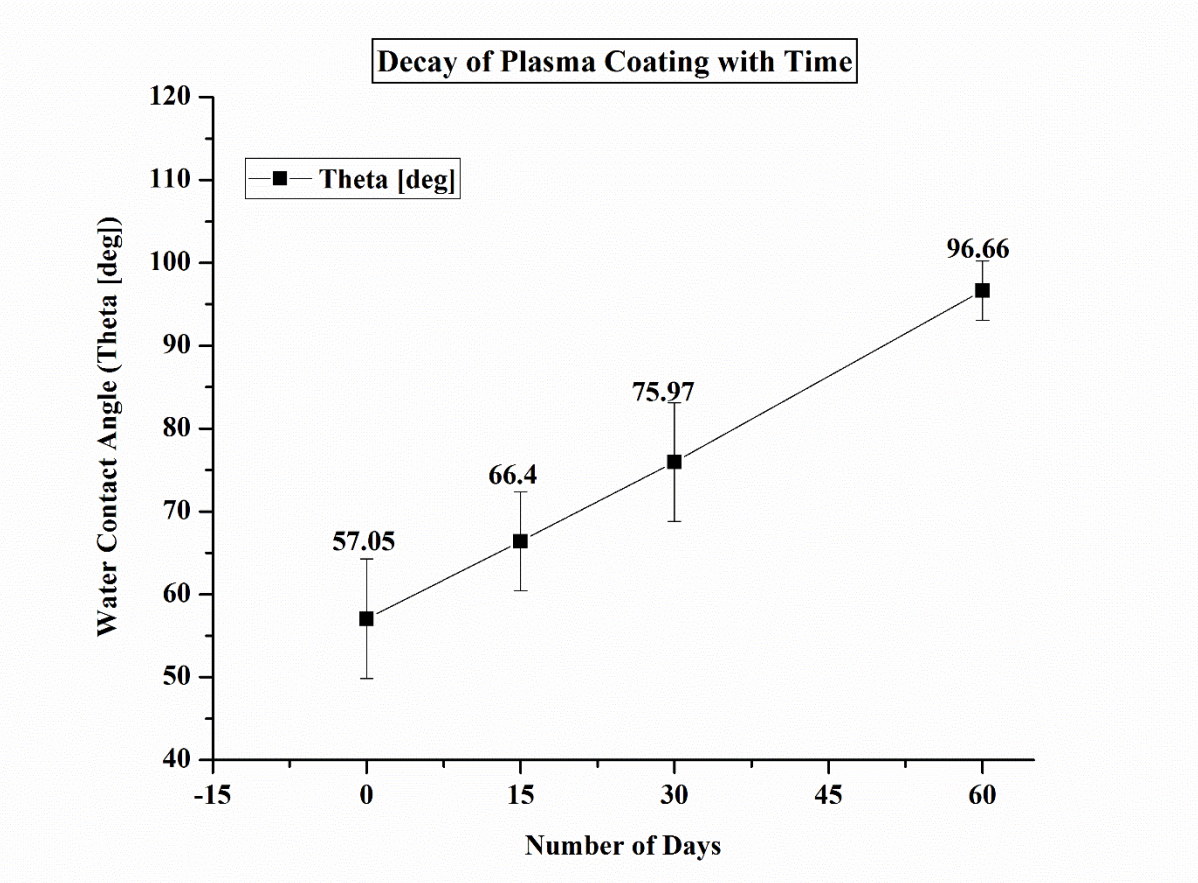

Figure 6.16: Decay of plasma treatment impact with time

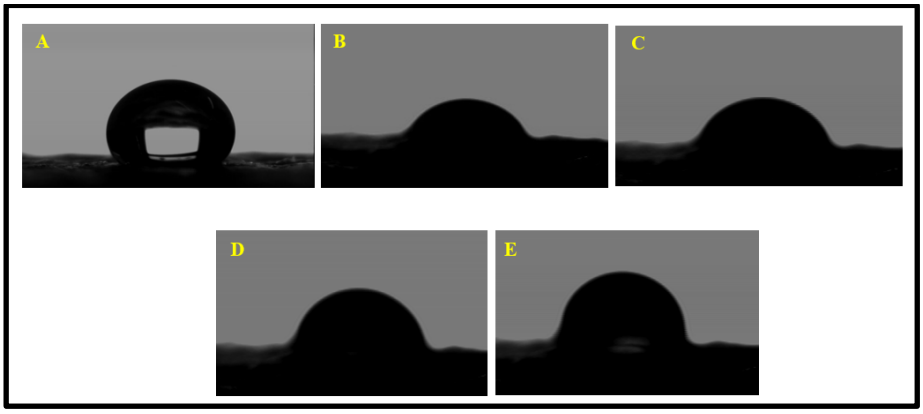

Figure 6.17: Decay of plasma treatment in terms of water contact angle: (A) contact angle of untreated PP sample 124°C (B) contact angle after treatment same day 57.05°C (C) contact angle after 15 days of treatment 66.4°C (D) contact angle after 30 days of treatment 75.97°C (E) contact angle after 60 days of treatment 96.66°C

6.4 Conclusion

In this study, a sandwich structured composite respiratory filters were developed by using CSNF coating and surface modification of the outer layer with the help of low pressure plasma treatment. The impact of CSNF nanofibres coating time and surface modification on filtration performance was studied with the help of filtration efficiency, pressure drop, and quality factor characterisation. Results illustrated that filtration efficiency and pressure drop increased with the rise of nanofibres coating time (h) due to the impact of enhanced thickness. Quality factor decreased significantly due to the rise of pressure drop with an increase of nanofibres coating time (h). The maximum filtration efficiency (%) value was 99.99% and the maximum quality factor was 0.068, while the lowest pressure drop value was 16.12 Pa. The sample of 50 GSM PP meltblown layers with 2h CSNF coating time and plasma surface modification showed best filtration performance. Sample exhibited 99.84% filtration efficiency with a pressure drop value of 82.13 Pa and highest quality factor 0.068. However, plasms surface modification impact was not significant in meltblown 50 GSM nanocomposite samples as they already

showed higher filtration efficiency results in untreated samples due to their fine fibre diameter of substrate and fine pore size formation in a resultant structure comparatively. However, 70 GSM and 100 GSM spunbonded nanocomposite samples showed significant impact of plasma surface modification on filtration efficiency. Thus, a combination of PP nonwoven substrate with nanofibre coating and low pressure plasma treatment can be used for the development of respiratory filter with high filtration performance in the field of air filtration.

The decay of plasma surface modification was analysed by using a water contact angle test on 50 GSM CSNF coated respiratory filter samples. Results showed the surface activation remained on the surface of PP respiratory filter for up to 30 days and samples became hydrophobic after 60 days of the surface modification. Conclusively, the effect of plasma treatment gradually decreased with the passage of time which bounds the application of this treatment in term of storage and immediate use after manufacturing.

Acknowledgement

I acknowledge the financial support of Punjab Education Endowment Fund (PEEF) for awarding a student grant to pursue my PhD. The author also thankful to University of Manchester and Xian Polytechnic University, China, for providing all research and characterisation facilities.

References:

[1] V. V. Kadam, L. Wang, and R. Padhye, “Electrospun nanofibre materials to filter air pollutants - A review,” *J. Ind. Text.*, vol. 0, no. 00, pp. 1–28, 2016.

[2] R. E. Shaffer and S. Rengasamy, “Respiratory protection against airborne nanoparticles: A review,” *J. Nanoparticle Res.*, vol. 11, no. 7, pp. 1661–1672, 2009.

[3] OSHA, “General Respiratory Protection Guidance for Respiratory,” 2016.

[4] A. Mukhopadhyay, “Pulse-jet filtration: An effective way to control industrial pollution Part I: Theory, selection and design of pulse-jet filter,” *Text. Prog.*, vol. 41, no. 4, pp. 195–315, 2009.

[5] V. Kadam, I. L. Kyratzis, Y. B. Truong, J. Schutz, and L. Wang, “2019 Electrospun bilayer nanomembrane with hierarchical placement of bead-on-string and fibres for low resistance respiratory air filtration.pdf,” *Sep. Purif. Technol.*, vol. 224, no. 1, pp. 247–254, 2019.

[6] R. Faki, O. Gursoy, and Y. Yilmaz, “Effect of Electrospinning Process on Total Antioxidant Activity of Electrospun Nanofibres Containing Grape Seed Extract,” pp. 912–918, 2019.

[7] J. Xue, T. Wu, Y. Dai, and Y. Xia, “Electrospinning and electrospun nanofibres: Methods, materials, and applications,” *Chem. Rev.*, vol. 119, no. 8, pp. 5298–5415, 2019.

[8] Y. Si, X. Tang, J. Yu, and B. Ding, “Electrospun Nanofibres for Energy and Environmental Applications,” *Nanostructure Sci. Technol.*, no. DOI 10.1007/978-3-642-54160-5__1, p. 525, 2014.

[9] M. Cao, F. Gu, C. Rao, J. Fu, and P. Zhao, “Improving the electrospinning process of fabricating nanofibrous membranes to filter PM2.5,” *Sci. Total Environ.*, vol. 666, pp. 1011–1021, 2019.

[10] R. S. Barhate and S. Ramakrishna, “Nanofibrous filtering media: Filtration problems and solutions from tiny materials,” *J. Memb. Sci.*, vol. 296, no. 1–2, pp. 1–8, 2007.

[11] C. V Stevens, “Chitosan as Antimicrobial Agent : Applications and Mode of Action Chitosan as Antimicrobial Agent : Applications and Mode of,” vol. 4, no. SEPTEMBER, 2003.

[12] H. Sashiwa and S. I. Aiba, “Chemically modified chitin and chitosan as biomaterials,” *Prog. Polym. Sci.*, vol. 29, no. 9, pp. 887–908, 2004.

[13] E. a El-hefian, M. M. Nasef, and A. H. Yahaya, “Chitosan Physical Forms : A Short Review,” *Aust. J. Basic Appl. Sci.*, vol. 5, no. 5, pp. 670–677, 2011.

[14] M. Arkoun, F. Daigle, M. C. Heuzey, and A. Ajji, “Mechanism of action of electrospun chitosan-based nanofibres against meat spoilage and pathogenic bacteria,” *Molecules*, vol. 22, no. 4, 2017.

[15] B. Simoncic and B. Tomsic, “Structures of Novel Antimicrobial Agents for Textiles - A Review,” *Text. Res. J.*, vol. 80, no. 16, pp. 1721–1737, 2010.

[16] C. Sen Wang, “Electrostatic forces in fibrous filters - A review,” *Powder Technol.*, vol. 118, no. 1–2, pp. 166–170, 2001.

[17] S. C. Rasipuram *et al.*, “Submicrometre particle filtration with a dc activated Plasma textile,” *J. Phys. D. Appl. Phys.*, vol. 47, no. 2, 2014.

[18] A. Jaworek, A. Krupa, and T. Czech, “Modern electrostatic devices and methods for exhaust gas cleaning: A brief review,” *J. Electrostat.*, vol. 65, no. 3, pp. 133–155, 2007.

[19] E. M. Liston, L. Martinu, and M. R. Wertheimer, “Plasma surface modification of polymers for improved adhesion: A critical review,” *J. Adhes. Sci. Technol.*, vol. 7, no. 10, pp. 1091–1127, 1993.

[20] P. Favia and R. d’Agostino, “Plasma treatments and plasma deposition of polymers for biomedical applications,” *Surf. Coatings Technol.*, vol. 98, no. 1–3, pp. 1102–1106, 1998.

[21] Michael Thomas and K.L. Mittal, “Selective Surface Modification of Polymer Materials by Atmospheric Pressure Plasmas,” in *Atmospheric Pressure Plasma Treatment of Polymers:*

Relevance to Adhesion, WILEY Publishers, 2013.

[22] S. M. Lemma, F. Bossard, and M. Rinaudo, "Preparation of pure and stable chitosan nanofibres by electrospinning in the presence of poly(ethylene oxide)," *Int. J. Mol. Sci.*, vol. 17, no. 11, 2016.

[23] M. Tang, J. Hu, Y. Liang, and D. Y. H. Pui, "Pressure drop, penetration and quality factor of filter paper containing nanofibres," *Text. Res. J.*, vol. 87, no. 4, pp. 498–508, 2017.

[24] R. M. Eninger, T. Honda, A. Adhikari, H. Heinonen-Tanski, T. Reponen, and S. A. Grinshpun, "Filter performance of N99 and N95 facepiece respirators against viruses and ultrafine particles," *Ann. Occup. Hyg.*, vol. 52, no. 5, pp. 385–396, 2008.

[25] J. P. Eshbaugh, P. D. Gardner, A. W. Richardson, and K. C. Hofacre, "N95 and P100 Respirator Filter Efficiency Under High Constant and Cyclic Flow," *J. Occup. Environ. Hyg.*, vol. 6, no. 1, pp. 52–61, 2008.

[26] S. Sundarrajan, K. L. Tan, S. H. Lim, and S. Ramakrishna, "Electrospun nanofibres for air filtration applications," *Procedia Eng.*, vol. 75, pp. 159–163, 2014.

[27] V. V. Kadam, L. Wang, and R. Padhye, "Electrospun nanofibre materials to filter air pollutants – A review," *J. Ind. Text.*, vol. 47, no. 8, pp. 2253–2280, 2018.

[28] R. A. Jelil, *A review of low-temperature plasma treatment of textile materials*, vol. 50, no. 18. 2015.

[29] H. Wan *et al.*, "Hierarchically structured polysulfone/titania fibrous membranes with enhanced air filtration performance," *J. Colloid Interface Sci.*, vol. 417, pp. 18–26, 2014.

[30] W. Sambaer, M. Zatloukal, and D. Kimmer, "3D air filtration modeling for nanofibre based filters in the ultrafine particle size range," *Chemical Engineering Science*, vol. 82. pp. 299–311, 2012.

[31] K. S. Chun, S. Husseinsyah, and H. Osman, "Utilization of cocoa pod husk as filler in

polypropylene biocomposites: Effect of maleated polypropylene," *J. Thermoplast. Compos. Mater.*, vol. 28, no. 11, pp. 1507–1521, 2015.

[32] A. Razzaz, S. Ghorban, L. Hosayni, M. Irani, and M. Aliabadi, "Chitosan nanofibres functionalized by TiO2 nanoparticles for the removal of heavy metal ions," *Journal of the Taiwan Institute of Chemical Engineers*, vol. 58. pp. 333–343, 2016.

[33] X. Liu, H. Shen, and X. Nie, "Study on the filtration performance of the baghouse filters for ultra-low emission as a function of filter pore size and fibre diameter," *Int. J. Environ. Res. Public Health*, vol. 16, no. 2, pp. 1–19, 2019.

[34] M. A. Hassan, B. Y. Yeom, A. Wilkie, B. Pourdeyhimi, and S. A. Khan, "Fabrication of nanofibre meltblown membranes and their filtration properties," *J. Memb. Sci.*, vol. 427, pp. 336–344, 2013.

[35] N. Wang, Z. Zhu, J. Sheng, S. S. Al-Deyab, J. Yu, and B. Ding, "Superamphiphobic nanofibrous membranes for effective filtration of fine particles," *J. Colloid Interface Sci.*, vol. 428, pp. 41–48, 2014.

[36] K. S. Chen, H. R. Lin, S. C. Chen, J. C. Tsai, and Y. A. Ku, "Long term water adsorption ratio improvement of polypropylene fabric by plasma pre-treatment and graft polymerization," *Polym. J.*, vol. 38, no. 9, pp. 905–911, 2006.

Chapter 7: Conclusion and future work

7.1 Conclusion

In this research work, a sandwich composite structure of two PP nonwoven layers and chitosan (CS) nanofibrous layer was fabricated for the development of respiratory filters. The performances of all developed respiratory filter samples were evaluated against the possible causes of byssinosis (COPD).

Chitosan nanofibre production was optimized to achieve a higher concentration of chitosan. Smooth and uniform chitosan nanofibres were electrospun by using 50% glacial acetic as solvent and 3% PEO solution as a co-spinning agent. Results illustrated that higher applied voltage and longer working distance developed finer nanofibres in all the samples of different concentrations. However, fibre production was only achieved up to 3.5% concentration of chitosan. The concentration of chitosan at 4% and above could not produce nanofibres due to high viscosity and high surface tension of solutions. The optimum nanofibre production conditions were 3.5% concentration of chitosan, 10cm working distance, and 20kv voltage.

Meltblown PP three layer composite filter samples were fabricated to analyse filtration performances. Results showed that the filtration efficiency increased with the rise of coating time (h) of CSNF, but pressure drop also increased. However, samples with 2h CSNF coating time showed a high filtration efficiency of up to 99.27% against the targeted aerosol range, a low pressure drop of 71.6 Pa, and a higher quality factor. Additionally, the antibacterial activity of CSNF against Pantoea agglomerans (*Enterobacter agglomerans*, Biosafety level 1, gram negative) bacterial strains were investigated. Quantitative analysis showed that CSNF has up to 91% antibacterial efficiency against the targeted pathogens. It can be concluded that the

fabricated PP respiratory filter with a 2-hour CSNF coating time offers a combination of high filtration efficiency, low pressure drop, and good antibacterial property. Filters made from such material are expected to effectively prevent byssinosis in textile cotton workers.

Additionally, the impact of low pressure plasma surface modification on filtration performance was studied. The samples of the respiratory filter were produced by using same three layer structure, having a CSNF coated layer sandwiched between two nonwoven layers. The outer layer of PP was surface modified by using low pressure plasma treatment. It was observed that respiratory filter sample of 50 GSM PP meltblown layer with 2h CSNF coating time and plasma surface modification showed the best filtration performance. Furthermore, 50 GSM PP meltblown sample exhibited 99.84% filtration efficiency with a combination of low pressure drop of 82.13 Pa and the highest quality factor of 0.068. However, plasms surface modification impact was not significant in meltblown 50 GSM nanocomposite samples as they already showed higher filtration efficiency results in untreated samples due to their finer fibre diameter of substrate layers and fine pore size formation in a resultant structure comparatively. However, 70 GSM and 100 GSM spunbonded nanocomposite samples showed significant impact of plasma surface modification on filtration efficiency. Thus, the combination of PP nonwoven substrate with nanofibre coating and low pressure plasma treatment can be used for the development of respiratory filter with high filtration performance in the field of air filtration. The decay of plasma surface modification effect on filtration performance was also analysed by using a water contact angle test on 50 GSM CSNF coated respiratory filter sample. The surface activation remained effective on the surface of the PP respiratory filter for up to 30 days and the sample became hydrophobic after 60 days of surface modification. This confirms the gradual decay of plasma treatment effect with the passage of time and restricts its application for longer period.

7.2 Future Work

The present research was specifically conducted to reduce byssinosis in textile workers. Therefore, targeted aerosol range and gram negative bacterial species were selected for investigation of performance. All the samples were produced by using the same substrate layers. Furthermore, the characterisation of all the samples was carried out in a laboratory environment. Therefore, research on the filtration performance of the developed respiratory samples can be further tested on the basis of targeted applications. The following are some possibilities for future work.

7.2.1 Industrial Evaluation of developed in Textile spinning environment

Industrial evaluation of filtration performance can be further investigated on factory floor in textile mill environment. The results will be more realistic for the targeted application, although the installation of the filtration setup will be a challenging task.

7.2.2 Evaluation of filtration performance below 100nm aerosols

The developed respiratory filter samples can be further evaluated for the filtration performance against aerosols less than 100nm size. Furthermore, the structure and nanofibrous coating design can be further modified to get better filtration performance against aerosols less than 100nm in size.

7.2.3 Combination of different PP nonwoven substrate for filter development

The current study investigated the performance of respiratory filter with the same GSM and PP substrate layers. Combinations of PP meltblown and spunbonded layers having different GSM can be used to design the respiratory filter for the filtration performance optimisation in future research.

7.2.4 Filtration performance against COVID-19 Virus protection

The developed respiratory filter with the best filtration performance can be further investigated against possible causes of COVID-19 virus to reduce the symptom or to offer protection.

7.2.5 Filtration efficiency test with aerosol particle size distribution

All the samples of developed respiratory filter material can be further analysed by using an instrument which can also provide the distribution percentage of interacted aerosol in addition to the range of particle diameter. So that, more detailed and precise analysis of filtration efficiency can be studied.

Publications Plan

1. "Process optimisation of chitosan nanofibres production" is ready to submit in Fibres and Polymers journal.

2. "Chitosan nanofibrous respiratory filter for byssinosis prevention" is ready to submit in Carbohydrate Polymers journal.

3. "Effect of low pressure plasma surface modification on filtration performance of chitosan nanofibrous membranes" is ready to submit in Carbohydrate Polymers journal.

Appendix A

Table A-1: Filtration performance results of CSNF coated 25 GSM filter samples

Filtration Efficiency (%) 25 GSM Meltblown Filter Samples									
Sr. #	**CSNF Coating Time (h)**	**Filtration Efficiency (ɳ) (%)**			**Average (%)**	**Standard Deviation**	**1- ɳ**	**Pressure Drop (P)**	**Quality Factor (Q)**
1	2	99.97	99.56	99.62	99.72	0.22	0.0028	71.60	0.089
2	4	99.89	99.85	99.94	99.89	0.04	0.0011	294.11	0.023
3	6	99.99	100	100	99.99	0.01	0.0001	472.39	0.021
4	8	99.99	99.99	100	99.99	0.01	0.0001	935.45	0.010

Table A-2: Antibacterial testing results of chitosan nanofibres

Antibacterial Efficiency (%) of Chitosan Nanofibres						
Description	**CFU (10^5)/ml**			**Average CFU (10^5)/ml**	**Standard Deviation**	**Antibacterial Efficiency (%)**
Standard Stock	52	48	50	50	2.00	
Sample 1 (12h)	13	11	12	12	1.00	76
Sample 2 (24h)	5	4	5	4.67	0.58	91

Table A-3: Filtration performance results of CSNF coated 50 GSM filter samples

Filtration Efficiency (%) 50 GSM Meltblown Filter Samples										
Sample #	**Plasma Coating**	**CSNF Coating Time (h)**	**Filtration Efficiency (%) (η)**			**Average (%)**	**Standard Deviation**	**1- η**	**Pressure Drop (P)**	**Quality Factor (Q)**
0	Yes	0	96.85	95.31	95.75	95.97	0.79	0.0403	-	-
1		2	99.83	99.81	99.87	99.84	0.03	0.0016	95.25	0.068
2		4	100.00	99.98	99.98	99.99	0.01	0.0001	615.58	0.015
3		6	99.99	99.97	100.00	99.99	0.01	0.0001	1970.17	0.005
4		8	99.997	99.999	99.998	99.990	0.00	0.0001	3956.80	0.003
0	No	0	96.49	94.31	95.65	95.48	1.10	0.0452	-	-
1		2	99.57	99.17	99.71	99.48	0.28	0.0052	93.53	0.064
2		4	99.83	99.93	99.86	99.87	0.05	0.0013	639.98	0.011
3		6	99.97	99.99	99.79	99.92	0.11	0.0008	1920.81	0.005
4		8	99.98	100.00	99.99	99.99	0.01	0.0001	4095.42	0.003

Table A-4: Filtration performance results of CSNF coated 70 GSM filter samples

Filtration Efficiency (%) 70 GSM Spunbonded Filter Samples										
Sample #	**Plasma Coating**	**Nanofibre Coating Time (h)**	**Filtration Efficiency (%) (η)**			**Average (%)**	**Standard Deviation**	**1- η**	**Pressure Drop (P)**	**Quality Factor (Q)**
0	Yes	0	8.23	7.21	7.80	7.75	0.51	0.92	-	-
1		2	96.69	97.87	96.92	97.16	0.62	0.03	82.13	0.044
2		4	99.99	98.45	99.45	99.30	0.78	0.01	347.26	0.018
3		6	99.75	99.77	99.79	99.77	0.02	0.00	673.39	0.009
4		8	99.97	99.99	99.996	99.99	0.01	0.00	1623.02	0.010
0	No	0	6.07	2.46	7.28	5.27	2.51	0.95	-	-
1		2	96.33	92.07	96.38	94.93	2.47	0.05	81.79	0.037
2		4	99.74	98.45	99.20	99.13	0.65	0.01	348.73	0.014
3		6	99.34	99.97	99.83	99.71	0.33	0.00	701.72	0.009
4		8	99.89	99.96	99.98	99.95	0.05	0.00	1645.00	0.005

Table A-5: Filtration performance results of CSNF coated 70 GSM filter samples

Filtration Efficiency (%) 100 GSM Spunbonded Filter Samples										
Sample #	**Plasma Coating**	**Nanofibre Coating Time (h)**	**Filtration Efficiency (%) (η)**			**Average (%)**	**Standard Deviation**	**1- η**	**Pressure Drop (P)**	**Quality Factor (Q)**
0	Yes	0	25.00	26.80	27.85	26.55	1.44	0.73	-	-
1		2	47.00	43.00	35.00	41.67	6.11	0.58	16.23	0.0340
2		4	64.95	60.19	51.21	58.78	6.98	0.41	45.63	0.0200
3		6	84.84	82.83	79.51	82.39	2.69	0.18	72.44	0.0210
4		8	89.66	87.47	91.85	89.66	2.19	0.10	211.25	0.0100
0	No	0	23.43	29.86	18.13	23.81	5.87	0.76	-	-
1		2	42.73	32.03	40.11	38.29	5.58	0.62	16.12	0.0300
2		4	54.00	48.00	57.11	53.04	4.63	0.47	42.38	0.0200
3		6	72.00	64.00	61.00	65.67	5.69	0.34	74.57	0.0150
4		8	87.17	84.60	88.75	86.84	2.10	0.13	210.58	0.0100

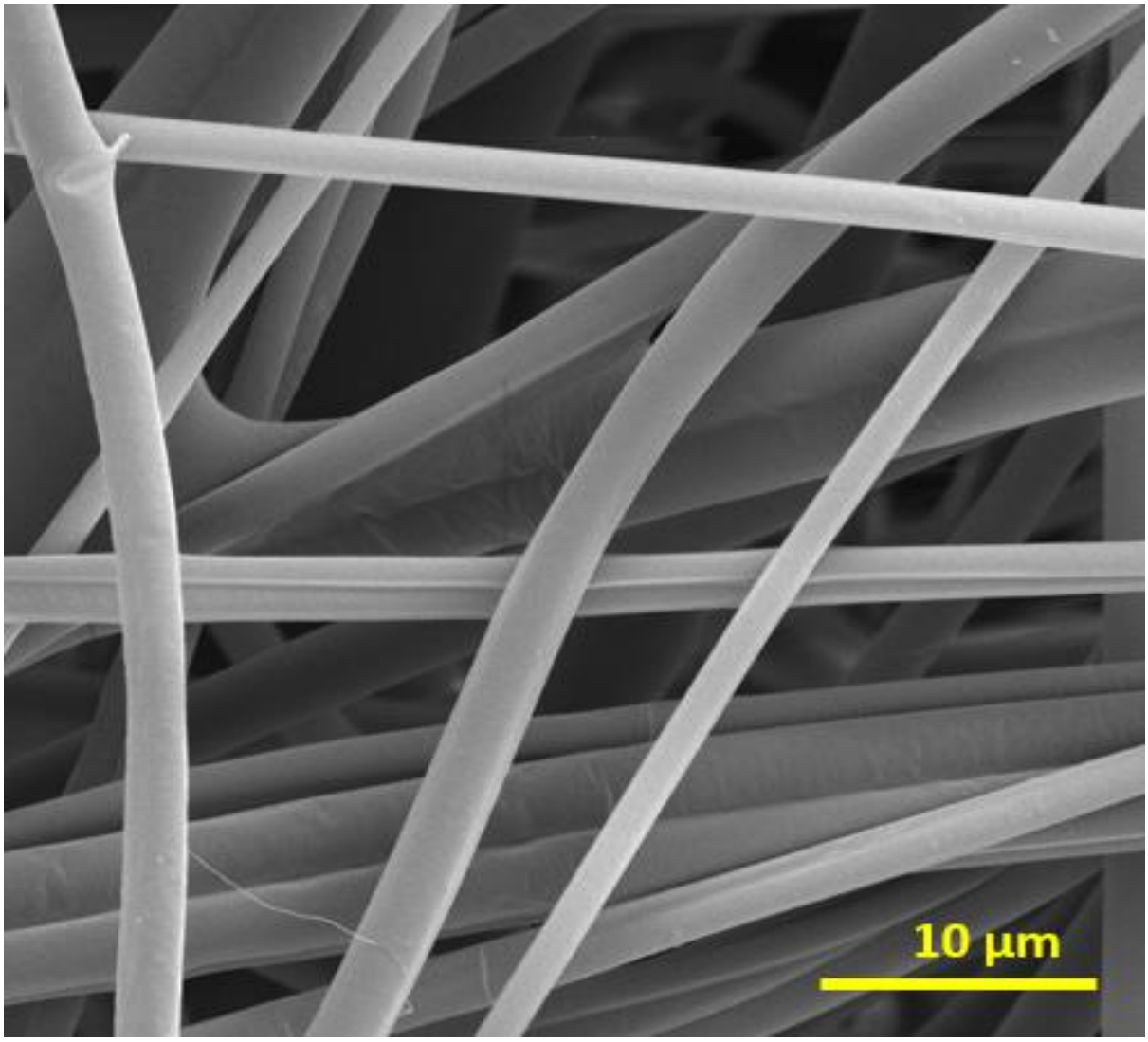

Figure A-1: SEM image analysis of 50 GSM Meltblown PP nonwoven substrate

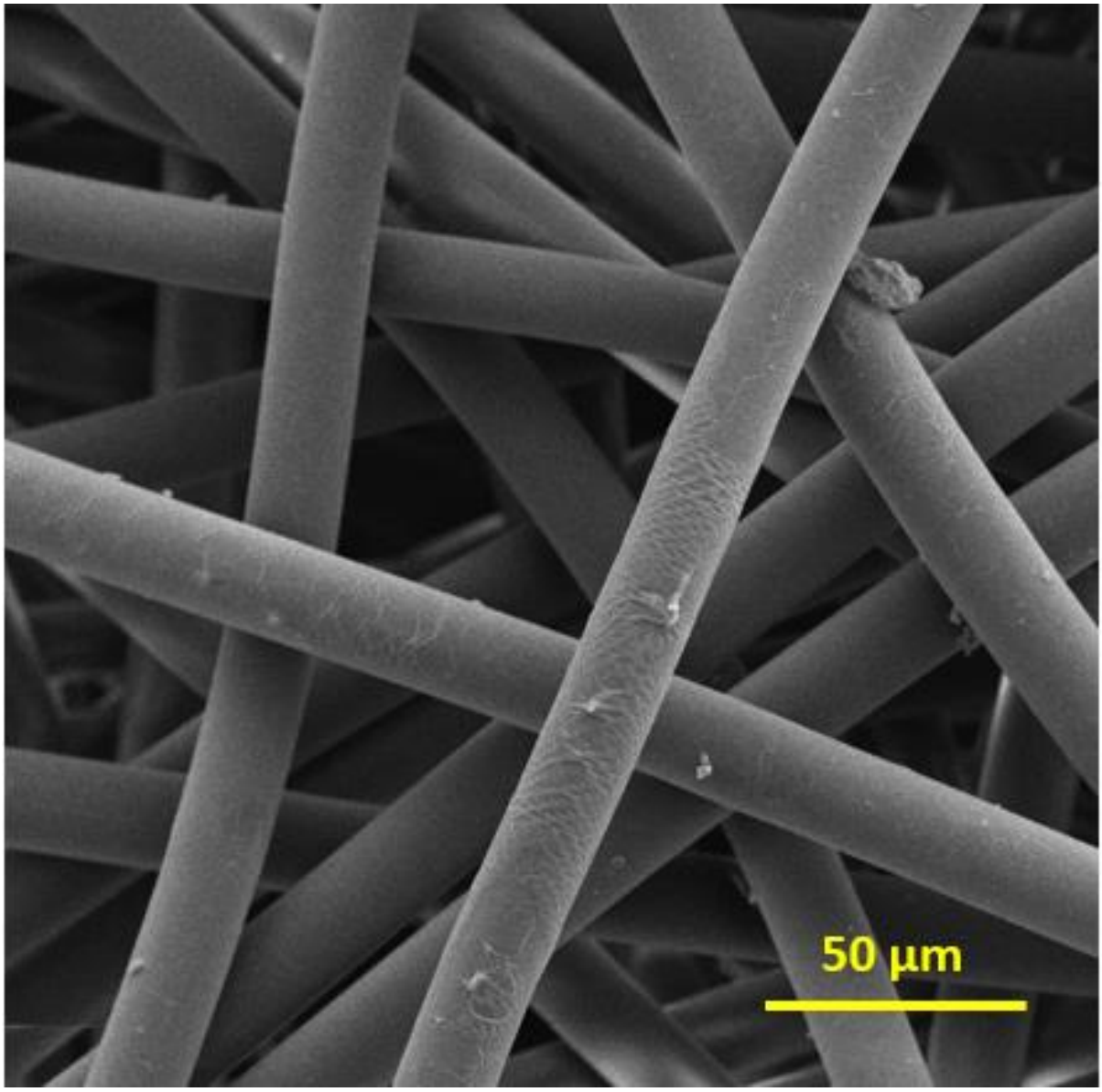

Figure A-2: SEM image analysis of 70 GSM spunbonded PP nonwoven substrate

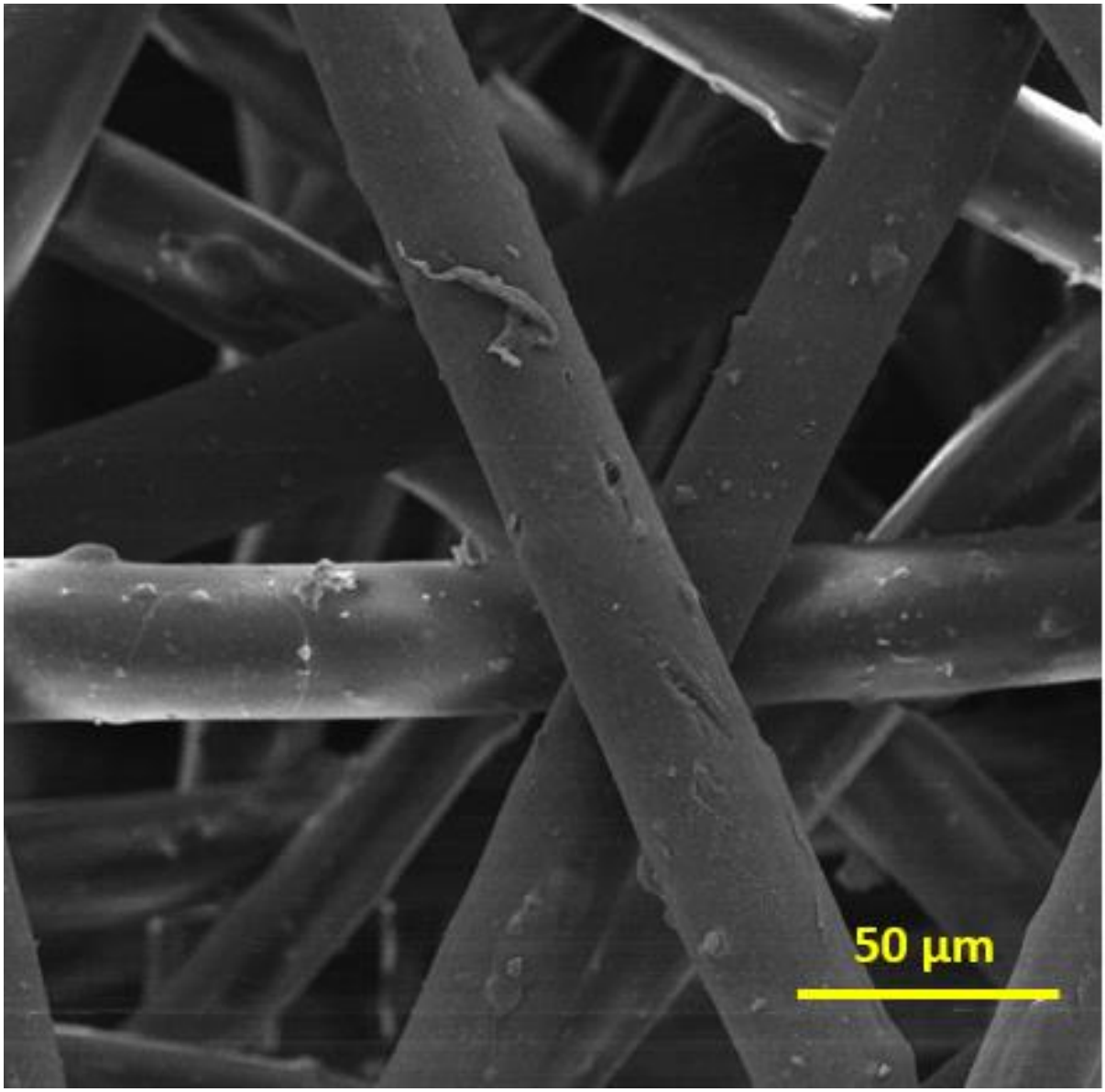

Figure A-3: SEM image analysis of 100 GSM spunbonded PP nonwoven substrate